EVALUATION OF INDUSTRIAL SLUDGE PRODUCED FROM TEXTILE AND LEATHER INDUSTRIAL WASTEWATER IN ENERGY AND ENVIRONMENTAL APPLICATIONS

Mostafa ABDUL WAHAB

Master's Thesis

Department of Chemical Engineering

Programme in Chemical Technology

Supervisor: Prof.Dr Funda ATEŞ

Eskişehir

Eskişehir Technical University

Institute of Graduate Programs

January 2022

17/01/2022

SUPERVISOR APPROVAL

Master's student Mostafa ABDUL WAHAB, whom I supervise, has completed this thesis titled EVALUATION OF INDUSTRIAL SLUDGE PRODUCED FROM TEXTILE AND LEATHER INDUSTRIAL WASTEWATER IN ENERGY AND ENVIRONMENTAL APPLICATIONS. According to my inspections, the work is scientifically and ethically appropriate for the student to the thesis defense exam.

Supervisor

Prof.Dr Funda ATEŞ

ABSTRACT

EVALUATION OF INDUSTRIAL SLUDGE PRODUCED FROM TEXTILE AND LEATHER INDUSTRIAL WASTEWATER IN ENERGY AND ENVIRONMENTAL APPLICATIONS

Mostafa ABDUL WAHAB

Department of Chemical Engineering

Programme in Chemical Technology

Eskişehir Technical University, Institute of Graduate Programs, January 2022

Supervisor: Prof.Dr Funda ATEŞ

In this study, catalytic (y-zeolite and activated alumina) and non-catalytic pyrolysis properties of sludge obtained from the biological treatment of leather and textile industrial wastewater plants were investigated by different methods. Iso-conversional model-free methods, such as Kissinger-Akahira-Sunose (KAS), Flynn-Wall-Ozawa (FWO), and Friedman were utilized to evaluate the kinetic and thermodynamic parameters. The calculated average E_a (activation energy) values of catalytic and non-catalytic pyrolysis with y-zeolite and activated alumina (Al2O3) were determined to be in the range of 170.63-182.77, 117.78-123.1 and 129.32-135.92 kJ/mol, respectively. GC/MS analyses showed that the oil obtained from the non-catalytic procedure was rich in fatty acids, steroidal compounds, and N-compounds. Activated alumina was very effective in removing nitrogen containing compounds from the oil. On the contrary, y-zeolite promoted de-oxygenation and de-acidification reactions and, as a result, the oil became rich in alkanes and alkenes which improved its quality as a fuel. As a result, y-zeolite can be used as an effective catalyst to improve the decomposition rate of sludge, and to upgrade the pyrolytic oil.

of the experimental studies, activated carbon was produced at different carbonization temperatures and saturation rate to evaluate the solid product obtained by the pyrolysis of the sludge. For this purpose, a two-factor experimental design method, 4-level carbonization temperature and 2-level saturation ratio, was carried out.

In the second stage, to evaluate the solid residue of sludge an activated carbon were produced at different carbonization temperature and different impregnation rate, for this reason a full factorial experiment was designed with two factors which are carbonization temperature with 4 levels and impregnation ratio with 2 levels.

As a result, Carbonization temperature (℃) was the most effected factors on surface area by 69.07 % contribution. Therefore, surface area increased with the increase of the temperature until achieved the maximum at 550 ˚C then decreased with the increasing of the temperature.

Keywords: Sludge, TGA Analysis, fast pyrolysis, catalyst, GC/MS, Activated Carbon.

ÖZET

DERİ SANAYI ATIK SUYU ÇAMURLARININ ENERJİ VE ÇEVRESEL UYGULAMALARDA DEĞERLENDİRMESİ

Mostafa ABDUL WAHAB

Kimya Mühendisliği Anabilim Dalı

Kimyasal Teknolojiler Bilim Dalı

Eskişehir Teknik Üniversitesi, Lisansüstü Eğitim Enstitüsü, Ocak 2022

Danışman: Prof. Dr. Funda ATEŞ

Bu çalışmada, tekstil ve deri sanayi atıksu arıtım tesislerinden oluşan biyolojik çamurun katalitik (y-zeolit ve aktive edilmiş alümina) ve katalitik olmayan piroliz özellikleri değişik yöntemlerle incelenmiştir. Kinetik ve termodinamik parametreleri değerlendirmek için Flynn-Wall-Ozawa (FWO), Kissinger-Akahira-Sunose (KAS) ve Friedman gibi izo dönüşümlü model içermeyen yöntemler kullanılmıştır. y-zeolit ve aktive edilmiş alümina (Al_2O_3) ile katalitik ve katalitik olmayan piroliz ile hesaplanan ortalama aktivasyon enerjisi (E_a) değerleri sırasıyla 117,78-123,1; ve 129,32-135,92; 170,63-182,77 kJ/mol aralığında belirlenmiştir. GC / MS sonuçlarına göre katalitik olmayan piroliz ile elde edilen sıvı ürün bileşiminin, yağ asitleri, steroidal bileşikler ve N-bileşikleri açısından zengin olduğunu bulunmuştur. Aktive edilmiş alümina, azot içeren bileşiklerin sıvı üründen uzaklaştırılmasında oldukça etkin saptanmıştır. Diğer taraftan, y-zeolit, oksijenli bileşiklerin uzaklaştırılması, ve asit giderme reaksiyonlarını teşvik ettiği tespit edilmiş, y-zeolitin katalizör olarak kullanıldığı deneylerde elde edilen sıvı ürün içerisinde alkanlar ve alkenler de saptanmıştır. Buraya kadar sonuçlar değerlendirildiğinde y-zeolitin, deri sanayi atıksu çamurunun bozunma reaksiyonlarında ve elde edilen sıvı ürünü iyileştirmek için etkin bir katalizör olarak kullanılabileceği sonucuna varılmıştır.

Deneysel çalışmaların ikinci aşamasında ise çamurun pirolizi ile elde edilen katı ürünü değerlendirmek için farklı karbonizasyon sıcaklıkları ve doyurma oranında aktif karbon üretilmiştir, bu amaçla 4 seviyeli karbonizasyon sıcaklığı ve 2 seviyeli doyurma oranı olmak üzere iki faktörlü deney tasarım yöntemi gerçekleştirilmiştir. Sonuç olarak, karbonizasyon sıcaklığı (℃) % 69.07 katkısı ile yüzey alanı üzerinde en çok etki eden faktör olarak belirlenmiştir. Bu nedenle yüzey alanı sıcaklığın artmasıyla artmış, 550 ˚C'de maksimuma ulaşmış, daha sonra sıcaklığın artmasıyla azalmıştır.

Under the abstract, there exists the Keywords section, which should contain at least 3, at most 5 keywords. Each of the keywords should start with a capital letter.

Anahtar Sözcükler: Atıksu arıtım çamuru, TGA analizi, Hızlı piroliz, Katalizör, GC/MS, Aktif Karbon.

ACKNOWLEDGEMENTS

I am grateful to my supervisor, Prof. Dr. Funda ATE, for giving me the chance to do this study. Furthermore, her monitoring, inspiration, and support from the beginning to the end of my master's degree allowed me to have a deeper grasp of the study issue. I am especially grateful for her time and tolerance when I was working in the laboratory and preparing my thesis. I'd want to also thank Dr. Eyüp YILDIRIR and Prof. Dr. Nihal ERGINEL for their advice and conversations, particularly throughout the journal publishing process.

Many thanks to my colleagues at Provable Cosmetics who providing aid, assistance and friendship Especially, **Adnan AKAT**, **Hakan KARAYAKA**, **Buse KOCER**.

and a private thanks to my best friend **Melek DERİN, Taha DERİN, Özlem Doktur**, **Zeki Doktur**, **Mohamad Mallouk** and **Asaad ALQUAISI.**

Many Thanks to my companion and my love **Aygül AKDAĞ** for her support, help and understanding.

Finally, I want to express my heartfelt thanks to my family, particularly my father Abdulnasser, brothers, and sisters, for their unwavering love and support during my master's degree. Especially to my Mother **Ghina ARNAOUT** for her unwavering love, support, and assistance, which I will never forget.

Mostafa ABDUL WAHAB

17/01/2022

STATEMENT OF COMPLIANCE WITH ETHICAL PRINCIPLES AND RULES

I hereby truthfully declare that this thesis is an original work prepared by me; that I have behaved in accordance with the scientific ethical principles and rules throughout the stages of preparation, data collection, analysis and presentation of my work; that I have cited the sources of all the data and information that could be obtained within the scope of this study, and included these sources in the references section; and that this study has been scanned for plagiarism with “scientific plagiarism detection program” used by Eskişehir Technical University, and that “it does not have any plagiarism” whatsoever. I also declare that, if a case contrary to my declaration is detected in my work at any time, I hereby express my consent to all the ethical and legal consequences that are involved.

Mostafa ABDUL WAHAB

CONTENTS

Page

LIST OF TABLES

Page

LIST OF FIGURES

Page

GLOSSARY OF SYMBOLS AND ABBREVIATIONS

Eα	:	Conversion Rate
Eα	:	Activation Energy
$\triangle H$	:	Enthalpy Change
△S	:	Entropy Change
△G	:	Gibbs Energy Change
FWO	:	Flynn-Wall-Ozawa
KAS	:	Kissinger-Akahira-Sunose

1. INTRODUCTION

Establishing sustainable processes to produce energy from waste is vital for the proposed circular economy, especially with increasing concerns over the effects of fossil fuels on climate change and global warming. Recently, utilizing organic waste as a resource for clean energy production has gained much attention. Activated sludge, as a by-product of the biological treatment of industrial or municipal wastewater, has great potential as organic waste since the amount of wastewater produced globally is nearly 330 km^3/year, which is the source for the sludge [1]. Depending on the type of the wastewater processed, it may contain hazardous and toxic compounds, hence the disposal of the sludge is important as it may create risks to the environment if it is not handled correctly. In developing nations especially, the quantity of sludge has increased noticeably in latest years. In the European Union alone, the total creation of sewage sludge was recorded as 9.2 million tons in 2010, and Turkey's share is around 0.6 million tons of sludge annually [2]. Mainly consisting of toxic and hazardous organic compounds, sludge could contain inorganic compounds, such as heavy metals and pathogenic compounds which are a major threat to the environment and human health [3]. Therefore, management of activated sludge is crucial for a sustainable environment and the economy.

Recent conventional treatment and removal methods of sludge consist of agricultural usage, landfilling, and incineration [4]. However, there is an increasing concern about these disposal methods due to their contribution to soil and water pollution in relation with the high amount of organic and inorganic toxic compounds in the sludge. As an alternative route, converting the sludge into fuel via thermochemical processes has been widely investigated. One of the most promising methods is the pyrolysis of sludge to produce oil, gas, char or activated carbon (AC). Bio-oil as a source of valuable chemicals or fuel with high calorific value could be obtained especially via fast pyrolysis of biomass and organic waste [5]. The fast pyrolysis of sewage sludge has been extensively studied, and the results have proven that the sludge amount decreases tremendously by converting it into liquid and gas products. However, the obtained liquid (bio-oil) has poor quality in terms of calorific value, water content, stability and oxygen content [6]. The bio-oil quality and the selectivity of the products could be enhanced by utilizing catalysts and/or modifiers. Several catalysts have been used in the past, such as CaO, Al_2O_3, HZSM-5 zeolite and steam as modifiers to increase the yield of the pyrolysis

and the quality of bio-oil [7]. Making AC from sludge has the possibility to be a cost-effective solution for waste treatment and low-cost adsorbent processing. In particular, the cost of production of sludge-based biomass, which depends on factors such as the supply of sludge and the necessary refining, including energy costs for pyrolysis and drying, has the potential to be equal to or even lower than the cost of production of commercial ACs [8].

(TGA) Thermo-gravimetric analysis is a widely applied technique to investigate the kinetics of the thermal decomposition process of solids. Knowing the kinetics of the mass loss of any material throughout their thermal decomposition is essential for characterization, new system development, feasibility assessment and design purposes [9,10]. Biomass thermal decomposition kinetic parameters could be determined by two techniques: model fitting and iso-conversional methods. Iso-conversional methods are more favorable as, according to Sanchez-Jimenez et. al., model fitting methods could yield uncertainties during the estimation of kinetic parameters and not represent the real case for a process [11]. The Friedman differential method [12], the Flynn-Wall-Ozawa linear integral method [13,14], and the Kissinger-Akahira-Sunose linear integral method [15], are the most referred iso-conversional methods, due to their simplicity and high accuracy. Many kinetic and thermodynamic parameters, such as activation energy, pre-exponential value, activation enthalpy change, activation Gibbs free energy and activation entropy change, can be obtained using the aforementioned methods by making use of transition state theory (active complex theory) [16] .

Liu et. al., estimate the activation energy of dried industrial sludge gathered from a chemical fiber factory and the woody industry using non-isothermal methods and the determined values are in the range of 170-593 kJ/mol and 125-756 kJ/mol, respectively [17]. Activation energy could be lowered with the help of the correct catalyst. Recent studies show that utilizing a CaO based catalyst, natural limestone, eggshell [18], Fe_2O_3, red mud [7], bifunctional HZSM-5/LS, HZSM-5 zeolite and limestone [19], have a substantial effect on minimizing the activation energy for the decomposition of biomass and organic waste.

Especially in developing countries such as Turkey, Bangladesh, Tanzania, South Africa etc., textile and leather industries are considered as one of the most important economy drivers. In general, low technology for production and waste management is

available and hence, the produced wastes contain vast amounts of toxic and hazardous materials [20]. The nitrogenous contaminants arising from the usage of azo-dyes and extensive usage of chromium during the tanning process, the produced sludge from these industries differs from the sewage and other industrial sludges. In this regard, as pyrolysis enables the routes not only producing liquid fuel, but also potential recovery of resources, can be a commercially available technology for a sustainable solution [21]. Although pyrolysis of sludge has been investigated in detail, there is very limited data on the pyrolysis of this kind of industrial sludge. The obtained oil could be enhanced with the catalyst addition and also determination of the kinetic data could contribute the literature in order to construct a commercial process, since there is not much research on the detection of kinetic parameters for catalytic thermal degradation of textile and leather industrial wastewater sludge in the presence of y-zeolite and Al_2O_3.

This Study divided into two parts; the first part was studying the thermal kinetic parameters of sludge estimated with the help of TGA analysis. Three different model free (iso-conversional) methods, Flynn-Wall-Ozawa (FWO), Kissinger-Akahira-Sunose (KAS) and differential Friedman, were used to determine the activation energy, pre-exponential factor, enthalpy, Gibbs's energy, and entropy change of activation during the pyrolysis of the sludge. The effects of y-zeolite and an activated alumina (Al_2O_3) catalyst on the activation energy and oil quality were also examined. Therefore, oil products obtained non-catalytic or catalytic procedure were analyzed by GC/MS to obtain product quality.

2. ENERGY RESOURCES

Energy can be described as a system's capacity to perform external work or movement. It is critical to identify and acquire energy sources efficiently. Energy Energy cannot be created or destroyed, according to the law of conversion of energy; however, it can be transformed from one type to another [22]. As a result, it is important to convert unexplored energy sources for sustainability which means addressing the demands of the present generation without endangering future generation's wealth. In other words, it must be worked to preserve the natural world for future generations while still meeting the basic needs [23]. Energy based on its resource's exhaustibility can be classified into non-renewable and renewable energy sources [22]. Figure 2.1 shows the growth of global energy consumption and the share of fuels for global energy consumption between 1990 and 2040.

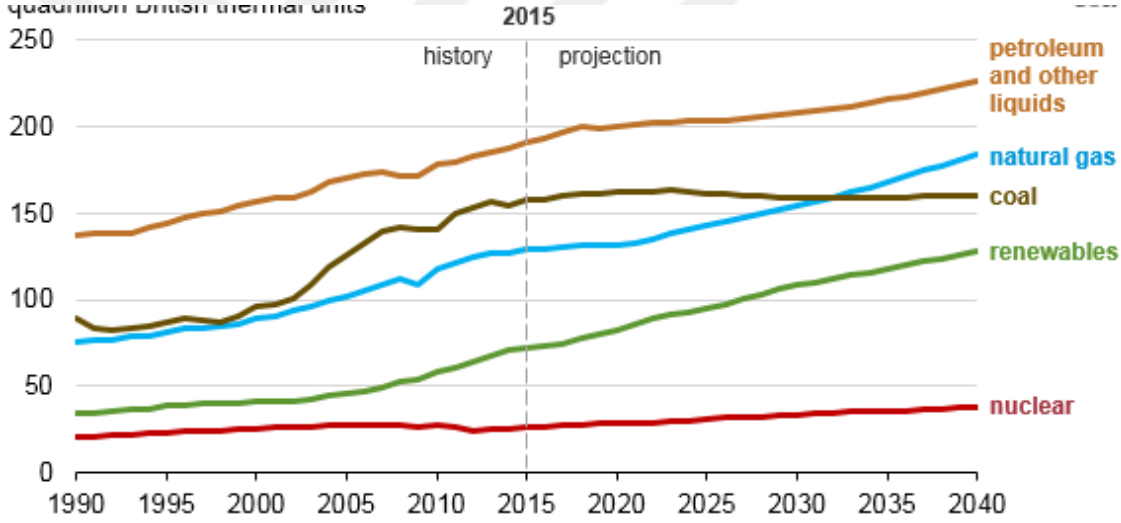

Figure 2.1. *Energy consumption between 1990 and 2040 (Source: U.S. Energy Information Administration, International Energy Outlook 2017)*

2.1. Non- renewable Resources

Non-renewable sources of energy include oil, coal, nuclear energy and Natural gas derived from sources that can deplete or cannot be restocked for thousands if not millions of years. Fossil fuels are the most abundant sources of non-renewable energy and were produced millions of years ago when the remains of marine creatures decomposed under enormous pressure and heat. The majority of fossil fuels are utilized to produce oil and electricity.

Unfortunately, for the time being, human civilization is reliant on non-renewable fuels as the main source of energy. Fossil fuels are energy-rich and quite economical to

process, that's why About 80% of the total volume of energy consumed globally per year is derived from fossil fuels. However, the main problem with fossil fuels, apart from their being in limited supply, is that burning them releases green-house gases CO_2, NO_x and SO_x into the atmosphere. Increasing levels of green-house gases in the atmosphere is the most important cause of climate change. Alternative energy sources, or in other word renewable energy such as wind, solar and biomass energy etc.., are a potential solution to reduce the using of non-renewable sources. Both clean energy sources are available in unlimited supply.

2.2. Renewable Energy sources

Renewable energy sources are mainly biomass-based and are usable in infinite amounts, as they can be recycled (i.e., regenerated through natural processes) within a fairly short period of time. Renewable energy sources are limitless, i.e., they can be replaced when we use them so they can produce energy again and again. Which include firewood (or fuelwood) originating from trees, Petro plants, plant biomass (as agricultural waste such as bagasse), animal dung, sludge, solar energy, wind energy, water energy (hydroelectric, ocean wave and tidal energy) and geothermal energy, etc. They can reproduce themselves in natural surroundings and can be harvested on an ongoing basis by good preparation and management [24].

2.3. Biomass Energy Sources

Biomass, a type of renewable energy, is organic material obtained from live beings, or recently living organisms, including herbaceous and wood biomass. Traditionally, biomass is utilized in direct incineration to create energy or produce heat. For example, forest residues (such as branches, tree stumps and dead trees), yard clippings, wood chips, municipal solid wastes, sewage sludge, and industrial sludge are regularly used to this objective. Nevertheless, biomass also contains plant or animal products used to produce fabrics or chemicals. Biomass can also contain biodegradable waste and can be used as coal. This includes organic materials such as fossil fuels which have been converted into substances such as coal or petroleum by geological processes [25].

Biomass, once administered, is often described as 'feedstock.' Different feedstocks used for energy purposes include sugar crops, oil seeds, wheat, sewage sludge, trees, agricultural residues, and algae grasses. Cellulosic biomass is used to characterize agricultural residues, trees, and grasses. The product extracted from biomass feedstock

depends on the biomass used and on the conversion process. Possible biomass-derived products include ethanol, methane, biodiesel, butanol, natural oils, and hydrocarbons which can be further refined into any number of suitable fuels [25].

3. SLUDGE

The world is currently seeing a dramatic increase in production of sludge, and this is supposed to stay in the early part of the next century. In both developed and newly industrialized countries, the increasing demand for consumer products and energy, together with the growing population, led to the rapid development of factories around the world, which increased the amount of waste produced. Among all the industries, textiles and leather have a large proportion, particularly in Turkey, as their share of global trade was around 5% in 2017 [26]. The processes involved in these industries contain a large quantity of water and a range of chemical intake, resulting in the development of Hazardous and toxic liquid and solid waste effluents close to those generated by municipal waste and other industries.

The history of the wastewater treatment plant of Usak City, Turkey provides a good illustration of the above case. Currently, about 200 ton/day of sludge per day is treated. The formed sludge is stored in a temporary waste field in accordance with the legislation then is sent to licensed landfill [27].

3.1. Sources and Treatment of Sludge

Sludge is a secondary product in wastewater sewage treatment. Werther and Ogada 1999 reported that wastewater is a mixture of liquid or water-carried waste separated from a domestic, commercial, or industrial establishment. Wastewater can include many harmful elements, including organic, inorganic and toxic compounds, and microorganisms that are pathogenic or disease-causing [28]. Wastewater is exposed to biological, physical, and chemical operations for the exclusion of wastewater components such as organic forms of carbon, solid settling, phosphorus, nitrogen, treated wastewater and sludge. The developed sludge has different characteristics according to the process applied to the wastewater [29]. There are three main types of sludge:

- Sludge from municipal wastewater treatment, consisting of either domestic wastewater or a combination of domestic wastewater with commercial wastewater and/or run-off rainwater.
- Sludge extracted from industrial wastewater treatment, that is water used in industrial processes.

- Sludge that treated from drinking water. Water must be processed before it is consumed. The volume of sludge produced by treating drinking water is considerably smaller than that created by treating wastewater [30].

3.1.1. Sludge pre-Treatment Process

Physical or Pre-treatment Operations utilized in the handling of wastewater require sedimentation and filtration methods. In the primary sedimentation phase, determined by gravity is the settling effective strong material of wastewater. Consequently, a semi-solid secondary product is created, known as primary sludge [29]. The pre-treatment processed effluent is then deposited in huge storage tanks that allow sludge to settle down at the bottom while materials such as oil and grease float upside down. The floating content shall be extracted. Werther and Ogada (1999) reported that the material removing from primary sludge, having 3-5 wt% solids which consists of 30 wt% inorganic and 70% organic matter [28]. Sedimentation is the most common form of treatment used at this point due to its convenience and low cost value [30]. This approach permits it possible to stabilize suspended solids under the control of gravity. The handled effluent is extracted from the bottom of the tank and brought to the chemical operation.

Chemical operations consist primarily of phase sequences that are called coagulation, flocculation, and sedimentation. To produce flocculants with different components such as heavy metals or phosphorus, chemical methods are added to wastewater. Sludge generated during chemical wastewater treatment involves added coagulants and flocculants, as well as the portion to be extracted from wastewater [31].

Biological stage: Biological activities are implemented to treat wastewater from nitrogen, phosphorus and organic carbon content. The purpose of biological wastewater treatment method is to accomplish wastewater elimination by creating an organic sludge that is collected in a pond where wastewater is applied. Biomass of activated sludge is mixed with wastewater during this process; although microorganisms use carbon and nutrients in wastewater as a source of energy for reproductive activity, wastewater control is accomplished. This cycle therefore creates enough biomass and is eliminated from the network. This part of wastewater is referred to as secondary (biological, excess) sludge [32].

3.1.2. Sludge Treatment Process

The main objective of treatment of sewage sludge is to increase the amount of dry matter and to maintain biologically stable residues. The dry matter volume of the waste sludge is raised by dewatering, thickening, and drying. Sludge stabilization is accomplished by chemical, anaerobic or aerobic methods [32]. Figure 3-1. show the sludge treatment process.

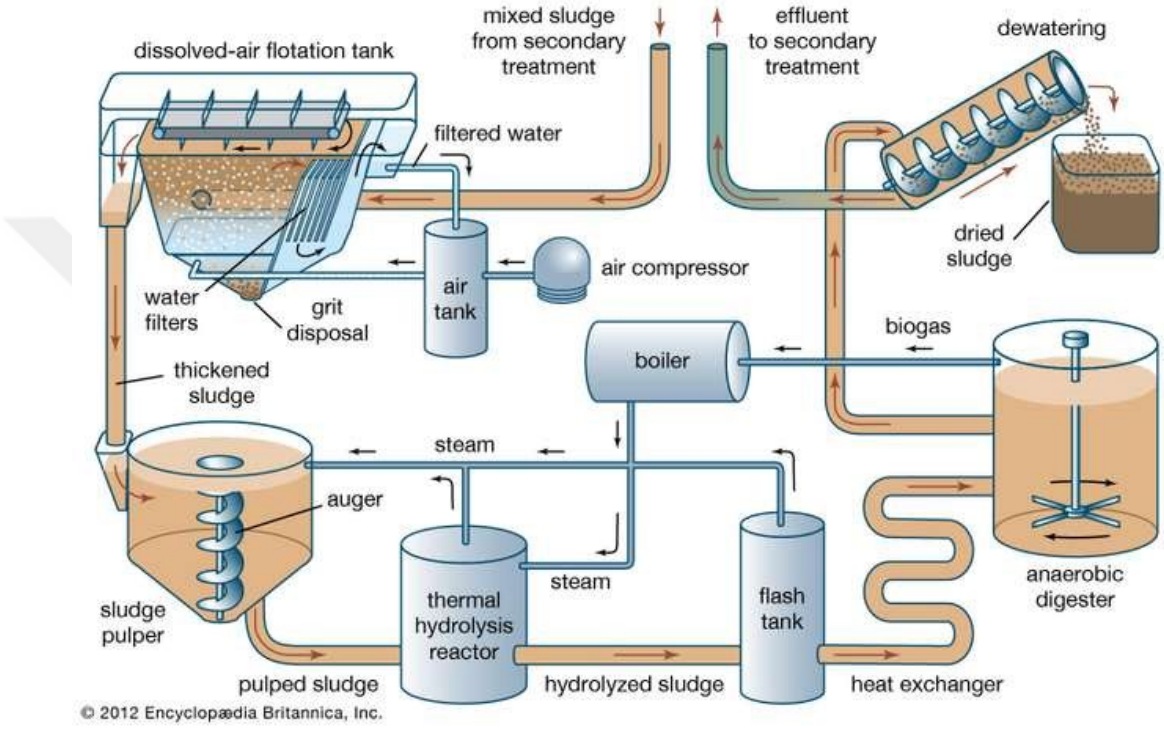

Figure 3.1. *Sludge treatment process (https://www.britannica.com/technology/wastewater-treatment/Sludge-treatment-and-disposal)*

3.1.2.1. Sludge thickening

Sludge thickening is a specific treatment procedure for sewage sludge that is often used to raise the content of biological sludge derived from the active sludge cycle [33] or to achieve a denser primary sludge. The sludge thickening cycle profits from both gravity and flotation impacts. If the amount of water in the sludge is decreased by 50 %, up to 5 % of the strong material of the sludge may be produced [34].

3.1.2.2. Sludge stabilization

Sludge stabilization is the following method of treatment with sludge added to thickened sludge. Stabilization may be accomplished by both chemical and biological cycle. Biological sludge stabilization is done in anaerobic or aerobic environments. The operation of microorganisms in the stabilization device is stimulated by the biological

stabilization phase of the sludge, thereby enabling microorganisms to utilize the organic fraction of the sludge as a resource of energy. As a consequence, the organic portion used is turned into gas and stable residues [28].

3.1.2.3. Anaerobic digestion

Anaerobic sewage sludge stabilization is a process controlled in the absence of oxygen. In anaerobic digestion, there are four phases in the metabolic reduction of organic matter. The goals of the anaerobic sludge stabilization process are to achieve hydrolysis, acidogenesis, acetogenesis, and methanogenesis. The organic portion of the sludge is transformed into CH_4, CO_2, and H_2S, as well as a solid residue that is removed as a process effluent. Anaerobically stabilized sludge with low pathogen matter and limited biological movement is described as the remaining sludge residue. [35].

3.1.2.4. Aerobic digestion

Aerobic digestion is a bacterial cycle that happens in the presence of oxygen. Organic matter is oxidized under aerobic conditions and products such as carbon dioxide, nitrate or phosphate are produced. Composting is a normal method of break down of organic matter by microorganisms under aerobic situations, providing adequate aeration by turning sludge daily. In this process, aerobic bacteria convert organic matter into energy, carbon dioxide and ammonia [36].

3.1.2.5. Sludge dewatering

Dewatering is applied following one of the steps of anaerobic digestion. The purpose of dewatering is to decrease sludge water content which results in lower transportation costs and reduces the sludge volume generated. Since it is easier to dry sludge which has a lower moisture content, it is also added to improve the mass loads to sludge drying activity. Stabilized sludge that has one to four percent of dry solids is converted into a substance called 'cake' with 20-30 percent of dry solids being dewatered. Pressure, vacuum or centrifugal forces are used to dewater sludge [37].

3.1.2.6. Sludge drying

Sludge drying is the final step in the disposal of untreated sludge. This is used to further minimize the amount of sewage sludge, to produce biologically resistant content that enables shipping or storage, and to make sewage sludge available in thermal processes [28]. Which demands a fully dry material such as thermal energy supplies or

cement kiln [38]. Solar energy is a used alternative as well as thermal energy for drying the sludge. Through spreading dewatered sludge into a managed land where high solar energy is accessible, the use of solar energy is brought. Sewage sludge thermal drying contains two separate mechanisms; direct drying is a high-level-rate process where elevated temperatures are attained. Indirect drying is accomplished by the countercurrent injection of low temperature air into waste sludge that is sprayed through a filter medium to produce a thin film. Nonetheless, both thermal drying methods make sewage sludge with a content of more than 90 percent dry solids [39].

3.2. Disposal Options of Sludge

The amount of wet sludge produced increases rapidly and the management with conventional methods become unsustainable day by day. Only in European Union the production of sewage sludge was around 10 million tons of dry solids in 2010 and 14% of it was disposed in landfills while 27% was incinerated. In addition, 39% of the sewage sludge was evaluated as fertilizer for agricultural usage however EU directive 86/278/EEC restricts such usage unless certain limits of contaminants and metals are satisfied [40]. Figure 3.2 shows the disposal routes of sludge in EU-12, EU-15 and EU-27 provinces in 2005 and 2011.

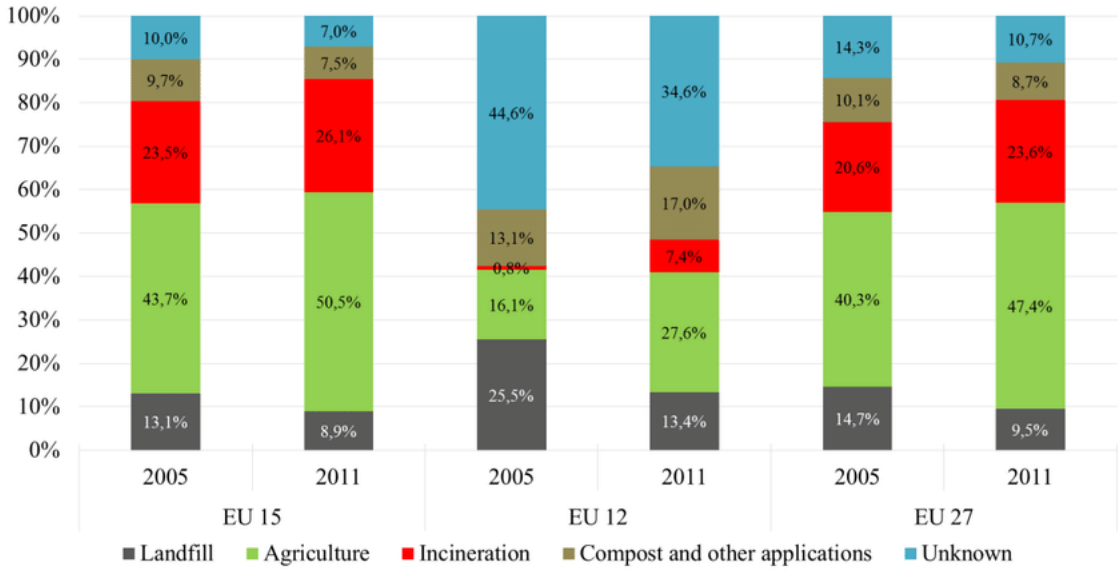

Figure 3.2. *Sewage sludge disposal routes in EU-15, EU-12 and EU-27 in 2005 and 2011 [41].*

Table 3.1. *Details on waste sludge development and disposal routes in Europe* [41].

Country (year)	ktons Dry Matter/year				
	Production	**Landfill**	**Agriculture**	**Incineration**	**Compost and other applications**
Belgium (2010)	176	0	17	113	0
Austria (2010)	263	21	44	115	83
Finland (2009)	149	4	8	0	133
Denmark (2010)	141	1	74	34	0
Germany (2010)	1,780	0	566	1004	317
France (2010)	966	42	727	181	0
Ireland (2011)	86	0	58	0	28
Greece (2011)	147	80	6	36	0
Luxembourg (2010)	10	0	5	1	0
Netherlands (2010)	351	0	0	330	0
Spain (2010)	1205	96	995	62	0
Portugal (2009)	344	22	226	0	0
UK (2010)	1,419	9	1118	260	0
Sweden (2010)	204	8	50	2	65
Bulgaria (2011)	52	28	18	0	1
Lithuania (2011)	52	0	10	0	11
Latvia (2009)	22	2	8	0	0
Estonia (2011)	18	2	1	0	15
Malta (2011)	6	6	0	0	0
Slovakia (2011)	59	8	0	0	38
Romania (2011)	114	54	2	0	0
Poland (2011)	519	51	116	42	31
Slovenia (2011)	26	2	0	15	2
Czech Republic (2011)	218	14	108	7	73
Cyprus (2010)	8	0	7	0	0
Hungary (2011)	168	2	78	30	43
Total	8503	452	4242	2232	840

3.2.1. Landfilling

Landfilling involves burying waste in a specified piece of land. This treatment process induces contamination from the breaking down of organic matter inside the

sludge to the ground water [42]. This is also a significant cause of air contamination, for methane and carbon dioxide [43]. Additionally, Landfilling induces air emissions from the supply automobiles and releases heavy metals into the soil impacting the harvest [42]. This technique of disposal is supposed to reduce especially with strict regulations and the need to minimize environmental pollution [43]. Landfilling of organic material is widely considered no longer acceptable from an economic point of view and this disposal method must definitely be heavily constrained by Directive 99/31 [44].

3.2.2. Fertilizer in agriculture

Spreading or applying sludge into the surface of farm land or pumping bio-solids beneath the surface of the soil layers, or fertilizing field-grown crops [45]. Due to its large nitrogen and phosphorus, sludge has healthy nutrient properties. Applying biosolids to farmlands enables processing of organic matter and nutrients to rebuild land. By adding to the bicycle, sludge use replaces synthetic fertilizers [45].

Dry sludge, typically in the form of granules or pellets, has the benefit of being suitable for transport owing to its decreased volume and strong dry matter content (85-95% DS) relative to dewatered sludge, which is just about 30 % DS. Farmers can now treat dried sludge more effectively and there is often a significantly reduced chance of contamination relative to older techniques for treating untreated sewage [45].

However, wastewater also includes heavy metals and other common contaminants such as organochlorine and brominated diphenyl ethers (BDEs), These toxic substances that present significant environmental hazards as a result of contamination of surface and ground water. By applying biosolid sewage in a harmful way, more contamination of plant animals by accumulation of food can be occur.

Nevertheless, this treatment of sludge through application to agriculture is commonly done and is generally believed to be environmentally friendly. Nonetheless, the treatment of waste sludge for grassland and forage crops must be closely controlled to avoid adverse effects on soil animal welfare [46].

3.2.3. Incineration

Combustion is a chemical reaction between a fuel and an oxygen which creates heat, CO_2, H_2O, and ash. Fuels are classified as heat-producing materials when reacting with an oxidant. Non-renewable carbon-based fossil resources generally are listed as

primary fuels but biomass and other renewable materials are listed as alternative fuels [47]. Thus sewage sludge may be categorized as alternative fuel and used in combustion processes due to the organic content. [28]. Incineration is one of the main forms of waste sludge disposal that has been commonly used in many developing countries and in some newly industrialized areas in previous years. Incineration can achieve stabilization, reduction in volume and recovery of sludge. It is an easy way to dispose of waste sludge [48]. But in the other hand it may release dioxin and furans, NO_x, SO_x and heavy metals hence causing air contamination [49]. Likewise, the obtained ash from incineration process is polluted with a high heavy metal content and is also costly to dispose of and requires special and costly filling sites [48]. Despite of incineration, there are other thermal methods for treating sludge, such as gasification and pyrolysis [50].

3.2.4. Gasification

Gasification method is the partial oxidation of biodegradable material in an environment that is limited by oxidants. The process occurs in the reactor for gasification, called the gasifiers [51]. The major aim of this process is the processing of flammable gas product namely gasification gas which consist of Hydrogen, carbon monoxide and methane. Gasification also creates a solid fraction which is a material rich in carbon [51]. Gasification of sludge contributes to a high-quality flammable gas which can be used for energy generation or to facilitate processes such as sewage sludge drying. Gasification is tolerant of complex, especially contaminated feedstocks. Taking into consideration that a reductive atmosphere characterizes gasification, the overall amount of generated gas is smaller than the amount of exhaust from the incineration process. As a result, sulfur in gaseous content is converted into H2S, nitrogen into NH3, chloride to HCl. It prevents the production of dioxins, SO2, and NOx and the installation of gas cleaning is smaller and less costly compared to traditional combustion [52]. Fig. 3-3 explain the flow diagram of gasification process.

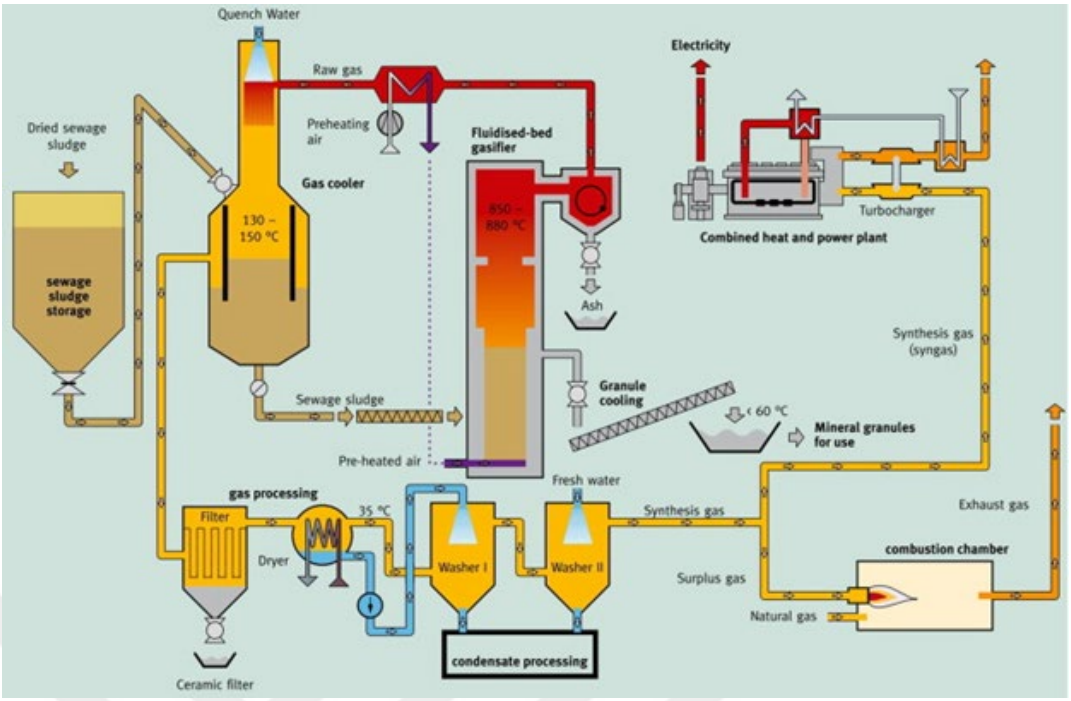

Figure 3.3. *Gasification flow diagram (http://www.biofuelsacademy.org/index.html%3Fp=456.html)*

3.2.5. Pyrolysis as an alternative disposal routes of sludge

Many studies on sludge pyrolysis process are based on the literature concerning lignocellulosic biomass pyrolysis. Indeed, significant attempts have been made to transform biomass to oil since the 1970s oil crisis [53].

4. PYROLYSIS

Pyrolysis is the thermal breakdown of materials in a vapor-producing environment created by condensable and non-condensable gasses and a solid product, namely char [53]. Pyrolysis is one of the alternatives that is used in sewage sludge treatment. Depending on the desired product result, the process takes place in the temperature range of 300 to 900 °C [30].

Biochar or char, bio-oil or pyrolysis oil and non-condensable gases or biogases are the principal products of the pyrolysis process. The oil obtained from pyrolysis process can be used for chemical manufacturing as a raw material or a fuel, the gas can be used for incineration, thus, biochar can also be used as fuel or used as fertilizer. Additionally, the pyrolysis process envelops the heavy metals in the bio-char except mercury [4].

Pyrolysis allows oil recovery with low N_2 and H_2S emissions. Werther and Ogada noted that in contrast with incineration, the production of toxic organic compounds such as dioxins is prevented at low operating costs [28]. It is a reliable oil source that can be used in several chemical processes and reduces sewage sludge to small amounts of inert residues [1]. The terms of the pyrolysis process can be changed to produce the required oil, gas and char as a product [54].

4.1. Pyrolysis Classification

Pyrolysis can be separated into three major groups, depending on the operating condition: Slow Pyrolysis, conventional Pyrolysis, fast Pyrolysis, and flash pyrolysis.

Table 4.1. *Typical functional parameters and pyrolysis products [55].*

Pyrolysis Process	Residence Time (s)	Particle Size (mm)	Heating Rate (℃/s)	Temp. (C)	Product Yield (%)		
					Char	Oil	Gas
Slow	450-550	5-50	0.1-1	177-277	35	30	35
Fast	0.5-10	<1	10-200	577-977	20	50	30
Flash	< 0.5	<0.2	>1000	777-1027	12	75	13

These differ in temperature of the plant, heating rate, time of solid residence, particle size of the biomass, etc. Relative product distribution, however, depends on the form of pyrolysis and the operating parameters of pyrolysis shown in Table 4.1. In addition, the following three sub-sections detail various forms of pyrolysis processes [55].

4.1.1. Slow Pyrolysis

Slow pyrolysis has been applied for many of years to increase charcoal formation at low heating rates and low temperatures. In this method, the vapor residence time is too high (5 min to 30 min) and the components in the vapor phase continue to react with each other, resulting in the formation of solid carbon and other liquids [55]. However, slow pyrolysis has certain technical drawbacks that have made it impossible to be ideal for bio-oil processing of good quality. Breaking of the primary product in a slow pyrolysis process is due to the long periods of residence and could negatively affect the yield and quality of the bio-oil. In addition, long periods of residence and low heat transfer demand extra energy reactant [56].

4.1.2. Fast Pyrolysis

In the case of fast pyrolysis, sludge or biomass decomposes quickly to create more vapors, volatiles, some char, and gas. After cooling and condensation, a dark brown homogenous mobile liquid is formed and has a heating capacity of about half that of standard fuel oil. Large yield of liquid is collected with the bulk of biomass feeds low in ash [57]. The basic characteristics of the method of fast pyrolysis to produce liquids are:

- Excessive heat transfer and excessive heating rates at the sludge particle reaction interface usually require a thinly ground sludge feed of typically less than 3 mm as sludge generally has a low thermal conductivity,
- Carefully regulated reaction pyrolysis temperature about 500 °C to optimize the liquid production for most of the sludge,
- Short hot vapor residence times of typically less than 2 s to minimize secondary reactions,
- Rapid elimination of product char to reduce cracking of vapors,
- Rapid cooling of the pyrolysis volatiles to give the bio-oil product [58].

During Fast pyrolysis liquid yield produce during a few seconds or less, heat and mass transfer processes as well as phase transition phenomena and chemical kinetics play an important role. The key issue is to ensure the optimum process temperature for the

reacting particles and to which their exposure to lower temperatures which promote the formation of charcoal. One way to achieve this aim is to use small particles, such as the later mentioned fluidized bed processes. Another alternative is that heat can be transferred very quickly only to the particle surface, touching the heat source used in ablative processes mentioned later [58]. Figure 4.1 shows process flow diagram of biomass pyrolysis process.

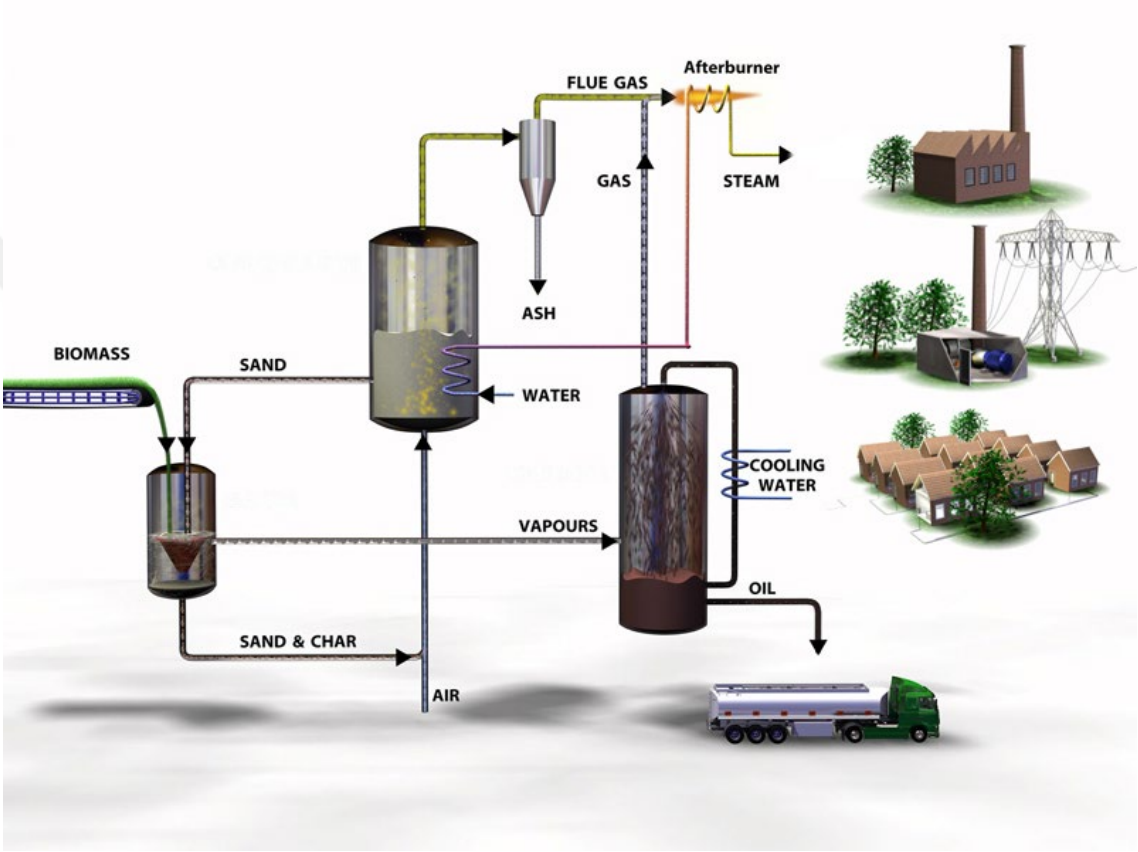

Figure 4.1. *Process flow diagram of biomass fast pyrolysis process*

The main product is bio-oil which produced by dry feed production of up to 75% wt. and secondary product charcoal and gas, that can be used during the process to supply the process heat requirements, so that waste streams are not available other than flue gas and ash. The liquid yield depends on the form of biomass, temperature, residence period in hot vapors, carbohydrate separation and content of biomass ash [57].

4.1.3. Flash Pyrolysis

Flash pyrolysis is an advantageous production process for liquid, gaseous, solid and fuel that can produce up to 75% of the oil yield. This process can be distinguished by quick inert devolatilization, high particle heating levels, high reaction temperatures of

450 °C to 1000 °C, and very short gas residence time (less than 1s). This method however has some technical limitations, such as: low thermal stability and oil corrosivity, solids in oil, increasing viscosity over time by catalytic char action, condensed alkals in char dissolves in oil and pyrolytic water production [55].

5. THERMOGRAVIMETRIC ANALYSIS (TGA)

The thermogravimetric analysis is the most widely used laboratory method for the study of pyrolysis kinetics [74,75]. Thermogravimetric analysis, referred to as TGA in this Thesis but also known as TG in some literature [75], TGA is a thermal analysis method used to analyze mass-change anomalies caused by variations in temperature. Temperature variations in the samples are caused by external heating or cooling, which may also be the result of processes inside the sample. Since the method measures mass transition, TGA can only be used to analyze thermal processes contributing to a shift in sample mass. Many thermally induced phenomena, such as melting and crystallization, cannot be tested using TGA, but are then analyzed using DSC, differential calorimetric scanning [76].

According to the restricted details that can be obtained using TGA, i.e. mass as a function of time and temperature, the technique is mostly paired with DSC in the so-called STA simultaneous thermal analyzer. In order to further improve the knowledge that can be obtained on a thermal occurrence, the evolution of gasses and/or vapors can be studied using an automated gas analysis (EGA) [74]. EGA can include either qualitative or quantitative information and examples of EGA include mass spectrometry (MS), Fourier-transform infrared (FTIR) spectroscopy and gas chromatography (GC). In addition to TGA and DSC, there are also other types of thermal analysis. Types include differential thermal analysis (DTA), thermomanometric analysis, thermomagnetic analysis, thermomechanical analysis (TMA), thermoacoustic analysis (TAA), thermoelectric analysis (TEA), and thermooptical analysis (TOA). An overview of thermal analysis methods can be found in [77].

There are several concepts that are applicable to the discussion of the TGA. The temperature program explains the variations in the sample temperature. it is the term used to denote the system created by the TGA operator, but it can also be used to describe the temperature of the sample, induced by both the programmed temperature schedule and/or the reaction heat. Thermal lag is another key in thermal decomposition kinetics studies. In addition, thermal lag means that the current temperature of the sample does not meet the desired temperature schedule used in the TGA [74].

This requirement to preserve the breakdown reactions that take place throughout the pyrolysis process within the kinetically regulated system ensures that certain

laboratory conditions and certain feedstock properties must be undeniably affected: their values will be conditioned to the goal of producing experiments within the kinetic control limits, preventing them to the full degree practicable. Some of the experimental parameters may have a significant impact on the essence of the reactions have been kinetically regulated or, quite the opposite, influenced by the limits of heat and mass transfer. are [78]:

- Collecting kinetic data
- Sample size and sample mass
- Temperature and heating rates
- Gas atmosphere and flow rate

By specifying the values of these constraints, which influence the structure of the reaction system within reasonable limits and reasonable ranges of values, so that the presumption of kinetic regulation is acceptable, the effects of heat and mass transfer may be assumed to be insignificant during the study of the experimental portion of this thesis. Values for all of these investigational parameters will be reviewed in a later section, where the need to search for the parameter values that best fit the conditions for maintaining the kinetic control regime throughout the experiments will be decisive [79].

5.1. Collecting Kinetic Data Using TGA

The available data from TGA is the difference in mass as a function of sample temperature and time. To collect data describing the kinetics of the sample decomposition process, the rate of operation (mass-change per time) must be determined by the rate of continuous chemical reactions. Other mechanisms that may regulate the rate include heat and mass transfer mechanisms, as well as thermodynamic phenomena such as equilibrium. Other processes that may control the rate include heat and mass transfer systems, as well as thermodynamic phenomena such as equilibrium. For more general, but comprehensive guidelines on how to gather thermal analysis data for clinical evaluation, see [75].

5.1.1. Sample size and sample mass

The sample size and mass will be selected to prevent thermal lag and to achieve a typical sample composition. Sample size also influences the presence of secondary reactions. During the planning of the experiments, the heterogeneous nature of the sludge

needs to be considered. To obtain representative kinetic parameters, each sample should be prepared in such a way that the entire biomass composition is represented. In the case of wood, this can be accomplished by milling and grinding and by extracting heterogeneous sections such as branches and bark. Milling can also decrease the particle size, which may minimize temperature gradients within the particle that would otherwise exist. Extensive milling can result in thick powders that may influence the process of pyrolysis due to the trapping of advanced gas species (secondary pyrolysis). Several tests with different sample layer thickness or different sample crucibles and gas flow conditions and flow speeds can be used to check whether this effect is present. If milling is not required, the number of repeats should be large to ensure that the kinetic properties are collected.

The total sample mass that can be used is typically based on the precision of the instrument and the necessary loads for the balance. The sample mass may also be constrained by the scale of the available crucibles. In general, a lower mass is favored for kinetic investigations because this reduces the thermal lag and the presence of secondary reactions (due to shortened vapor hold-up time in the solid matrix). Small mass improves the signal-to-noise ratio and the difficulties of collecting homogeneous samples. Ideally, experiments of different sample mass and heating levels are carried out to ensure that the sample mass selected does not result in a thermal lag for the selected heating rate. A last thing to consider is that a reduced sample size will increase the surface to the volume ratio. Unless the surface reactions are isolated from those in the bulk, this could be of concern [74].

5.1.2. Gas atmosphere and flow rate

For convenience, the gas flow and atmosphere is usually chosen in kinetic studies of sludge pyrolysis to reduce the impact of secondary pyrolysis processes [75]. This can be checked by adjusting the rate of gas flow and making sure the mass-loss curve is not disturbed. In these situations, no lid on the sample crucible is used and a high rate of gas flow is necessary. The structure of the gas flow would also be a major factor for varying. The gas ought to be inert, i.e. there should no oxidizing agent as water or oxygen be present. This is especially relevant over long periods and runs at high temperatures, where only trace amounts of oxygen can contribute to measurable mass loss [75]. Choosing inert gas depends on price, quality, thermal conductivity, and density. Higher thermal

conductivity of gas should increase the flow of heat between the reactor and the sample, which can reduce thermal lag.

5.1.3. Temperature and heating rates

The aim with kinetic studies is to describe the decomposition process of pyrolysis reaction and find the demand energy and thermodynamic parameters. But In some industrial applications, the heating intensity may be several hundred Kelvin per second [80]. In most commercial TGAs, the maximum heat rates attainable are much lower than this, partially due to the high thermal inertia in the furnaces used. The question to be asked then is whether the kinetics dictated in the TGA at lower heating rate situations can be used to model high heating rate processes in the industry. One thing that really matters to remember is that although the heating rate is high on the particle surface, the internal heating rate is not necessarily high [80,81], which implies that TGA may provide relevant information at least at lower process temperatures. From a scientific point of view, low heating rates are advantageous as they decouple overlapping mass-loss peaks which enable detailed evaluation of sub-processes. The lower heating rate also will reduce the thermal lag. The sample mass must be small if high heat rates are required.

Necessary for model fitting methods but also very important for isoconversional methods is that the experiments be performed with a minimum of three different heating rates or temperature systems (preferably more).

5.1.4. How to ensure high accuracy of the collected data

The precision and the quality of the data obtained impact on the sample volume, the mass of the sample, the temperature system, gas flow rate and the form of gas. In addition, it will rely on the consistency of the temperature calibration, the calibration of the balance, the correction of the buoyancy effect, the cleanliness of the device and the crucibles, as well as on the reproducibility of the preparation and handling of the samples. In addition, all the hard work done during calibration, washing, and preparation will go to waste when the TGA is put under constant atmospheric conditions in a vibrational free environment. The sampling rate and the automated smoothing that occurs in some commercial TGA applications are two final issues which can affect the data quality [76].

5.2. Thermal Decomposition Kinetics and Definition of Main Parameters

It's crucial to understand the kinetics of biomass degradation in order to analyze the different processes of thermal decomposition and forecast their behavior. Biomass decomposition is a difficult mechanism because numerous activities occur simultaneously, both in parallel and in succession. As a result, the number of components degrading simultaneously during a thermochemical decomposition process is quite large. Furthermore, the process analysis is more complex due to the already degradable elements that impact the breakdown of the residual biomass fraction, the secondary reactions happening between the vapors and gasses produced as a result of biomass decomposition and the solid fraction of the non-decomposed biomass components, and the secondary reactions happening between the vapors and gasses produced as a result of biomass decomposition [79].

Until providing a description of the modeling work performed on the kinetics of sludge pyrolysis, isoconversional methods used in the literature are briefly listed with a emphasis on their specific accuracy.

5.2.1. Non-isothermal Experiments

Kinetic analysis is established in a different way based on whether the breaking down process is isothermal or non-isothermal.

Isothermal methods are those in which the temperature of the structure is upraised as quickly as possible to the desired sample temperature; because the temperature of the system is raised so quickly, there is not enough time for the main phase of decomposition of the feedstock and, as a result, the main reactions to occur [78]. It is only when the targeted experimental temperature has been attained that the primary breakdown processes begin to take place. The temperature remains steady all throughout process, with time being the only variable that changes during the decomposition process. As opposed to isothermal tests, in non-isothermal experiments, decomposition processes occur during the heating phase of the system; however, this heating process occurs considerably more slowly than in isothermal experiments. Consequently, the feedstock decomposes as the temperature increases. Depending on the temperature and time conditions, the state of decomposition will be determined in this situation [79].

The key characteristic of the TGA experiments that were developed for this Thesis is that they were non-isothermal experiments, i.e. devolatilization of one sample under non-constant temperature situations. Therefore, the kinetic models specific to non-isothermal studies will be discussed in this section. In addition, all tests are carried out under constant pressure circumstances to ensure reproducibility.

Throughout the process of the TGA tests, the temperature increases and the mass loss of one sample were reported under these non-isothermal terms at a constant pressure: these signals defined feedstock breakdown. The signals obtained from the TGA were used by various kinetic models for the achievement of kinetic parameters, as it is described later in the current research. A successful simulation of the TGA signals was followed by this process. The basis for the application of the particular kinetic models was developed by specifying the thermal breakdown of the raw material for non-isothermal experiments, as will be discussed in this section. α

The rate of decomposition in non-isothermal decomposition tests done under constant pressure is determined by the temperature, T, and the degree of conversion of the breaking down of organic matter. The degree of conversion, may be calculated using mass loss experiments and is defined as follows:

$$\alpha = \frac{m_i - m_t}{m_i - m_f} \quad (1)$$

Where m_i is the initial sample weight, m_t is the weight of the sample at any time t and at temperature T, m_f is the weight of the sample at the end of the pyrolysis reaction.

Thermal kinetic studying the process initiated by a change in temperature. The reaction rate for these processes, without dependency on the pressure, is often defined as:

$$\frac{d\alpha}{dt} = k(T).f(\alpha) \quad (2)$$

Where $\frac{d\alpha}{dt}$ is rate of mass loss conversion, α is the mass loss conversion, k is the constant of the reaction rate, T is function of temperature, t is the time, the $f(\alpha)$ is described as reaction mechanism function. Eq 1 describes the rate of a single step process. Depending of the process tested, a fraction of the overall mass lost, or a fraction of the total heat consumed or emitted in the process will be measured. No matter what fraction α signifies, it still rises from 0 to 1 as the process proceeds [76]. Although the rate of

decomposition during thermal analysis of complex structures represents the total transition of the reactant to the component, the rate of constant obtained for a process found to implement a single step equation is unlikely to represent a single step process [82].

The Arrhenius equation is used almost without exception to explain temperature dependency of the phase of thermal decomposition

$$k = A.exp^{-\frac{E_\alpha}{R.T}} \quad (3)$$

Where A defined as pre-exponential Factor (1/min), Eα is activation energy of the pyrolysis degradation reaction kJ/mol, where, R is the gas constant (8.314 kJ/mol. K) and T is the absolute temperature.

In addition, the activation energy, E, is defined as the lowest possible energy needed to enable molecules and atoms to a state where they are capable of undergoing a chemical reaction; thus, it is the amount of energy that is necessary at least so that the reaction can begin. With respect to the pre-exponential or frequency component, this implies the frequency at which the input compound molecules collide with each other [83,84]. While it is commonly defined as a temperature-independent parameter, it is influenced by temperature as it defines the frequency of molecular collisions, and this frequency depends on temperature. The Arrhenius equation (3) is used almost without exception to explain temperature dependency of the phase of thermal decomposition [82]. Although the process studied is limited by the reaction rate, the quantities measured reflect the sum of all ongoing reactions, and likely not the rate of a single elementary reaction step. In the thermal analytics community, there is currently a robust debate as to whether or not the Arrhenius expression can be used as a temperature feature in solid state reactions [74].

The temperature-dependent rate constant is the product of the total of the independently named major cracking constants of oil, char, and volatiles, which are k1, k2, and k3, respectively, when the process is thought to follow the pattern of a first-order reaction.

$$k(T) = k_1 + k_2 + k_3 \quad (4)$$

Thus, considering the definition provided by Equation 2, Equation 3 stays as:

$$\frac{d\alpha}{dt} = A.exp^{-\frac{E_\alpha}{R.T}}.f(\alpha) \quad (5)$$

At the same time, mass loss conversion rate can be written as follows

$$\frac{d\alpha}{dT} = \frac{d\alpha}{dt}\frac{dt}{dT} \quad (6)$$

where the term dT/dt indicates to the value of the heating rate.

For non-isothermal experiments performed under non-constant heating rate conditions, and thus where the magnitude of the heating rate changes as a function of time, Equation 5 cannot be simplified; but in the case of non-isothermal studies with linear, constant heating rate, as developed for this thesis by the TGA experiments, it is entirely possible to rewrite the expression as following.

$$\beta = \frac{dT}{dt} \quad (7)$$

Thus, Equation (6) can be written as:

$$\frac{d\alpha}{dT} = \frac{d\alpha}{dt}.\frac{1}{\beta} \quad (8)$$

Therefore, by applying this Equation (8), the decomposition rate equation can be expressed as function of temperature [84]:

$$\frac{d\alpha}{dt} = \frac{A}{\beta}.exp^{-\frac{E_\alpha}{R.T}}.f(\alpha) \quad (9)$$

Equation 9 is the equation used to explain the feedstock's thermal decomposition for non-isothermal TGA experiments with a constant heating rate, written according to the reaction process, f(α).

This Equation 9 describes the due to the differences of the non-isothermal rate equation, which is the expression usually used to measure the sample kinetic parameters. The rate of biomass decomposition at a certain temperature is dependent upon the degree of conversion at that temperature.

As a result, while working on the formation of the kinetic analysis of the thermal degradation phase of the samples measured in this study, the kinetic parameters provided in Equation 9 were checked for the specific case of each of the samples undergoing the

non-isothermal degradation experiments. As a result, while introducing the selected kinetic model, the purpose of this kinetic modeling approach was to identify the values of the pre-exponential component, A, and activation energy, E. Nonetheless, the reaction processes had to be thoroughly reviewed and specified before the calculations could begin, so that the conversion function f() could be replaced in Equation 9. Aside from the parameters and coefficients given, it may also be necessary to measure the values of certain additional unknown variables, depending on the reaction mechanism and kinetic model that was chosen. In the next part, all of this will be thoroughly examined [19].

5.2.2. Isoconversional methods

The calculation of the activation energy, E, is obtained using isoconversional methods independent of the reaction mechanism. No inference was therefore required for the reaction process since this will not be part of the computations. These isoconversional methods were commonly used to explain the thermal degradable processes in solid state. While the thermal behavior of the samples is not completely modelled, the importance estimation of the activation energy represents an essential step to research the thermal conduct of the different species, although consideration of the reaction mechanism is not required. This part explains the basis of these methods and the basis for their use.

The methods used in isoconversional can be separated into differential and integral methods. The Friedman method is a differential method established in 1964 [76]. It is called differential because it analyzed the rate expression in its differential form. The fundamental equation of Friedman's differential system is conveniently obtained by taking the logarithm of Eq 10. as following

$$\ln\left(\frac{d\alpha}{dt}\right) = \ln\big(Af(\alpha)\big) - \frac{E}{RT} \tag{10}$$

This approach is very easy to use and it is the process of isoconversional based on the lowest number of assumptions [82,85]. A often stated drawback with the Friedman approach is the need to separate the results, i.e. to approximate the $\frac{d\alpha}{dt}$ derivative, which may lead to large noise levels in the case of TGA results [82]. To avoid this problem integral methods can be used for this purpose. The first integral methods were the Ozawa method [14], introduced in 1965, and the Flynn and Wall methods [86] introduced in 1966. Integral methods are based on the integral form of the equation of rates.

In non-isothermal applications, establishing a set of temperatures that result in a specified conversion rate for diverse heating rates is critical. This is in keeping with the process's name: isoconversional suggests that different experimental sites with the same degree of conversion should be taken into account. The temperatures required to produce these experimental points with an equivalent, constant conversion rate are calculated for only a few different heating rates: Tf(β), where "f" refers to the fixed conversion rate. As a result, Tf(β) refers to the different temperatures at which a variety of identical conversion degree values may be attained throughout the conversion process [85,87].

Following the first stage, there are two distinct approaches to dealing with the modeling difficulty for non-isothermal studies using isoconversional methods:

1.) *By estimating the temperature in the integral* [64]

One approach is to consider the integration of Equation (5) and to add an approximation to solve the integral temperature that is obtained; for this, a set of Tf(β) temperatures is only necessary. The equations KAS and the FWO will be studied amongst the equivalences and models which follow this trend to obtain the thermogravimetric parameters.

2.) *Without mathematical method for resolving the temperature integral* [64]

There is no integrated approach to this alternative. It contains of defining the different breakdown at the fixed value of conversion's degree α. With respect to this form of isoconversional modeling, the Friedman approach will be clarified.

Each unique, regarded value of the conversion's degree is given a different value of the activation energy utilizing these isoconversional procedures. It can be determined whether it is suitable to find a single-phase reaction with a single, overall average of the activation energy or if the degradation process can be separated into various regions with respect to two various targets of activation energy by analyzing the differences between the obtained values of the activation energy. A brief overview of these multiple forms of solving the issue of modeling by applying isoconversional methods will be presented.

5.2.2.1. By resembling the temperature integral

This method is based on integrating Equation (5) by separating the variables in the following way: [85]

$$g(\alpha) = \int_0^{\alpha} \frac{d\alpha}{f(\alpha)} = \frac{A}{\beta}\int_{T_0}^{T_f} \exp\left(\frac{-E}{R.T}\right) dT = \frac{AE_\alpha}{\beta R}\, P\left(\frac{E}{RT}\right) = \frac{AE_\alpha}{\beta R}\, P(x) \qquad (12)$$

The integral version of the equation (5) with variable separation is represented by the function $g(\alpha)$. The sublimit of the temperature integral, T_0, has been estimated to zero on the right side of the equation since the decomposition processes at temperatures just below atmospheric temperature are relatively low, and so this estimation is totally authorized.

The function represents the integral form of the equation (5) with the separation of variables. As far as the right side of the equation is concerned, the sublimit of temperature integral, T_0, has been approximated to zero as the decomposition reactions at temperatures just under the ambient temperature are quite low and therefore this approximation is fully permitted.

The procedure used for the estimation required to solve the integral temperature of the equation (12) should allow a difference between the different methods based on this approach.

Both the different methods that implement this approach of resolution the problem of modeling include a plotting procedure, where the following is represented: 1 / T_f is plotted against a logarithmic equation, which will vary based on the particular system used and which will depend on the value of the rate of heating and, in some situations, will also base on the temperature. The form that this logarithmic function would take depends on the method used to estimate the defined temperature integral.

As there are several different means of mathematically approximating the integral temperature, there is also a wide variety of different approaches for extracting activation energy using this strategy.

Now the findings obtained from two separate approaches to temperature integral resolution will be addressed and their reliability and accuracy will also be tested based on previous publications:

Kissinger-Akahira-Sunose (KAS) linear integral method

The KAS method is one of the commonly used iso-conversional method to find the activation energy [88], for constant mass loss conversion without specification of reaction

of mechanism [89]. The KAS method followed by replacement of the integrant by an empirical approximation function (Eq. (8)) and this treatment has led to establishment of the following equation,

$$\log P(x) \cong \frac{e^{-x}}{x^2};\ \text{for}\ 20 \leq x \leq 50 \tag{13}$$

$$ln\left(\frac{\beta}{T^2}\right) = ln\left(\frac{AE_\alpha}{Rg(\alpha)}\right) - \frac{E_\alpha}{RT} \tag{14}$$

Under the iso-conversional assumption the function g(α) reaches a given value thus a constant. Therefore, activation energy Eα can be calculated from the slope of the plot of $ln\left(\frac{\beta}{T^2}\right)$ against 1/Tα, the result will be a straight line with a slope $\frac{E_\alpha}{RT}$ and intercept $ln\left(\frac{AE_\alpha}{Rg(\alpha)}\right)$.

Flynn-Wall-Ozawa linear integral method

The FWO method is another commonly used iso-conversional method to find the activation energy [88], Flynn, Wall and Ozawa tried to rewrite Eq. (7) in an integral form, followed by a replacement of the integrant by Doyle's approximation function (Eq.(10)). This replacement has led to the following equation.

$$\log P(x) \cong\ -2.315 - 0.4567x;\ \ \text{for}\ 20 \leq x \leq 60 \tag{15}$$

$$\ln(\beta) = \ln\left(\frac{AE_\alpha}{Rg(\alpha)}\right) - 2.315 - 0.4567\left(\frac{E_\alpha}{RT}\right) \tag{16}$$

Since g(α) has a constant value, the activation energy can be calculated from the slope of the plot of $\ln(\beta)$ against 1/Tα, the result will be a straight line with a slope -0.4567 $\frac{E_\alpha}{RT}$ and intercept $ln\left(\frac{AE_\alpha}{Rg(\alpha)}\right)$.

5.2.2.2. Without mathematical approach for solving the temperature integral

In the case of isoconversional techniques, which do not employ a mathematical approach or approximation to compute the integral temperature, data on Tf, i.e. the temperature value at a certain heating rate at which an equivalent, fixed conversion degree is obtained, is still required. The value of the conversion rate at Tf temperature is also significant [90].

Among the approaches that are based on this method, the Friedman method will be presented here

Friedman differential method

According to Cai, J et al 2018, the most widely used method is Friedman Method because of its accuracy and simplify [91], the FR method developed by taking logarithms for Eq. (5). Which leads to the equation below.

$$ln\left[\left(\frac{d\alpha}{dt}\right)_{\alpha,i}\right] = \ln[A_\alpha f(\alpha)] - \frac{E}{RT_f} \quad (17)$$

To apply this Friedman method, a series of experiments should be performed by concerning different linear heating rates, β; for such experiments, it should be possible to record the times when a certain conversion degree is accomplished for the various heating rates and temperatures, T_f, at which that conversion degree is achieved. As the conversion function f(α) depends only on the conversion rate, this is constant at all experimental stages.

Under the isoconversional hypothesis, the function f(α) reaches a given value when α is a constant. Consequently, the plot of ln(dα/d*t*) against $1/T_f$ results in a straight line with slope $-E_\alpha/R$ and intercept $\ln[A_\alpha f(\alpha)]$.

Nonetheless, it is normally much desirable to use the equation as a function of the conversion degree temperature derivative, defined by Equation (9), rather than using the conversion degree time derivative. Therefore, in most cases the following variation from Equation (17) will be used, resulting in an expression dependent on the heating rate:

$$ln\left[\beta\left(\frac{d\alpha}{dt}\right)_{\alpha,i}\right] = \ln[A_\alpha f(\alpha)] - \frac{E}{RT_f} \quad (18)$$

When using Equation (18), the plot in this issue will be $1/T_f$ against ln(βdα/dt), therefore, The values of the activation energy, E, will be defined from the slope of the taken axes, without having to presume some kind of reaction process for determining f(α). As previously stated, the method has no reliance on the reaction mechanism.

5.2.3. Thermodynamic Parameters

The thermodynamic parameters, including A, ΔH, ΔG, and ΔS, indicate the pyrolysis behavior of the feedstock.

5.2.3.1. Pre-exponential factor (A, 1/s)

The A-value is the number of collisions per unit of time, which obtains the correct direction for the reaction to take place. A-values elucidate the reaction chemistry that is crucial to the efficiency of the pyrolysis cycle. A values are important for the optimization of pyrolytic sludge [92]. High pre-exponential value means that more energy is necessary to be moved to a higher molecular collision and is adjacent to the activation energy needed. With small A values (≤109) it can be stated that there is a constraint of particle rotation of the activated complex relative to the original reagent and that there is a broad surface reaction. Therefore, the intensity is expected to increase by its size and hence the contact with the adjacent molecule will become more powerful. In the meantime, the value of A of the order of ≥109 showed there is no change in the rotation of the active complex and the mixture in the pyrolysis reaction is calculated by a simplified reaction [93].

Pre-exponential factor (A) can be estimated as following

$$A = \beta E_\alpha exp\left(\frac{E_\alpha}{RT_p}\right)/RT_p^2 \tag{19}$$

5.2.3.2. Enthalpy Change (ΔH, kJ/mol)

The enthalpy change defines the changes in enthalpy detected in a thermodynamic system's constituents when a chemical or transformation reaction occurs. This is the difference between enthalpy after completion of the process, i.e. the product enthalpy, and the initial system enthalpy, namely the reactants. The change in enthalpy (ΔH) is an essential thermodynamic factor. For pyrolysis, ΔH implies the energy consumed in the reaction when sludge is transformed into gas, char, and oil [93]. It can be found as following equation.

$$\Delta H = E_\alpha - RT \tag{20}$$

5.2.3.3. Gibbs free energy (ΔG, kJ/mol)

Gibbs's energy change is using to determine the spontaneity of the process. Moreover, ΔG, exhibits the amount of available energy from biomass upon pyrolysis. It can be expressed as the follow.

$$\Delta G = E_\alpha + RT_p ln\frac{K_B T_p}{hA} \tag{21}$$

Where K_B is Boltzmana constant (1.381×10^{-23}J/K) , h is planck constant and (6.626×10^{-34} J.s) and T_p is the peak temperature.

5.2.3.4. Gibbs free energy (ΔG, kJ/mol)

Entropy change, ΔS, is a function of the state, and a measure of disorder or randomness. Also, ΔS, a direct expression of the system 's degree of disturbance, elucidates the system 's approach to its thermodynamic equilibrium in reaction to various circumstances. It can be calculated by the following equation.

$$\Delta S = \frac{\Delta H - \Delta G}{T_p} \quad (22)$$

5.2.4. Effect of heating rates on decomposition process of biomass

The information on the effect of the heating rate is important because it affects the conversion, product delivery and provides an understanding of the reactor to be used [99]. They found that the increase in heating rates shifts the peak temperature to higher value. The change in behavior is due to poor heat transfer and change in the reaction mechanism. Lower heating rates were generally preferred as heating of biomass particles occurs constantly, and it provides better heat transfer to the inner part of the biomass. Increasing the heating rate releases more volatile materials and less residues were left after the pyrolysis.

Zhang X et al investigated the impact of heating rate on pyrolysis of siderite at different heating rates and they concluded that as the heating rate increased from 5 to 30 °C/min, the start and end pyrolysis temperatures and temperate where maximum weight loss rate happened increased where the maximum weight loss rate increased, while the total weight loss was fundamentally the same. Every heating rate within a specified range was in favor of reducing the time of each reaction step, so with a short period the optimum conversion rate could be achieved. Moreover, the related activation energies and pre-exponential factors increased with rising heating rate from 446.13 to 505.19 kJ / mol, and from 6.67 1018 to 2.40 1021, respectively [100].

Viet D Q et al studied the thermal decomposition of farming residue such as rise corn cob (CC), husk (RH) and sugarcane bagasse (SG) in inert atmosphere by TGA. Parameters of the reaction kinetics of biomass pyrolysis were calculated using FWO method. It’s found that the activation energy of rice husk, corn cob and sugarcane bagasse where 157.17, 194.43 and 171.56 kJ/mol, respectively. They found that the weight loss

increased with increasing heating rate. The phenomenon associated with this important change could be explained by the fact that biomass possessed a heterogeneous structure and several constituents. Those constituents in the pyrolysis process gave their characteristic weight loss range for individual decomposition. During pyrolysis, when heating rate was low enough, most of these temperature ranges could be small broken lines or vibrations. However, separate peaks did not occur at high heating rates because some of them were simultaneously decomposed and several sequential temperature ranges were united to form overlapped, broader and higher peaks [101].

5.2.5. Effect of Catalyst on Kinetic Analysis and Decomposition of Different Type of Biomass

Ouyang W et al studied the pyrolytic properties and kinetics of corn straw using a thermogravimetric analyzer under a nitrogen atmosphere from ambient temperature to 900 °C at four different heating rates ranged from 10 °C min−1 till 40 by adding10 °C min−1 each step. Moreover, authors studied the mass loss and weight loss curve rate results from corn straw biochar pyrolysis and biochar with the addition of 5 % (wt.%) ammonium dihydrogen phosphate (ADP) catalyst. in addition, three different isoconversionel method the FWO, modified CRM and KAS free method and Kissinger method were used to calculate the activation energies and pre-exponential factors of the pyrolysis process. It was concluded that three stages occurred in the pyrolysis process of corn straw, initial stage was in temperature range 25-220 °C due to evaporation of moisture content. Second stage ranged between 220-600 °C, the main pyrolysis reaction occurred in this stage decomposition of hemicellulose cellulose and lignin was observed in this stage. Moreover, the observed peak in the final stage was due to repolymerized and the converting of levoglucosan into tar. The pyrolysis process was finished in this stage. Also, it's shown that the catalytic pyrolysis process was predominantly characterized by water removal including free water and mixed water, hemicellulose, cellulose and lignin decomposition, and carbonization [102]. The authors found that that the ADP had a catalytic impact on the biomass pyrolysis activity and was able to reduce the biomass pyrolysis activation energy. The catalyst will also boost the pyrolysis reaction and has tremendous potential to increase the performance of crop residue treatment [102].

Gan D K W et al used thermogravimetric analysis to investigate the thermodynamic and kinetic characteristics of rice husk (RH) catalytic pyrolysis utilizing two distinct

catalysts, namely eggshells (ES) and natural limestone (LS), at varied heating rates of 10-100 K/min and temperatures ranging from 323 to 1173 K. Two free kinetic iso-conversional models, FWO and multi-step reaction model (Distributed Activation Energy Model), were utilized for this aim. They discovered that using a catalyst during biomass pyrolysis improved the conversion of oxygenated molecules into simple hydrocarbons through dehydration (H2O), decarboxylation (CO2), and decarbonylation (CO), as well as depolymerization processes. Additionally, adding these catalysts to RH pyrolysis boosted the secondary reaction rate, where RH molecules diffused on the porous structure of catalysts, removing tar and increasing product gas output. In addition, the DTG curves show that RH's catalytic pyrolysis has a lower average rate of deterioration. Reducing the maximum rate of degradation has a significant impact on the energy consumption of the pyrolysis process. The average activation energy was determined to be between 175.4 and 177.7 kJ mol1 for RH, 123.3–132.5 kJ mol1 for RH-LS, and 96.1–100.4 kJ mol1 for RH-ES. As a consequence, the major finding was that centrifuged eggshell (ES) had a greater catalytic impact than regular limestone (LS) in terms of boosting syngas production and lowering activation energy value [18].

TGA was used to investigate the kinetics of catalytic pyrolysis of chlorella vulgaris by Fong M J B et al. The catalysts were limestone (LS), HZSM-5 zeolite, and bifunctional HZSM-5 / LS, and the samples were heated at a rate of 10-100 °C/min from 50 °C to 900 °C. The kinetic parameter was determined using three distinct iso-conversional Model free methods: FWO, KAS, Starink, and Vyazovkin (Activation energy). The thermodynamic parameters were assessed using the FWO and KAS techniques. The Ea values for non-catalytic and catalytic pyrolysis of HZSM-5 zeolite, LS, and bifunctional HZSM-5 / LS were calculated to be 156,16–158,10 kJ / mol, 145,26–147,84 kJ / mol, 138,81–142,06 kJ / mol, and 133,26 kJ / mol. In comparison to HZSM-5 and LS, catalytic pyrolysis with the presence of bifunctional HZSM-5 / LS resulted in lower average Ea and H, resulting in decreased energy consumption requirement. In reality, microalgae degradation was seen throughout the pyrolysis and catalytic pyrolysis processes, which were split into three key phases of volatilization. The first stage occurred between ambient temperature and 180 °C, with minor mass loss owing to dehydration of moisture. Furthermore, the second stage began at 180 degrees and finished at 550 degrees. The degradation of protein, carbohydrate, and fats resulted in a considerable mass loss at this stage. The third stage occurred between 550 and 900 degrees Celsius, with minimal mass

loss owing to the breakdown of carbonaceous components contained in the solid leftovers. Furthermore, the highest degradation peak of the DTG of catalytic pyrolysis was determined to be lower than the one without the catalyst.

6. ACTIVATED CARBON

Activated carbons also called activated charcoal are extremely microporous carbons with high internal surface area and porosity that are commercially used as an adsorbent to remove organic and inorganic contaminants from air and water sources. Any inexpensive material with a high carbon content and low inorganics can be used to produce activated carbon [103].

Activated carbon consumption will benefit from the global environmental movement's further intensity as well as rising industrialisation. The usage of AC in the pharmaceutical industry has the best development prospects in most emerging and established nations. Furthermore, environmental concerns in emerging nations will drive additional development in water treatment applications, which are currently the biggest single market in industrialized countries. Apart from the need for safe drinking water, government environmental restrictions that differ by location have a considerable influence on the need for air conditioning in this industry.

Activated Carbon's properties such as surface area, pore volume, and pore size distribution are the cause of their high adsorption capacities. These distinct characteristics are determined by the raw materials used in the preparation of AC as well as the method of activation. Literature survey indicates that there have been many studies to obtain low-cost activated carbons from different agricultural wastes and biomass such as rice husk [104], coconut shells [105], hazelnut shells [106], walnut shells [107], spent mushroom compost [108], corn cob [109] and others.

Due to the increasing demand for air conditioning, it is critical to find creative precursors for the manufacture of air conditioning that are both cost-effective and equivalent to commercially available air conditioning. Since sewage sludge is a renewable, carbon-rich, and abundant resource that can be achieved at low cost, an alternative use of sludge is to produce activated carbon (AC), which are used to eliminate a broad variety of pollutants from air and water. Sludge has been shown to generate high-quality carbons for adsorption of metals, phenols and dyes in water [110]. Making AC from sludge has the possibility to be a cost-effective solution for waste treatment and low-cost adsorbent processing. In particular, the cost of production of sludge-based biomass, which depends on factors such as the supply of sludge and the necessary refining,

including energy costs for pyrolysis and drying, has the potential to be equal to or even lower than the cost of production of commercial ACs [8].

6.1. Thermal Decomposition Kinetics and Definition of Main Parameters

Carbonization and activation are the two reactive phases in the production of AC. Carbonization and activation may be done in one or two steps, depending on the manufacturer's desire and equipment availability. AC may be made from of a variety of raw materials, including sludge, agricultural wastes, and garbage. The majority of the carbon-rich precursors utilized in the production of activated carbon are carbon-rich raw material [111]. Physical activation, chemical activation, and a combination of both were the most common methods for producing AC.

Physical activation starts with the carbonization of the raw material. Then, the activation takes place at high temperatures (between 800 and 1100 °C) in the presence of oxidizing gases such as carbon dioxide or steam [8]. whereas Chemical activation mechanisms are mature and include the use of alkaline metals, acids, and salts, e.g., KOH, NaOH, H_3PO_4, H_2SO_4, $ZnCl_2$ and $CaCl_2$. Moreover, chemical activation induces the interaction of swelling, dehydration and condensation of aromaticity compound with carbon, creating a large number of uniform mesoporous structure and high-specific activated carbon surfaces [112].

In most cases, activated carbon is made by heating the raw material in a way that doesn't use oxygen. The carbonized product is then activated [113]. On the other hand, chemical activation is better than physical activation because it allows for better porous structures to be formed in a single process at lower temperatures than physical activation does.

6.1.1. Physical Activation

The process of physical activation is two-fold. Carbonization of the raw material is followed by activation at high temperatures in the presence of oxidative greenhouse gases such as carbon, steam, air, or combinations of these gases. Carbonization temperatures vary from 400 to 800 degrees Celsius, whereas activation temperatures range from 800 to 1100 degrees Celsius. CO2 is often employed as an activation gas because it is clean, simple to handle, and the slow reaction rate at high temperatures allows for better control of the activation process.

On the other hand, chemical activation is better than physical activation because it allows for better porous structures to be formed in a single process at lower temperatures than physical activation does. Chemical activation may be chosen as the preferred activation mechanism because it is completed in a single step and results in higher yields and well-developed microporosity. Furthermore, activated carbons can be generated at lower temperatures than those used in physical activation in many cases. By affecting the overall process's operating costs, this results in a significant reduction in energy costs in manufacturing.

6.1.2. Chemical Activation

Chemical activation of activated carbon is a one-step process that involves both carbonization and activation at the same time. The precursor is first combined with a chemical activating agent, which serves as a dehydrating and oxidizing agent. The most used chemical activating agents are KOH, NaOH, H_3PO_4, H_2SO_4, $ZnCl_2$ and $CaCl_2$ etc...

Chemical activation has many benefits over physical activation, the most notable of which are:

i- The physical activation temperature (800 – 1100 °C) required higher activation temperature compared to the chemical activation (< 800 °C)
ii- Single stimulation step
iii- Larger harvests
iv- Better porous characteristics, and Shorter activation times

Chemical activation, on the other hand, has a cost disadvantage because of the washing processes required to separate and recover the leftover activating chemical after the reaction. In addition, for each chemical employed in the production process, unique materials are required to create the reactor. Because KOH is a powerful oxidizing agent, a reactor composed of stainless steel or quartz would be inappropriate owing to the corrosive chemical's attack. Physical activation is a more attractive manufacturing technique than chemical activation because of the cleaner activation process and reduced plant maintenance expenses.

6.2. Physical Properties of Activated Carbon

Adsorption is used to separate and purify a variety of substances using activated carbons. Adsorption is the aggregation of substances at a solid's interface. Because of the

forces involved in the adsorption process, the concentration of a material at the interface between a fluid and a solid appears to be higher than the concentration in the fluid. The adsorption mechanism may be either physical or chemical, and depending on the existence of the surface forces, the terms physical and chemical adsorption can be called physisorption and chemisorption, respectively [114].

The enormous surface area of activated carbon distinguishes it from other sorbents, making it distinctive, helpful, and popular. The large surface area is due to the microporous structure, and the spaces between the crystallites are what make this microporous structure possible. An activated carbon's interior surface area ranges from 250 to 2500 m2/g. Some activated carbons having a surface area more than 2500 m2/g may be suitable for particular applications requiring a large amount of accessible surface area.

Pore characteristics such as surface area, pore size distribution, and pore depth, as well as chemical surface properties, are important factors to consider when evaluating the quality and application fields of the activated carbon. Their properties are influenced by the raw material, carbonization process, carbonization temperature, impregnation rate, and activation methods. Agricultural raw materials are superior to other precursors in the manufacture of activated carbon in terms of adsorptive properties. Low ash and high carbon content, including precursors, are also preferable to the alternatives.

6.3. Application of Activated Carbon

Activated carbon is used in hydrogen and methane storage, solvent recovery, air purification, gold purification, decaffeination, metal extraction, water purification, medicine, sewage treatment, air filters in respirators, filters in compressed air, teeth whitening, production of hydrogen chloride and many other applications.

Activated carbon is a versatile adsorbent with a wide range of applications, including the adsorptive removal of color, odor, flavor, and other unwanted organic and inorganic impurities from drinking water; industrial waste water treatment; air purification in the food manufacturing and chemical industries; purification of certain chemical, food, and pharmaceutical products; operate in hostile conditions respirators; and a variety of other gas-phase applications. Liquid phase applications account for over

80% of total activated carbon use, and both granular and granular activated carbons may be employed [103].

6.4. Literature Review of Activated Carbon

By using a KOH activation procedure through one-stage or two-stage co-pyrolysis, B. Yang et al. was able to create adsorbent material with outstanding performance attributes from waste biomass and sludge in two separate ways. Then, in terms of physicochemical attributes and adsorption capabilities for methylene blue, investigate the consequences of both strategies. They discovered that the two-stage activated carbon had a greater surface area than the one-stage activated carbon, which was better for methylene blue adsorption. In conclusion, two-stage co-pyrolysis increases activated carbon adsorption capacities, resulting in higher economic value from waste material [115].

In another work, T. L. Silva et al. produced activated carbon from industrial laundry sewage sludge using slow pyrolysis followed by physical activation CO2 and used it to remove the reactive dye Remazol Brillant Blue R from aqueous solutions. The scientists investigated the influence of activation temperatures of 750 °C, 800 °C, and 850 °C on surface area, and the findings were 159 m2/g, 156 m2/g, and 65 m2/g, respectively, with average pore diameters ranging from 4.56 to 5.88 nm [116].

Liang et al. produced a low cost activated carbon from coconut shell and municipal sludge via two-stage co-pyrolysis. A single factor experiment was used to optimize the variables of the synthetic process. Also, The Box-Behnken design (BBD) of response surface methodology (RSM) was used to further optimize the preparation conditions and interactions between variables. The authors found that the optimal activation temperature of sludge was 800 °C, with an activation time of 60 min, carbonization time of 45 min and impregnation concentration of 2.5 mol/L. Other wise when a %50 of cococunt shell was added to the system the optimal carbonization temperature decreased to be 500 °C, and the carbonization time 45 min with the same impregnation ratio. As a result The most important factor influencing the iodine value of AC was found to be the activation temperature [117].

Li et al. investigated the influence of various carbonization temperatures on porosity properties in carbonized coconut shell char and activated carbon generated from carbonized coconut shell char with varying activation durations. The results showed that

high temperature carbonized coconut shell char and activated carbon samples derived from high temperature carbonized coconut shell chars had higher BET surface area, total volume, micropore volume, and yield than low temperature carbonized coconut shell char and activated carbon samples derived from low temperature carbonized coconut shell chars [118]. Based on the data, we concluded that physical activation (steam activation) with optimum carbonization temperature and activation time choices might produce high surface area activated carbons from coconut shells [118].

In other study Katesa, Junpiromand, and Tangsathitkulchai investigated the effect of the carbonization temperature in the range from 250 to 750 °C on the properties of char and activated carbon from coconut shell. The results showed that the surface area, pore volume, and mean pore size of activated carbon decreased as the carbonization temperature increased, with activated carbon derived from char prepared at the lowest temperature of 250 °C having the highest surface area and pore volume of 1,056 cm2 /g and 0.533 cm3 /g, respectively. The majority of pores formed in activated carbon are micropores, accounting for 78-81 percent of total pore capacity [119].

Varil et al. investigated the impact of impregnation rate and activation temperature on the specific surface area, total carbon content, pore size distribution, and yield of peat-based activated carbon. The peat was impregnated with varying amounts of ZnCl2, and the impregnated peat was activated at various temperatures. The results revealed that a high impregnation ratio (1:2) and a high activation temperature increased the clear surface area and microporosity of the activated carbon of peat (1072 K). Most samples provided highly porous activated carbon with a specific surface area of about 1000 m2 /g and a total pore volume greater than 0.5 cm3 /g [120].

7. MATERIALS AND METHODS

This chapter explains the instruments used in the laboratory scale, and analytical methods used to obtain the findings described in this study.

7.1. Raw Material

The sludge sample used in this study was supplied from Leather and Textile Industry-Wastewater Treatment Plant, Uşak. The wet sludge content almost 70 wt% of water therefore the sample has dried at 110 ℃ for 15 days and then grounded into small particles to make particle size fraction of 0.6 mm < Dp < 0.85 mm. Figure 7.1 shows the sludge used in pyrolysis and activated carbon production processes

Figure 7.1. *Sludge Sample used in the experiments.*

7.1.1. Ultimate and proximate analyses

Table 7.1 shows the proximal, ultimate, ICP/MS analyses, and HHV data for sludge. The weight fractions of carbon, hydrogen, and nitrogen were determined using a Thermoscientific Flash Smart elemental analyzer, with the weight fraction of oxygen derived by difference. The Dulong formula was used to get the heating value. The EPA 6020A technique was used for the ICP/MS analysis of the sludge sample. The raw material has large concentrations of Al, Cr, Na, and other elements.

$$\text{Moisture (\%)} = (wt_1 - wt_2)/wt_2 \quad (23)$$

wt_1: weight of initial sample before drying test,

wt_2: weight of sample after drying test

To evaluate the ash content, a dried sludge sample weighing to the closest 0.1 mg was placed in the crucible (of known weight). The crucible was put in the muffle furnace at 650 °C, and searing was finished when consistent weight was reached. In a desiccator, the crucible is cooled to room temperature, and the percentage weight of the sample that remains is used to calculate the ash content. Fixed carbon is a monetary value that has been calculated.

$$\text{Ash (\%)} = (wt_1/wt_2) \times 100 \quad (24)$$

Thus.

wt_1= Weight of sample used, (g)

wt_2= Weight of sample after heating, (g)

The proportion of volatile matter (VM) in the sludge samples was calculated using the technique outlined below. A total of 1.0 g of the material was placed in a crucible with a lid (of known weight). For 7 minutes, the covered crucible was put in a muffle furnace set at 95020 °C. The covered crucible was then cooled to room temperature in a desiccator and the weight was measured. The proportion of volatile stuff was considered as the percentage of weight loss.

$$VM=[[(g1-g2) / g1] - ASH] \times 100 \quad (24)$$

g_1= Weight of sample used, (g)

g_2= Weight of sample after heating, (g)

and it is the resultant of summation of percentage moisture, ash, and volatile matter subtracted from 100.

$$\text{Fixed carbon (\%)} = 100 - (\text{moisture \%} + \text{ash \%} + \text{volatile matter \%}) \quad (25)$$

Al_2O_3 and y-zeolite was used as catalyst in the experiments. y-zeolite purchased from Zeolyst and it has the following properties: SiO_2/Al_2O_3 mole ratio= 5:1; nominal cation form: Hydrogen; Na_2O content= 2.8 wt%; Surface Area= 730 m^2/g.

Table 7.1. *Proximate, ultimate and ICP/MS analysis (wt%) of sludge*

Proximate analysis (%)		Ultimate analysis (%)		ICP/MS analysis (%)		HHV(MJ/kg)
Volatiles	43.1	C	46.49	Al	3.26	13.14
Fixed C	15.8	H	3.65	Cr	1.38	
Ash	32.3	N	6.25	Na	0.95	
Moisture	8.8	O	43.61	Mg	0.66	
				Ca	0.58	
				Fe	0.52	
				K	0.27	
				Sr	0.019	
				Ba	0.016	
				Mn	0.015	
				Zn	0.012	

7.1.2. TGA and kinetics analysis

Thermogravimetry (TG) or thermal gravimetric analysis (TGA) is a technique that measures the mass of a sample against time or temperature while varying the sample's temperature in a controlled environment. This test was performed to investigate the thermal reaction of sludge samples after being heated in nitrogen ambient under inert conditions. The research allows us to estimate the time it would take for sludge carbonization to be completed.

In this study, A thermogravimetric analyzer (Perkin Elmer Simultaneous Thermal Analyzer, STA 6000) coupled with differential thermal analyzer (DTA) was used. Sample's weigh was between 10 and 15 mg then was put in alumina crucible and heated from 30 ℃ to 800 ℃ under nitrogen ambience with a flow rate of 50 ml/min. Mixture of catalyst and sludge were prepared by mechanical mixing method, after mixing, the mixture has ground to obtain uniform sludge and catalyst samples. Figure 7.2 show the thermogravimetric analyzer (Perkin Elmer Simultaneous Thermal Analyzer, STA 6000) used in TGA experiments.

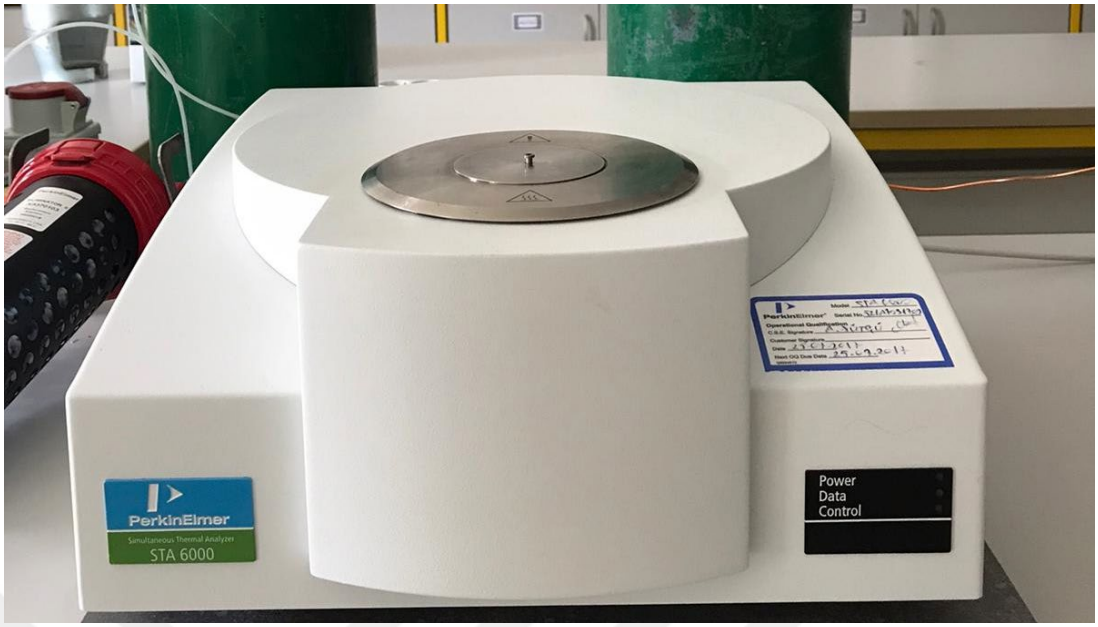

Figure 7.2. *Thermogravimetric analyzer (Perkin Elmer Simultaneous Thermal Analyzer, STA 6000)*

Three samples were prepared for these purposes: sludge without any additivity, with Al_2O_3 and with y-zeolite as catalysts. These three different samples were heated at four different heating rates 5, 10, 15 and 20 ℃/min. At least two repetitive were carried out to confirm the accuracy of the results.

7.1.3. TGA and kinetics analysis

Sludge pyrolysis was performed in a fixed bed, thin tube reactor in a nitrogen (N2) environment at a pyrolysis temperature of 500 °C and a heating rate of 500 °C/min. Nitrogen was added into the reactor from the top before each experiment began. An automated temperature controller was used to regulate the temperature. A steel wool is used to fix 3 g of sludge sample and catalysts (10 wt percent), a thermocouple is placed into the reactor from the top, and flanges are fixed at the top and bottom of the reactor for closing. In this research, two designs were used: catalytic and non-catalytic models. Steel wool was inserted to a height of 20 cm from the bottom of the reactor using an iron rod for the non-catalytic model studies, with biomass placed above it. Two different catalyst beds were constructed in the catalytic model to catalyze the volatiles. The reactor was then loaded with steel wool, catalyst, steel wool, catalyst, steel wool, and biomass, in that order. The reactor was filled with 3 g of sludge, 0.6 g of steel wool, and 0.3 g of catalyst. Figure 7.3 shows the fixed bed reactor scheme.

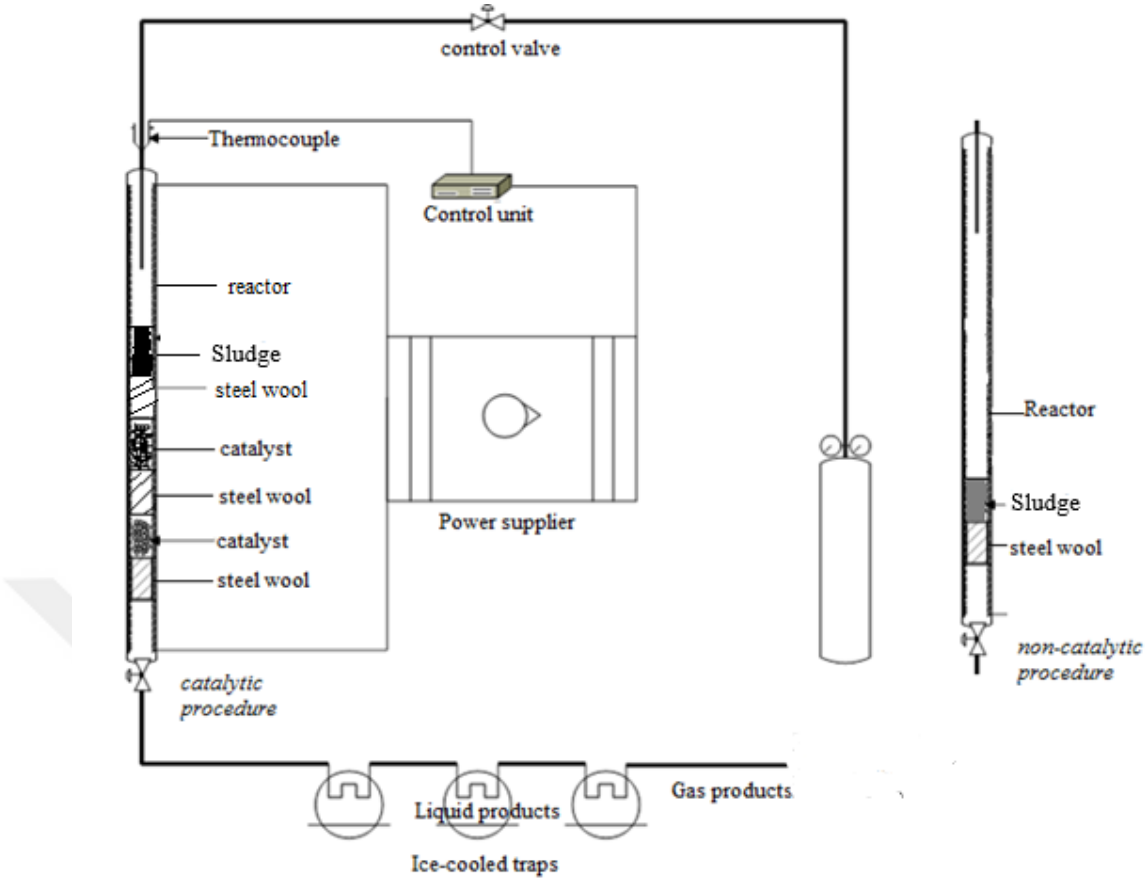

Figure 7.3. *Fixed Bed Reactor Scheme*

The reactor system is retained in place for 60 seconds after reaching the required temperature. The carrier gas was used to transfer the reactor's non-condensable and condensable products. Condensable volatiles were recovered by dichloromethane (DCM) washing after being chilled and condensed using ice-cooled traps; the aqueous were separated from the oil using a separating funnel. A rotary evaporator was used to remove DCM, and the residual bio-oil was weighed. The tubular reactor's solid residue was collected and weighed as char product. The difference was used to calculate the gas product. More details on the reactor may be found in the prior paper [121].

All the product's yields were calculated on a dry basis and ash free basis additionally at least two repetitive were carried out to confirm the accuracy of the results for each experiment therefore each experimental condition and reproducibility of the experiment data was calculated to be within ±2 %.

7.2. Preparation of Activated Carbon

Preparing activated carbon from sludge can be divided into two stages, activation stage, and carbonization stage. ZnCl2 was used as an activating agent in this study. Distilled water was combined with a known quantity of activating agent. impregnation ratio defined as the mass ratio of dried sludge to activating agent, in this study sludge was impregnated in two different ration 1:1 and 1:2. The impregnated samples were dried in an oven for 24 h at 110 °C to remove the residual water. Then 14 g of the impregnated sample was used for carbonization. Carbonization process was carried out at 10 °C/min heating rate and 100 ml/min nitrogen flow rate at different carbonization temperatures (400 °C, 450 °C, 500 °C, 550 °C and 600 °C) for 1 hour in a fixed bed reactor (Figure 7.4). The produced activated carbons were kept in hot deionized water overnight and then washed with hot ultrapure water; the washing process has been carried out until the pH achieved the value of the used water. Then the obtained wet activated carbon was dried in an oven at 110 °C ± 2 to constant weight then removed from the oven and cooled to room temperature. The obtained activated carbons were stored in a sealed box at room temperature.

Figure 7.4. *(a) Experimental setup for carbonization, (b) Carbonization Reactor.*

7.3. Oil Analysis

The oil products that were shown in figure 7.5 were analyzed by GC / MS using a Hewlett – Packard HP 7890 gas chromatograph coupled with an HP 5975 quadruple detector. 30 m×0.25 mm

Figure 7.5. *Oil product*

temperature was 45 °C, which was maintained for 2 minutes before being regulated from 45 to 290 °C at 5 °C/min with an isothermal hold for 10 minutes. At 290 C, a splitless injection was given. The temperatures of the ion source and the transfer line were 230 and 300 °C, respectively. Data was collected in full-scan mode between m/z 33–533, with a solvent delay of 3 minutes.

Figure 7.6. *GC-MS for Oil Analysis*

When available, chromatographic peaks were detected using the WILEY mass spectral data database, and retention durations were calculated using the standard substance. Peak percentages were determined using the TIC's peak area (total ion chromatography). The oil extracted from the traps was diluted in DCM before being tested by GC/MS. Oils were injected into the vials, which were then placed in the autoinjector port, which had a capacity of 8 vials. Figure 7.6 depicts GC/MS analysis using a Hewlett-Packard HP 7890 gas chromatograph.

8. RESULTS AND DISCUSSION

8.1. Thermal Decomposition of the Sludge at Different Heating Rates

Thermal decomposition behaviour of sludge under N_2 atmosphere from ambient temperature to 800 °C was investigated at heating rates of 5, 10, 15 and 20°C/min. The resulting TG and DTG thermographs are shown in Figures 8.1 (a) and 8.1 (b) respectively and indicate that the thermal decomposition of the sludge could be classified in three main stages; dehydration (Stage 1), degradation of volatiles (Stage 2) and decomposition of carbonaceous materials (Stage 3).

The weight loss during the pyrolysis of sludge in Stage 1 was mainly due to the moisture content of the sludge and observed between the ambient temperature and 180.29 °C when the heating rate was 5°C/min. The organic constituents of the sludge such as proteins, lipids and carbohydrates started to degrade in Stage 2, taking place between the temperatures of 180.29 and 516.66°C. Two major peaks were detected in the DTG curve as one at 306.55°C representing the degradation of proteins and carbohydrates, and at 444.03°C showing the decomposition of lipids [66]. The total weight loss observed in the Stage 2 was 50.84 wt.% at the same heating rate. When the temperature exceeded 516.66°C, the decomposition of carbonaceous materials started, and the weight loss occurred at the last Stage was 6.99 wt.%. The total weight loss during the thermogravimetric analysis of the sludge was determined as 69.72 wt.% at 5°C/min heating rate. The initial and final temperatures (T_i and T_f) together with peak temperatures (T_{m1} and T_{m2}) and mass losses for pyrolysis of sludge at different heating rates were summarized in Table 8.1.

The total weight loss during the pyrolysis of the sludge did not vary noticeably with the changing heating rates and remained in the range of 69.72 to 66.54wt.%. Similarly, the mass loss in each Stage were close to each other as they are shown in Table 8.1. However, the maximum degradation rates dramatically increased with the increasing heating rate such as in Stage 2, it was 1.290 at 5°C/min heating rate and became 5.196 at 20°C/min heating rate. The maximum degradation rate is one of the important parameters for the energy analysis of pyrolysis since lowering its value means decreasing the energy input for pyrolysis process [122]. Hence, increasing the heating rate would increase the energy demand of the pyrolysis process for sludge degradation. In addition, increasing heating rates shifted the boundaries of the Stages to higher temperatures as well as the

peak temperatures. Similar effects were reported in the studies with sludge and compost of sludge during pyrolysis at different heating rates [123,124].

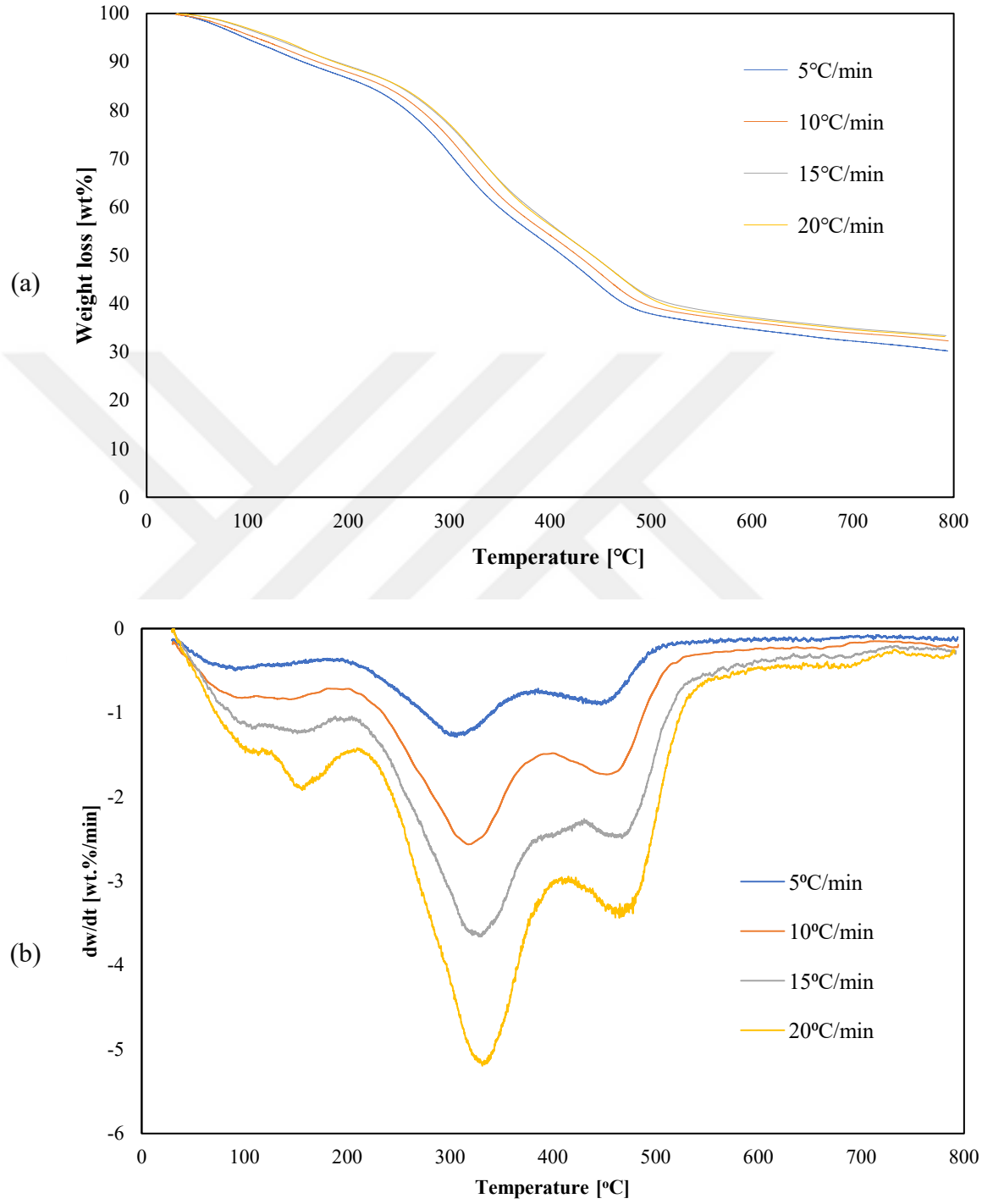

Figure 8.1. *(a) TG curves and (b) DTG thermographs for sludge pyrolysis at various heating rates*

Table 8.1. *Initial, final and peak temperatures, weight loss and -DTG values during non-catalytical pyrolysis of sludge at various heating rates*

Heating Rate [°C/min]	Temperatures [°C]				Mass Loss [wt.%]	-DTG [wt.%/min]	
	T_i	T_f	T_{m1}	T_{m2}			
Stage 1							
5	30	180.29	91.60	-	11.89	0.499	
10	30	181.64	143.71	-	10.77	0.842	
15	30	204.31	151.45	-	11.08	1.249	
20	30	209.72	156.33	-	11.62	1.920	
Stage 2							
5	180.29	516.66	306.55	444.03	50.84	1.29	0.91
10	181.64	525.00	317.77	452.15	50.86	2.57	1.73
15	204.31	533.33	327.82	467.07	49.49	3.66	2.49
20	209.72	555.56	331.36	464.66	50.26	5.20	3.44
Stage 3							
5	516.66	800	-	-	6.99	-	
10	525.00	800	-	-	5.94	-	
15	533.33	800	-	-	5.96	-	
20	555.56	800	-	-	4.85	-	

8.2. The Effect of Catalysts on Thermal Decomposition of the Sludge

Thermal decomposition behaviour of sludge from ambient temperature to 800°C was investigated at constant heating rate of 10°C/min and under N_2 atmosphere. The effects of Al_2O_3 and y-zeolite as catalysts were also determined and the resulting TG and DTG thermographs are shown in Figure 8.2 (a) and 8.2 (b). The addition of catalysts greatly affected the thermal decomposition rate of the sludge as when Al_2O_3 was used as catalyst, the total weight loss was 64.05 and in the presence of y-zeolite the total weight loss was increased to 70.62 wt.% while it was 67.57 wt.% in non-catalytical pyrolysis.

Catalytic effect of y-zeolite during the pyrolysis of the sludge was discrete compared to catalytic effect of Al_2O_3, especially in Stage 1, different thermal decomposition behaviour was observed. The weight loss in Stage 1 was due to the moisture content of the sludge as it was 10.77 and 11.55 wt.% in case of non-catalytical pyrolysis and catalytic pyrolysis via Al_2O_3, respectively. When sludge with y-zeolite was fed to the TGA analyser, the weight loss was decreased in Stage 1 to value of 4.81 wt.%. This dramatic decrease in the weight loss could be a result of the zeolite's capacity to adsorb water even at low and moderate temperatures. Zeolites are being used in low and

medium temperature air-drying processes due to their ability to remove water from fresh air [125]. In addition, the adsorbed moisture on the y-zeolite surface then released during Stage 2, yielding a weight loss of 61.91 wt.% which was 47.63 wt.% in the presence of Al_2O_3. However, it should be pointed out that this increase in weight loss in Stage 2 in the presence of y-zeolite was not only due to the release of water, but also the enhancement in the degradation of organics since the weight loss in the same stage was 50.86 wt.% during non-catalytic pyrolysis.

The change in the maximum degradation rates also indicate the catalytic effects of Al_2O_3 and y-zeolite since there was a certain decrease in -DTG (wt.%/min) values compared to non-catalytical pyrolysis. The values of the maximum degradation rates were detected as 2.565 wt.%/min for the non-catalytical pyrolysis, and it was decreased to 2.354 and 1.737 wt.%/min in the presence of Al_2O_3 and y-zeolite as shown in Table 8.2. This can also be observed in Figure 8.2 (a) as the peak heights in the Stage 2 lowered in the catalytic cases. As a summary, it could be concluded that both catalysts affected the degradation rates and lowered the required energy for the pyrolysis of the sludge.

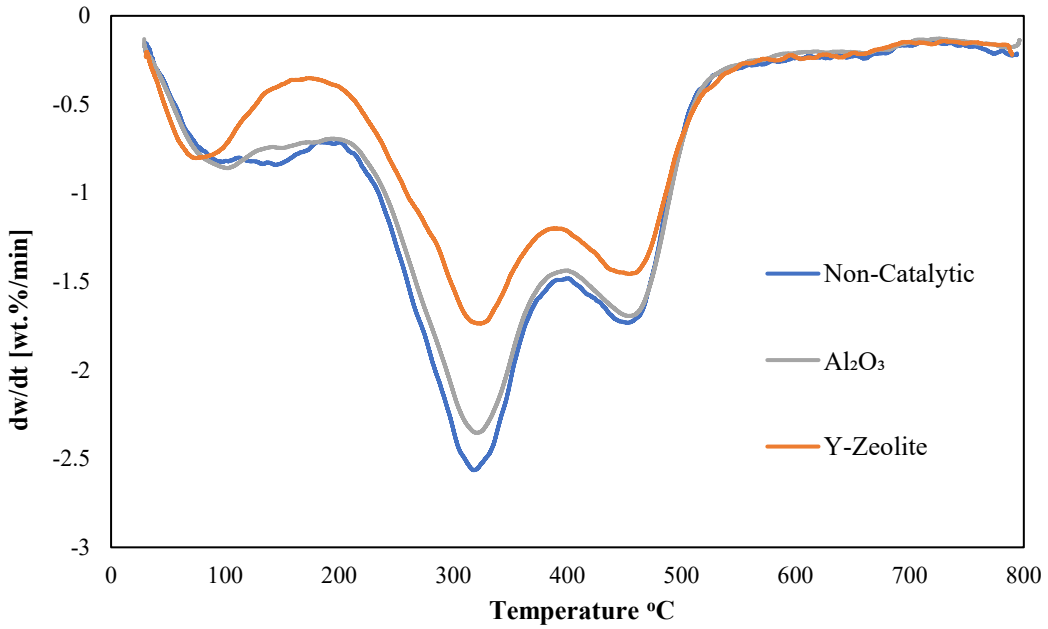

(a)

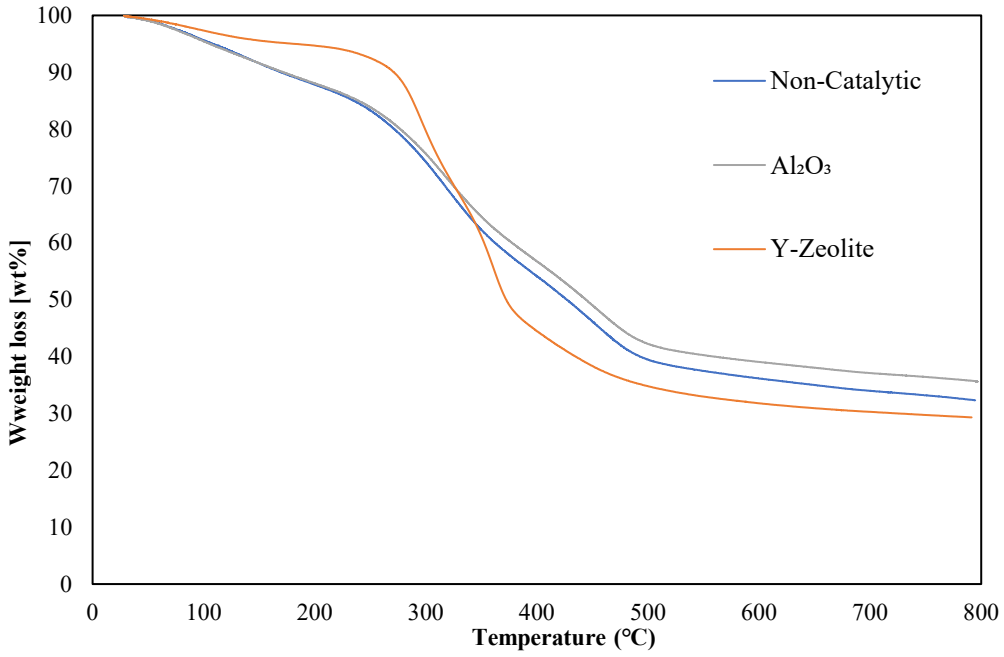

Figure 8.2. (a) TG and (b) DTG thermographs for non-catalytic and catalytic sludge pyrolysis at constant heating rate of 10 °C/min

(b)

Table 8.2. *Initial, final and peak temperatures, weight loss and -DTG values during pyrolysis of sludge at constant heating rate of 10 °C/min.*

	Temperatures [°C]				Mass Loss [wt.%]	-DTG [wt.%/min]	
	T_i	T_f	T_{m1}	T_{m2}			
Stage 1							
Sludge	30	181.64	143.71	-	10.77	0.842	
Sludge+Al_2O_3	30	195.24	102.17	-	11.55	0.860	
Sludge+y-zeolite	30	174.03	74.54	-	4.81	0.803	
Stage 2							
Sludge	181.64	525.00	317.77	452.15	50.86	2.565	1.734
Sludge+Al_2O_3	195.24	533.34	320.55	453.54	47.63	2.354	1.694
Sludge+y-zeolite	174.03	541.67	321.71	454.62	61.91	1.737	1.457
Stage 3							
Sludge	525.00	800	-	-	5.94	-	
Sludge+Al_2O_3	533.34	800	-	-	4.87	-	
Sludge+y-zeolite	541.67	800	-	-	3.90	-	

8.3. Kinetic and Thermodynamic Analysis

KAS, FWO and Friedman methods as isoconversional kinetic models were utilized to determine the kinetic and thermodynamic parameters during the pyrolysis of sludge. The kinetic plots for all methods are shown in Figure 8.3 for non-catalytical pyrolysis of sludge, Figure 8.4 for Al_2O_3 catalytical pyrolysis of sludge, Figure 8.5 for y-zeolite catalytical pyrolysis of sludge. Activation energies (E_A) were calculated from corresponding slopes of each line drawn for conversion degrees (α) from 0.1 to 0.8 and the correlation coefficients (R^2) for all cases were above 0.90, proving the high accuracy of the kinetic models. All values of activation energies and pre-exponential factors (A) per conversion degrees for all cases calculated from the corresponding slopes of the kinetic plots are shown in Table 8.3.

The determined average activation energy values for non-catalytical pyrolysis were 182.77, 170.63 and 175.84 kJ/mol according to KAS, FWO and Friedman models respectively. Application of isoconversional kinetic methods is relatively new and due to its simplicity and good accuracy, it has gained much of the attention. In this methods the

thermal degradation of the solid is defined as a single reaction and small differences in the calculated activation energies by different kinetic models could be a result of this approach as seen in pyrolysis of biomass and biomass constituents such as cellulose, hemicellulose and lignin [126–128]. Kinetic modelling of sewage sludge was investigated, and model fitting method was applied in various articles which considers the sludge as two or more pseudo components. The activation energy depending on the degree of conversion in these studies were roughly in the range of 100 to 400 kJ/mol [129–132].

In this work, in all methods, activation energy and pre-exponential factor values increased with the increasing conversion degree. When KAS method was used, activation energy was increased from 84.66 to 291.18 kJ/mol as conversion degree was increased from 0.1 to 0.8 during the non-catalytical pyrolysis. Similar trends can be observed in other kinetic models as listed in Table 8.3, as well as in other reports in the literature investigating the kinetics of pyrolysis of leather wastes and biomass samples [19,88].

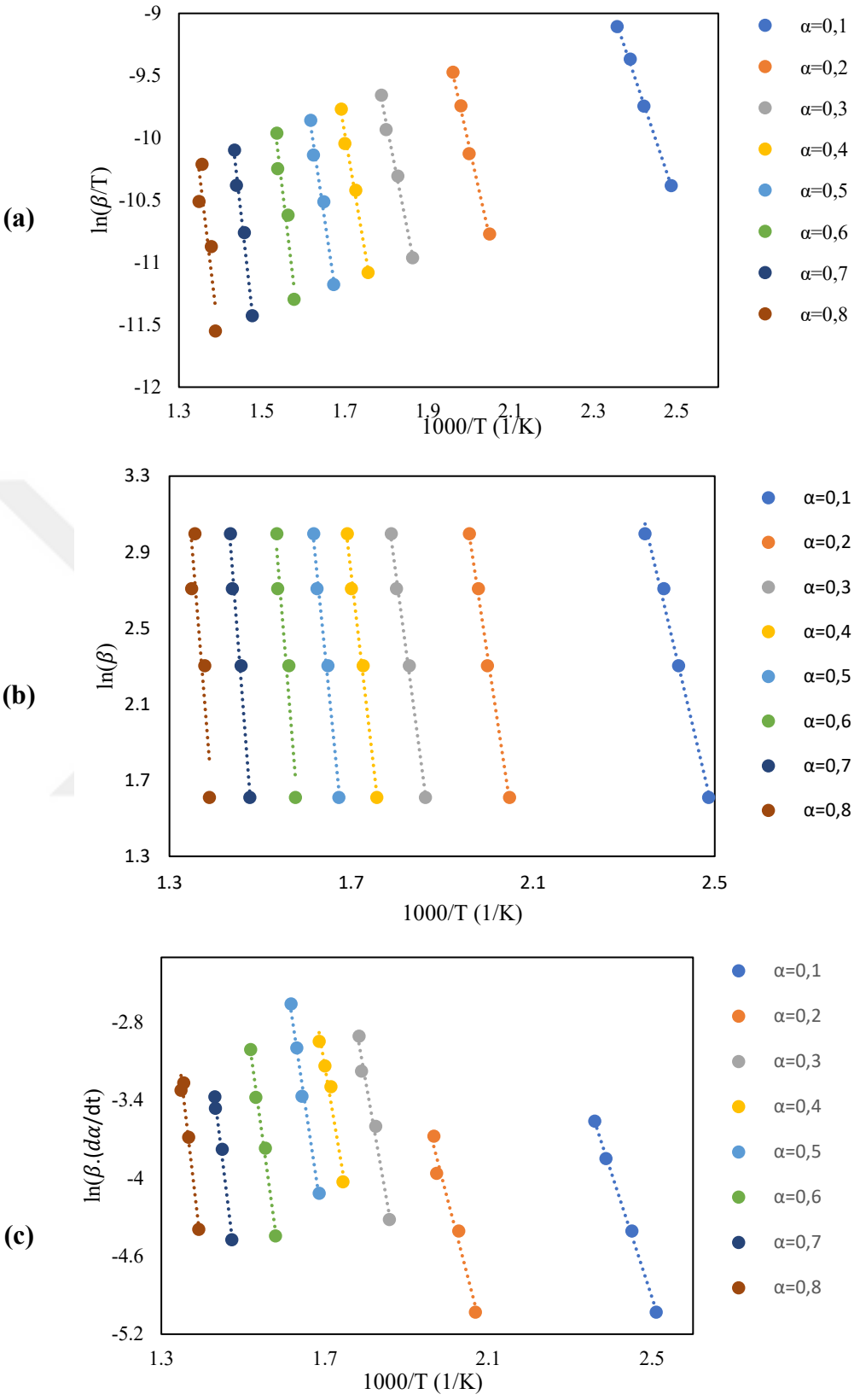

Figure 8.3. *Kinetic Plots of (a) KAS, (b) FWO and (c) Freidman model for non-catalytical pyrolysis of sludge*

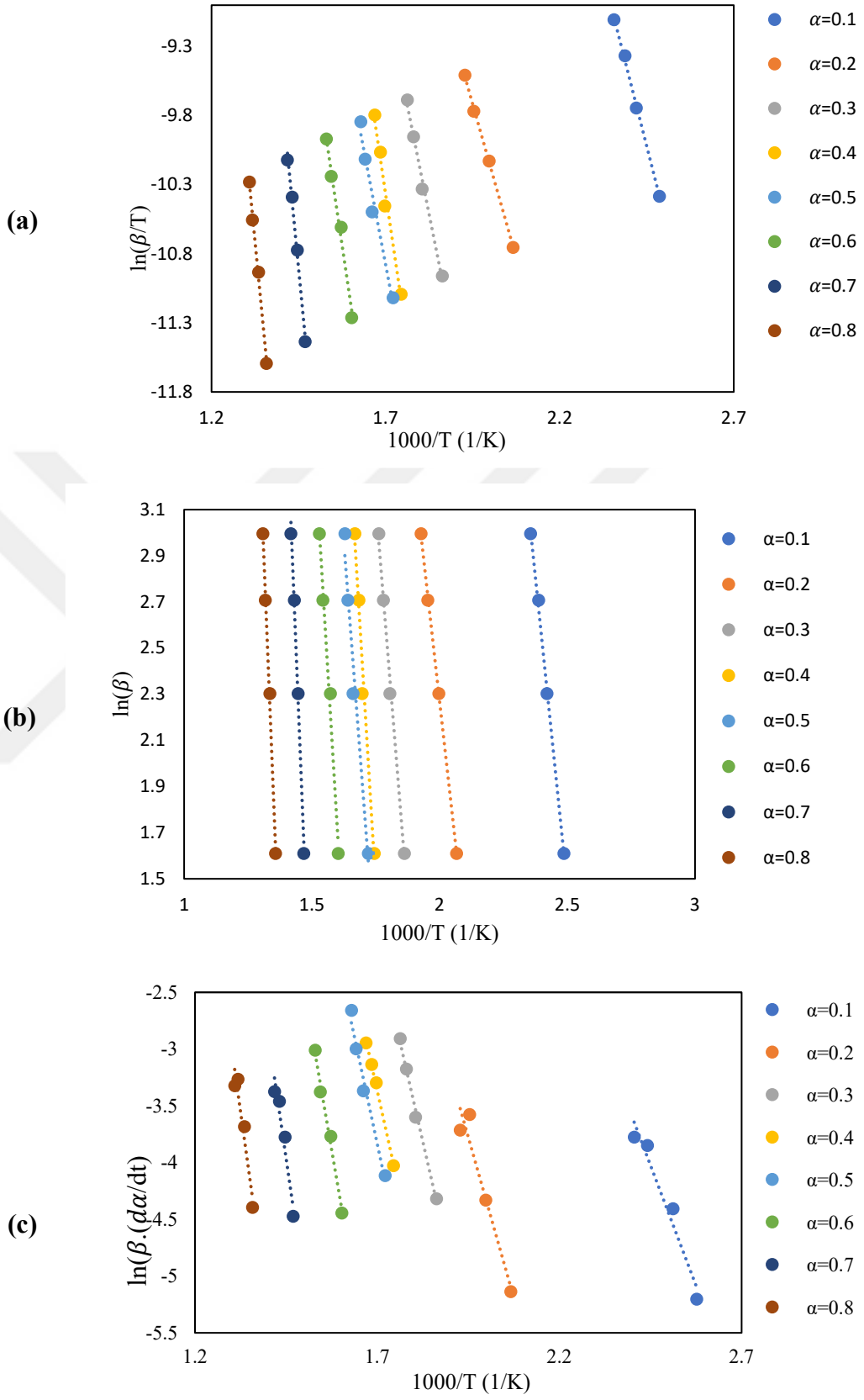

Figure 8.4. *Kinetic Plots of (a) KAS, (b) FWO and (c) Freidman model for Al2O3 catalytical pyrolysis of sludge*

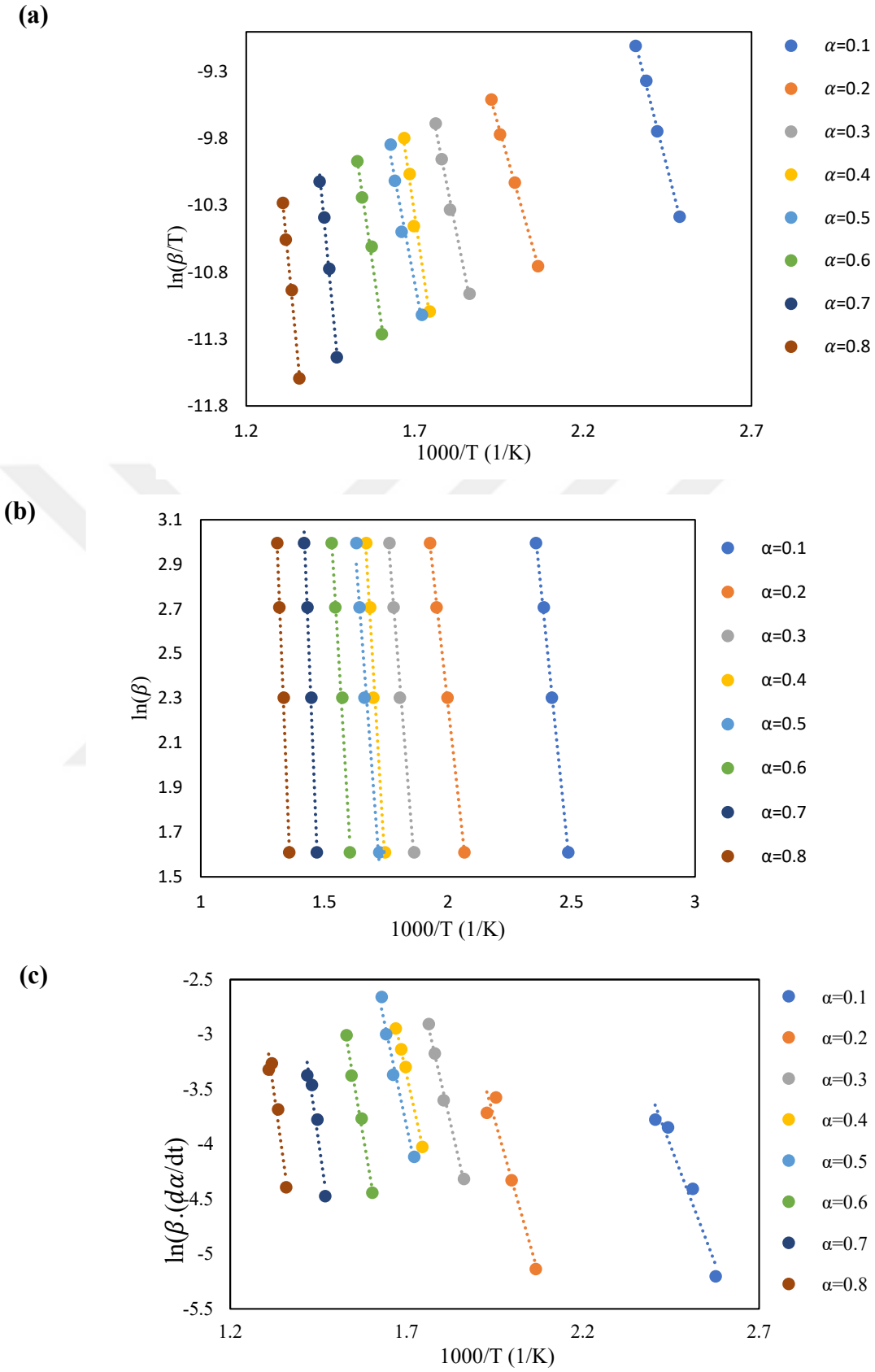

Figure 8.5. *Kinetic Plots of (a) KAS, (b) FWO and (c) Freidman model for y-zeolit catalytical pyrolysis of sludge*

Table 8.3. *Kinetic Parameters for pyrolysis of sludge via KAS, FWO and Friedman models*

		KAS			FWO			Freidman		
	α	E_A [kJ/mol]	A [s^{-1}]	R^2	E_A [kJ/mol]	A [s^{-1}]	R^2	E_A [kJ/mol]	A [s^{-1}]	R^2
Sludge	0.1	84.66	$7.05x10^{06}$	0.9980	84.43	$6.71x10^{06}$	0.9977	90.38	$2.38x10^{07}$	0.9821
	0.2	123.11	$2.33x10^{10}$	0.9944	124.25	$2.96x10^{10}$	0.9960	128.47	$7.16x10^{10}$	0.9872
	0.3	139.45	$7.07x10^{11}$	0.9937	140.48	$8.76x10^{11}$	0.9941	152.23	$1.01x10^{13}$	0.9959
	0.4	161.27	$6.58x10^{13}$	0.9888	161.63	$7.08x10^{13}$	0.9894	130.36	$1.06x10^{11}$	0.9959
	0.5	186.54	$1.22x10^{16}$	0.9815	185.96	$1.09x10^{16}$	0.9823	203.41	$3.97x10^{17}$	0.9331
	0.6	232.09	$1.45x10^{20}$	0.9300	229.59	$8.66x10^{19}$	0.9338	246.41	$2.74x10^{21}$	0.9733
	0.7	243.87	$1.63x10^{21}$	0.9798	241.42	$9.84x10^{20}$	0.9999	209.92	$1.52x10^{18}$	0.9254
	0.8	291.18	$2.63x10^{25}$	0.9517	292.68	$3.57x10^{25}$	0.9999	245.43	$2.24x10^{21}$	0.9629
	Avg	182.77			170.63			175.83		
Sludge+Al_2O_3	0.1	84.66	$7.05x10^{06}$	0.9974	84.43	$6.71x10^{06}$	0.9977	70.51	$3.41x10^{05}$	0.9547
	0.2	73.93	$7.11x10^{05}$	0.9990	77.78	$1.62x10^{06}$	0.9991	94.23	$5.37x10^{07}$	0.9361
	0.3	104.65	$4.85x10^{08}$	0.9948	107.63	$9.08x10^{08}$	0.9957	116.63	$6.01x10^{09}$	0.9949
	0.4	141.88	$1.17x10^{12}$	0.9784	143.37	$1.60x10^{12}$	0.9811	120.21	$1.27x10^{10}$	0.9968
	0.5	110.30	$1.59x10^{09}$	0.9743	113.68	$3.24x10^{09}$	0.9784	125.09	$3.53x10^{10}$	0.9760
	0.6	142.10	$1.23x10^{12}$	0.9852	144.41	$1.99x10^{12}$	0.9871	155.78	$2.10x10^{13}$	0.9881
	0.7	217.44	$7.13x10^{18}$	0.9999	216.52	$5.89x10^{18}$	0.9999	184.89	$8.71x10^{15}$	0.9395
	0.8	212.42	$2.54x10^{18}$	0.9999	216.96	$6.46x10^{18}$	0.9999	192.24	$3.97x10^{16}$	0.9361
	Avg	135.92			129.31			132.45		
Sludge+y-zeolite	0.1	73.12	$5.98x10^{05}$	0.9652	64.05	$8.44x10^{04}$	0.9712	69.66	$2.48x10^{05}$	0.9622
	0.2	77.04	$1.38x10^{06}$	0.9387	80.59	$2.96x10^{06}$	0.9491	94.01	$5.12x10^{07}$	0.8760
	0.3	102.40	$3.02x10^{08}$	0.9847	105.43	$5.72x10^{08}$	0.9869	104.99	$5.21x10^{08}$	0.9951
	0.4	115.73	$4.97x10^{09}$	0.9761	118.59	$9.05x10^{09}$	0.9795	121.58	$1.69x10^{10}$	0.9891
	0.5	129.36	$8.62x10^{10}$	0.9491	131.97	$1.49x10^{11}$	0.9558	137.73	$4.94x10^{11}$	0.9058
	0.6	127.71	$6.10x10^{10}$	0.9907	130.91	$1.19x10^{11}$	0.9920	156.99	$2.71x10^{13}$	0.9897
	0.7	162.24	$8.03x10^{13}$	0.9999	164.23	$1.21x10^{14}$	0.9999	167.74	$2.51x10^{14}$	0.9529
	0.8	197.17	$1.10x10^{17}$	0.9999	202.21	$3.10x10^{17}$	0.9999	180.34	$3.40x10^{15}$	0.9502
	Avg	123.10			117.78			129.13		

The pre-exponential factors for non-catalytical pyrolysis of sludge ranged from 10^6 to 10^{25} s^{-1} obtained by KAS and FWO, while they were in the range of 10^7-10^{21} s^{-1} according to Friedman method. While the high values of pre-exponential factor indicate that numerous chemical reactions taking place during the pyrolysis of sludge, the wide range of the values shows the complex structure of the sludge since A is defined as degree of collision of a reaction per unit time [100].

The presence of Al_2O_3 and y-zeolite affected the values of both activation energy and pre-exponential factor values. According to all methods used, the average activation energy decreased during the catalytical pyrolysis of sludge. It was decreased from 182.77 to 135.92 kJ/mol when Al_2O_3 was used as the catalyst and it was 123.10 kJ/mol in case of y-zeolite addition when calculations were carried out via KAS model. The same decrease was observed in the calculations via Friedman and FWO methods, showing that both catalysts were effective to reduce the activation energy. Although the values of pre-exponential factor decreased slightly, they were still high ranged between 10^6-10^{18} s^{-1}

The changes in enthalpy, Gibbs free energy and entropy as thermodynamic parameters were determined for the pyrolysis of sludge and all values per conversion degree are shown in Table 8.4. Enthalpy change (ΔH) refers to the energy absorbed by the sludge during the pyrolysis to degrade into bio-oil, syngas and char. The ΔH values with the changing conversion degree were positive, showing the reactions occurred during pyrolysis were endothermic. In addition, while the ΔH increased with the increasing conversion degree, the difference between E_A and ΔH were around 5 kJ/mol, indicating product formation was easily achievable [133]. The catalyst addition decreased the ΔH values, for example, they were in the range of 79.69 to 286.21 kJ/mol during the non-catalytical pyrolysis and decreased to the range of 79.69 to 207.45 kJ/mol in the presence of Al_2O_3, according to KAS model. Y-zeolite addition further lowered the ΔH values, ranging from 68.15 to 192.20 kJ/mol, showing that it was the most effective catalyst in this study.

Gibbs free energy (ΔG) represents the increase in the total energy of a system necessary for the development of the activated complex [99]. The ΔG values were in a very narrow range and slightly increased with the increasing conversion degree, and were between 156.2 kJ/mol and 150 kJ/mol, according to all three kinetic models.

Table 8.4. *Kinetic Parameters for pyrolysis of sludge via KAS, FWO and Friedman models*

		KAS			FWO			Freidman		
	α	ΔH [kJ/mol]	ΔG [kJ/mol]	ΔS [kJ/mol]	ΔH [kJ/mol]	ΔG [kJ/mol]	ΔS [kJ/mol.K]	ΔH [kJ/mol]	ΔG [kJ/mol]	ΔS [kJ/mol.K]
Sludge	0.1	79.69	156.21	-127.92	79.46	156.22	-128.33	85.41	155.88	-117.81
	0.2	118.13	154.34	-60.54	119.28	154.30	-58.54	123.50	154.13	-51.21
	0.3	134.48	153.72	-32.18	135.51	153.69	-30.39	147.26	153.29	-10.08
	0.4	156.30	153.00	5.51	156.66	152.99	6.13	125.38	154.06	-47.94
	0.5	181.57	152.28	48.97	180.99	152.29	47.98	198.44	151.85	77.89
	0.6	227.12	151.19	126.94	224.62	151.24	122.66	241.44	150.89	151.38
	0.7	238.90	150.94	147.04	236.45	150.99	142.87	204.95	151.69	89.04
	0.8	286.21	150.06	227.61	287.71	150.04	230.17	240.46	150.91	149.70
Sludge+Al_2O_3	0.1	79.69	156.21	-127.92	79.46	156.22	-128.33	65.54	157.12	-153.10
	0.2	68.96	156.88	-146.99	72.81	156.63	-140.13	89.26	155.67	-111.04
	0.3	99.68	155.15	-92.74	102.66	155.01	-87.53	111.66	154.61	-71.82
	0.4	136.91	153.64	-27.97	138.40	153.59	-25.39	115.23	154.46	-65.59
	0.5	105.33	154.89	-82.86	108.71	154.74	-76.96	120.12	154.26	-57.09
	0.6	137.12	153.63	-27.60	139.44	153.55	-23.59	150.80	153.17	-3.97
	0.7	212.47	151.52	101.90	211.54	151.54	100.32	179.92	152.32	46.13
	0.8	207.45	151.63	93.32	211.99	151.53	101.09	187.27	152.13	58.75
Sludge+y-zeolite	0.1	68.15	156.93	-148.43	59.07	157.59	-164.71	64.69	157.18	-154.63
	0.2	72.07	156.68	-141.45	75.62	156.45	-135.14	89.04	155.69	-111.43
	0.3	97.43	155.26	-96.69	100.46	155.11	-91.37	100.02	155.14	-92.15
	0.4	110.76	154.65	-73.39	113.61	154.53	-68.41	116.61	154.41	-63.19
	0.5	124.39	154.10	-49.67	127.00	154.00	-45.13	132.76	153.79	-35.16
	0.6	122.73	154.16	-52.54	125.94	154.04	-46.98	152.02	153.14	-1.87
	0.7	157.26	152.97	7.17	159.25	152.91	10.60	162.77	152.81	16.65
	0.8	192.20	152.00	67.20	197.24	151.88	75.84	175.36	152.45	38.32

Entropy change (ΔS) at conversion degrees less than 0.3 were negative during the non-catalytical pyrolysis while it remained negative until the conversion degree reached 0.6 in the presence of catalysts according to KAS and FWO models. The Friedman model suggested that in non-catalytical pyrolysis ΔS remained constant for conversion degree less than 0.4 and in catalytical pyrolysis, at conversion degrees higher than 0.7, ΔS became positive. The negative values of ΔS indicate that the produced substances are more organized in molecular structure compared to the initial substances, showing that before reaching the thermodynamic equilibrium, substances undergo a chemically or physically aging process [134]. Therefore, it can be concluded that the addition of catalyst enhanced the production of substances with more organized molecular structure.

8.4. The Effect of Catalyst on Fast Pyrolysis Product Yields

Due to sludge sample contains a high fraction of ash and fixed carbon content as seen in Table 7.1. Therefore, oil yield obtained by pyrolysis of sludge is expected as low whereas char is expected to be high [135,136]. From Figure 8.6, it was showed that low oil yield (24.7%) was produced during the self-pyrolysis of sludge, which might be attributed to the low volatile matter (organic content) in the sample. [136–138].

Fig. 8.6 also shows the product yields (catalytic or non-catalytic models) of sludge sample. Compared to the non-catalytic results, all product yields are differed using catalysts in the experiments. The oil yield increased from 24.7 percent to 25.8 % in the presence of Al_2O_3 [72]. A few studies examined the influence of catalyst on sewage sludge pyrolysis and the similar results obtained using Al_2O_3. For example, Sun et. al., studied the effect of composite alumina on sewage sludge pyrolysis and reported increased liquid and gas yields using composite alumina [70]. Furthermore, Lin et. al., obtained the bio-oil yield at a limit of 22.60%, but it is as improved by 5.16% relative to those without a catalyst with iron oxide [139]. In the other hand the oil yield decreased using y-zeolite catalyst. As a result, reactive thermal and catalytic cracking reactions were more likely to decrease the bio-oil yield. Some studies showed similar results: Xie et. al., studied the pyrolysis of sewage sludge with HZSM-5 catalyst and reported that when catalyst was used, the yield of oils reduced [72]. In other study et. al., proposed that Fe2O3 was responsible for an increase in gas yield but a decrease in bio-oil and biochar yield, while CaO was in favour of increasing the yield in gas and bio-oil but of decreasing biochar yield [6].

It was also found that the pyrolysis of sludge sample with Al_2O_3 and y-zeolite catalysts results an increasing in gas yield and decreasing in char yield relative to without catalyst. The highest gas yield (30 %) was obtained using y-zeolite. Yu et. al., studied the effects of six catalysts (CaO, $CaCO_3$, NiO, Ni_2O_3, y-Al_2O_3 and TiO_2) in the pyrolysis of sewage sludge under the microwave irradiation. It was showed that a significant improvement in the gas fraction relative to that tested without catalysts [71].

Minimum char production (40.5%) was observed using Al_2O_3 catalyst in the experiments.

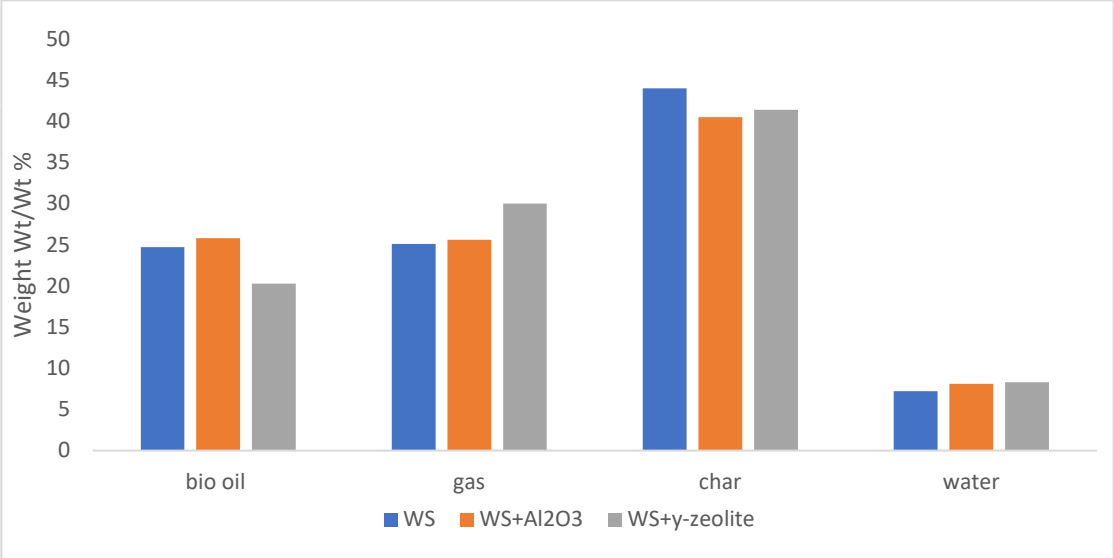

Figure 8.6. *The product yields of sludge with and without the presence of catalyst.*

8.5. Oil Composition

The oils were analyzed by using gas chromatography/mass spectroscopy (GC/MS) and it is given in Figure 8.7, Tables 8.5, Tables 8.6, Tables 8.7, show the detailed component analysis of the bio-oils by GC/MS, including retention time (min), compound name, peak number and peak area. Figure 8.8 shows the classification of oils.

The sludge oil obtained without catalyst, contained about 69.7% fatty acids, 5% N-compounds, 2.8% aliphatics (alkanes and alkenes), 3.1% amides and 3.3% oxygenated phenolic compounds. Also present amongst the sludge pyrolysis products were four steroidal hydrocarbons (16.1%), Cholesterol, Cholest-5-en-3-ol (3. beta), Cholesta-3,5-diene and Cholest-4-en-3-one. The nitrogenous compound, and oxygenated phenolic compounds are likely derived from the sources of the sludge, which contain a high amount of nitrogen and oxygen in proteins and/or amino acids [142]. In addition, the main source

of the fatty acids is pyrolysis of lipid [143]. The presence of the oxygenated phenolic compound can cause the bio-oil to become unstable during long term storage and transportation. The latter descriptions indicate that a higher quality of oil will contain high hydrocarbons, low oxygen and nitrogen compounds, as well as low acidity.

Two catalysts were used in this study for improving the quality of oil.

In principle, the use of both catalysts reduces fatty acid which are classified as long chain organic compounds since they have a carbon distribution between 13 and 18, Steroidal hydrocarbons were major compounds in non-catalytic sludge pyrolysis. These compounds were diminished using catalyst. It was though that the hydrothermal alteration reactions are dominant on conversion of the steoredials [144].

Nonetheless, the effects of both catalysts on the liquid product are specific in view of the compounds created. Methoxy phenols are abundant in Al2O3 studies. Al2O3 has a cracking effect on the liquid component and shortly afterwards a unifying effect. Supporting results can be seen from the table 8.6. Fatty acids decreased from 69.7 % to 24.6 % and steroidal compounds decreased from 16.1 % to 2.7 %. Al2O3 can be described as effective in removing nitrogen-containing components. Since methoxy phenols are oxygen-containing compounds, Al2O3 is not considered to be very effective in removing oxygen from liquid products.

Positive and important changes in the product composition were observed in experiments with y-zeolite. The most obvious effect of y-zeolite catalyst on sludge oil is related to the fatty acid, aliphatics, N-compounds, and steroidal compounds. The decrease in fatty acids and increase in aliphatic content is seen while the pyrolysis process is conducted in the presence of the y-zeolite. Oil product obtained at non-catalytic procedure only contains 2.75% aliphatics (C14-C15) whereas oil product obtained with y-zeolite contain significant amount aliphatic components of 31.1%. The formation of lower molecular weight hydrocarbons is dominant during sludge pyrolysis with y-zeolite. While mono-ring aromatic components and naphthalenes with the use of Al2O3 are not observed, these componenets were detected 3% and 3.4% with using of y-zeolite, respectively. N-compounds in oil obtained using y-zeolite have been found to be increased. These components, obtained as 5 % without catalyst, increased by y-zeolite to 18.1 %.

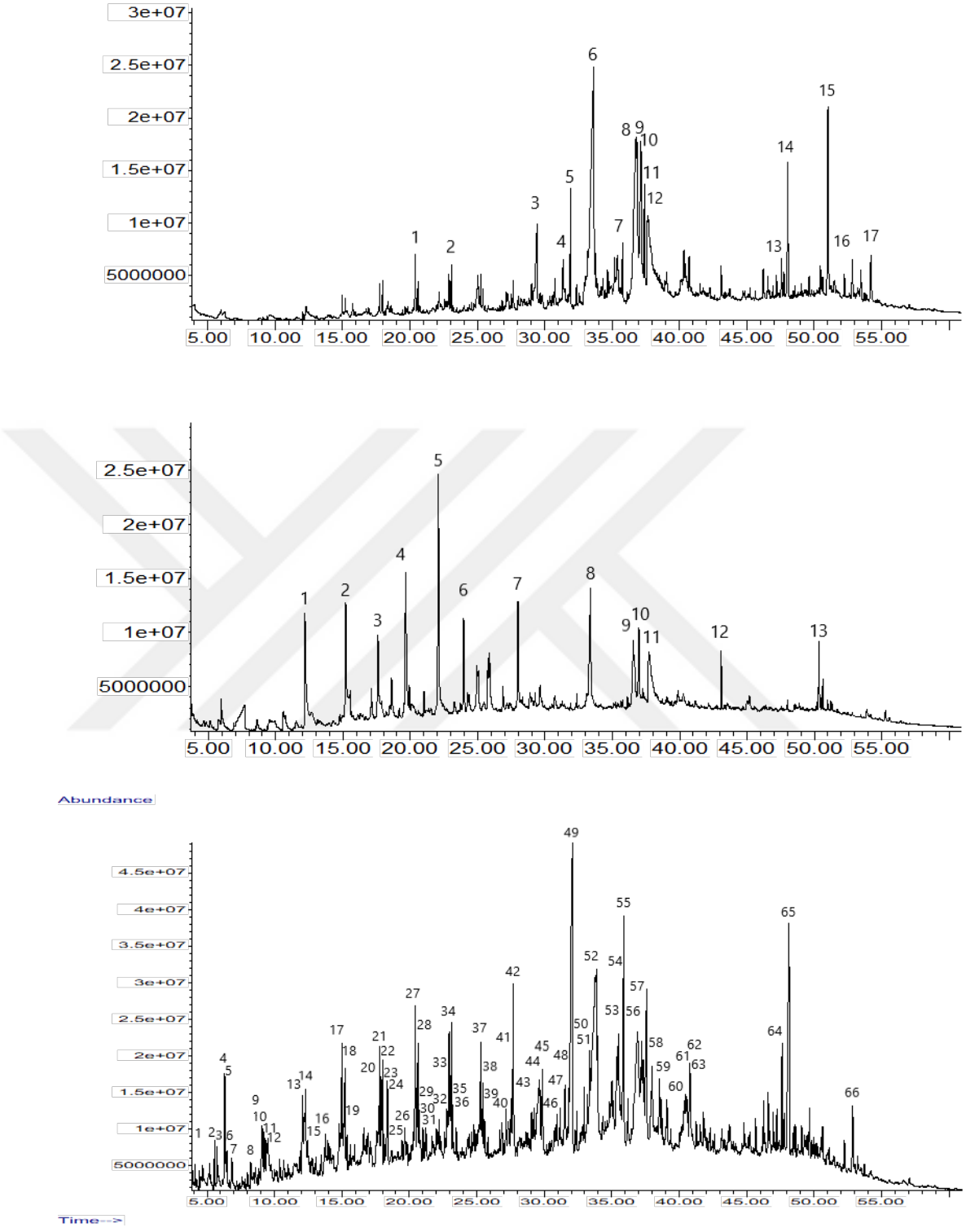

Figure 8.7. *GC/MS chromatogram of bio-oils obtained at pyrolysis of sludge without catalyst (a), sludge with Al_2O_3 (b) and Sludge with y-zeolite(c).*

Table 8.5. *Main and relatively large compounds (area percent) in oils derived from pyrolysis of sludge without catalyst.*

Peak Number	Retention Time (min)	Compound Name	Area (%) (Peak Number)
1	20.41	1-Tetradecene	1.67
2	23.09	Pentadecane	1.08
3	29.43	Tetradecanoic acid	4.61
4	31.37	Pentadecanoic acid	1.16
5	31.92	Hexadecanenitrile	3.1
6	33.65	Hexadecanoic acid	27.83
7	35.2	Heptadecanoic acid	1.42
8	35.79	Heptadecanenitrile	1.94
9	36.78	9-Octadecenoic acid	25.11
10	37.15	Octadecanoic acid	9.56
11	37.41	Hexadecanamide	3.1
12	37.71	Phenol, 4,4'-(1-methylethylidene)bis	3.3
13	47.58	Cholesterol	1.06
14	48.05	Cholesta-3,5-diene	4.92
15	51.01	Cholest-5-en-3-ol (3.beta.)	6.73
16	52.84	Cholest-4-en-3-one	1.35
17	54.21	Lanosta-8,24-dien-3-ol, (3.beta.)	2.05

Table 8.6. *Main and relatively large compounds (area percent) in oils derived from pyrolysis of sludge with Al2O3 catalyst.*

Peak Number	Retention Time (min)	Compound Name	Area (%) (Peak Number)
1	12.18	Phenol, 2-methoxy	8.91
2	15.2	Phenol, 2-methoxy-4-methyl	6.23
3	17.6	Phenol, 4-ethyl-2-methoxy-	4.8
4	19.65	Phenol, 2,6-dimethoxy	11.71
5	22.08	Phenol, 2-methoxy-4-(1-propenyl),	16.29
6	23.97	2.3.5-Trimethoxytoluene	4.62
7	25.76	Phenol, 2,6-dimethoxy-4-(2-propenyl)	12.93
8	33.39	Hexadecanoic acid	13.27
9	36.57	9,-Octadecenoic acid	7.72
10	36.98	Octadecanoic acid	3.64
11	37.75	(Phenol, 4,4'-(1-methylethylidene)bis-	4.93
12	43.09	1-2,benzenedicarboxylic acid	1.88
13	50.35	Chloest-5-en-3-ol(3.beta)	2.73

Table 8.7. *Main and relatively large compounds (area percent) in oils derived from pyrolysis of sludge with y-zeolite catalyst.*

Peak Number	Retention Time (min)	Compound Name	Area (%) (Peak Number)
1	3.62	Toluene	0.3
2	5.56	Benzene, ethyl-	0.22
3	5.76	p-Xylene	0.28
4	6.27	1-Nonene	0.15
5	6.31	Styrene	0.73
6	6.35	Benzene, 1,2-dimethyl-	0.39
7	6.84	2-Cyclopenten-1-one, 2-methyl-	0.36
8	8.25	Benzene, 1-ethyl-2-methyl-	0.21
9	9.09	1-Decene	0.56

10	9.18	Benzene, 1,2,3-trimethyl	0.42
11	9.33	Decane	0.32
12	9.51	Phenol	0.87
13	12.08	1-Undecene	0.77
14	12.28	Phenol, 4-methyl-	1.68
15	13.8	1-Methylindene	0.58
16	14.81	Naphthalene	1.07
17	15.07	1-Dodecene	2.15
18	15.23	Dodecane	1.32
19	15.38	Dodecane, 4,6-dimethyl	0.32
20	17.6	Phenol, 4-ethyl-2-methoxy-	0.34
21	17.79	1-Tridecene	1.53
22	17.92	Naphthalene, 1-methyl-	0.94
23	18.02	Tridecane	1.09
24	18.38	Naphthalene, 2-methyl-	1.26
25	19.67	Phenol, 2,6-dimethoxy-	0.42
26	20.45	1-Tetradecene	2.04
27	20.71	Tetradecane	1.51
28	21.19	Naphthalene, 1,7-dimethyl-	0.17
29	22.01	1-Tetradecanol	0.64
30	22.62	Cyclododecane	0.31
31	22.78	trans-7-pentadecene	0.67
32	22.98	1-Pentadecene	3.49
33	23.23	Pentadecane	0.43
34	23.48	Pentadecanol	0.71
35	25.25	1-Hexadecene	2.27
36	25.47	Hexadecane	0.61
39	26.87	Benzene, decyl-	0.44
40	27.16	1-Heptadecene	0.49
41	27.33	Heptadecane	0.77
42	27.61	Tetradecanenitrile	2.61
43	29.43	Tetradecanoic acid	2.69
44	29.64	1-Octadecene	1.07

45	29.86	Octadecane	1.09
46	30.77	1-Nonadecene	0.42
47	30.95	Nonadecane	0.68
48	31.18	Pentadecanoic acid	0.72
49	32	Hexadecanenitrile	9.78
50	33.53	Hexadecanoic acid	6.76
51	35.02	Heneicosene	0.81
52	35.4	Heneicosane	1.7
53	35.5	Heptadecanitrile	5.75
56	36.98	9-Octadecenoic acid	6.59
57	37.22	Octadecenoic acid	2.78
58	37.59	Hexadecanamide	2.79
59	38.643	4-Methylheptanamide	0.3
60	39.08	1-Tricosene	0.58
61	40.42	Tricosane	1.25
62	40.58	1-Tetracosene	0.4
63	40.81	Tetracosane	1
64	47	Cholesterol	3.49
65	48.15	Cholestadiene	4.43
66	52.87	Cholest-4-en-3-one	1.01

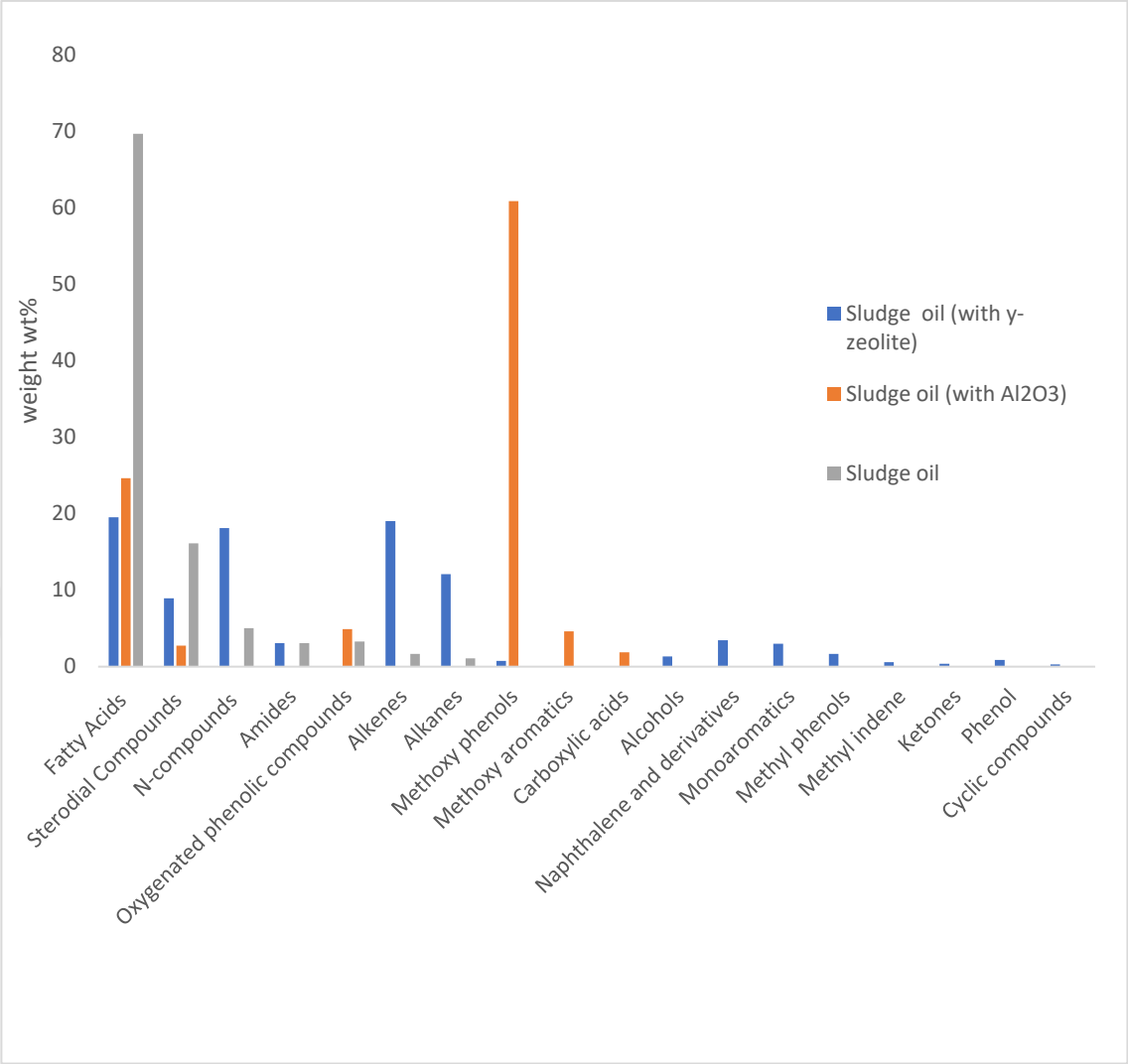

Figure 8.8. *Classification of pyrolysis oils*

8.6. Surface Area of The Activated Carbon

The effect of carbonization temperature on surface area within the range 400 to 600 ℃ was investigated for the samples which activated at different impregnation ratio. To understand the effect of the carbonization temperature and impregnation ratio, a full factorial design with second-order model applied on the results shown in table 8.8. The maximum surface area found in carbonization temperature 550 ℃ and impregnation ratio 1:2. Also, it can be observed that the surface area values increased with the increase of the carbonization temperature. E.g., when the impregnation ratio was 1;1 the surface area of the activated carbon produced at 400 ℃ was 147 g/cm2 but this value has increased to achieve the value 513.886 g/cm2 at 550 ℃ then decreased to be 456.795 g/cm2 at 600 ℃.

Table 8.8. *Surface areas obtained by different experimental parameters*

The code of the sample	Carbonization Temperature	impregnation rate (Sludge's weight: impregnation rate weight)	Obtained surface area (g/cm^2)
MW1AC	400	1:1	147
MW2AC	550	1:2	556.388
MW3AC	500	1:1	388.918
MW4AC	450	1:2	468.135
MW5AC	600	1:1	456.795
MW6AC	400	1:2	236.871
MW7AC	550	1:1	519.516
MW8AC	500	1:2	451.908
MW9AC	450	1:1	345.969
MW10AC	600	1:2	501.806
MW11AC	400	1:1	158.352
MW12AC	450	1:2	427.46
MW13AC	550	1:1	513.886
MW14AC	500	1:2	489.667
MW15AC	600	1:1	503.167
MW16AC	550	1:2	564.687
MW17AC	400	1:2	281.407
MW18AC	600	1:2	530.432
MW19AC	450	1:1	386.364
MW20AC	500	1:1	421.405

8.6.1. Full factorial design with second-order model

Full factorial design means that all possible combinations of levels for all factors are carried out in random order. These combinations can be repeated to estimate error. The first-order model considers main effect of factors, interactions, and error. In some cases, the curvature in the response function is required second-order model where quadratic effects of factors are added to the model as follows [1] :

$$\hat{y} = \beta_0 + \sum_{i=1}^{k} \beta_i x_i + \sum_{i=1}^{k} \beta_{ii} x_i^2 + \sum \sum_{i \neq j} \beta_{ij} x_i x_j + \varepsilon$$

Where yˆis the estimated response, β_0 is a constant, β_i is the effects of i. factor, β_ii represents the quadratic effect of i. factor, β_ij shows the interaction effect between i. factor and j.factor, and ε is the error term. Also, fixed effect model where levels/treatments are determined by experimenters are chosen. The test hypothesis is conducted on treatment means at fixed effect model. If there is a statistically significant difference at least two treatment means, the factor is effective on the response. In this study, a full factorial experiment was designed with two factors which are carbonization temperature with 4 levels and impregnation ratio with 2 levels as explained in Table 8.9 and table 8.10.

Table 8.9. *Selected factors and levels*

	Levels				
Carbonization Temperature (°C) Levels	400	450	500	550	600

Table 8.10. *Selected factors and levels*

	Levels	
Impregnation Ration Levels	1	2

Twenty experiments (5 levels of carb.temp. x 2 levels of impreg. ratio x 2 replicates) are carried out in random order, and surface area (m^2/g) is measured as response. Due to the nonlinear structure of surface area versus carbonization temperature, we conducted the second order model with interaction. But the carbonization temperature and impregnation ratio interaction are insignificant, so the interaction term is considered into

the error term. ANOVA table is constituted by calculating sum of square terms for each factor. ANOVA is a statistical technique that compares treatment means and define if there is a significantly differences among means by using F test. F test is a ratio of between treatment means variance and within treatment variance given in Table 8.10. P-value shows the effective factors when p-value < 0.05 significance level that is selected as 0.05 % in general. Also, contribution column represents the explanation ratio of total variance by effective factors. We can set the regression model that include the effective factors defined by ANOVA table. 8.10 The coefficients of effective factors, confidence intervals and the p-values based on t distribution present in Table 3. In addition, the coefficient of determination (R-square-adj.) explains the total variability accounted by the regression model. It is desired greater than 75% generally.

In this study, analysis is implemented by using MINITAB 17 statistical software. As you can see in Table 8.10, both linear and square terms are affected on surface area. Carbonization temperature (°C) is the most effected factors on surface area by 69.07 % contribution with p-value (0.000 < 0.05). Also, square term of carbonization temperature (°C) is the second effective factor by 16.47 % with p-value (0.000 < 0.05). Impregnation ratio is the third effective factor on surface are by 7.5 % with p-value (0.001 < 0.05). The interaction between carbonization temperature and impregnation ratio is insignificant due to the p-value (0.119 < 0.05). So, this interaction term is removed model and added this sum of square value into the error. The coefficient of determination (R-square-adj.) ratio is found to be 91.73 % which is quite a big value, given in Table 8.11. So, the conducted regression model explains the variation of surface area very well.

Table 8.11. *ANOVA table on surface area*

Analysis of Variance

Source	DF	Seq SS	Contribution	Adj SS	Adj MS	F-Value	P-Value
Model	3	276172	93.04%	276172	92057	71.25	0.000
Linear	2	227288	76.57%	227288	113644	87.96	0.000
carbon. temp.	1	205018	69.07%	205018	205018	158.68	0.000
impreg. ratio	1	22270	7.50%	22270	22270	17.24	0.001
Square	1	48884	16.47%	48884	48884	37.83	0.000
carbon. temp.*carbon. temp.	1	48884	16.47%	48884	48884	37.83	0.000
Error	16	20673	6.96%	20673	1292		
Lack-of-Fit	6	15198	5.12%	15198	2533	4.63	0.017
Pure Error	10	5475	1.84%	5475	548		
Total	19	296845	100.00%				

Table 8.12. *Model summary with R-square-adjusted*

S	R-sq	R-sq(adj)	PRESS	R-sq(pred)
35.9450	93.04%	91.73%	31677.2	89.33%

The coefficients of terms in model are significant with their p-value < 0.05. The variance inflation factor (VIF) detects the multicollinearity in regression model. Multicollinearity shows the correlation between one factor and the other factors in a model whose presence can adversely affect to regression model. The interpretation of VIF is 1: not correlated, 1-5: moderately correlated, and greater 5: high correlated. In our regression model, VIF values of factors are equal to 1. So, it is impossible to mention the multicollinearity. It is the independence of factors that is desired in a regression model. The regression model of surface area was given in table 8.12.

Table 8.13. *Regression Model of Surface Area*

Coded Coefficients

Term	Effect	Coef	SE Coef	95% CI	T-Value	P-Value	VIF
Constant		476.6	12.5	(450.0; 503.2)	38.05	0.000	
carbon. temp.	286.4	143.2	11.4	(119.1; 167.3)	12.60	0.000	1.00
impreg. ratio	66.74	33.37	8.04	(16.33; 50.41)	4.15	0.001	1.00
carbon. temp.*carbon. temp.	-236.4	-118.2	19.2	(-158.9; -77.5)	-6.15	0.000	1.00

$$\hat{y}_{surface\ area} = -3294 + 13.25\, x_1 + 66.7\, x_2 - 0.01182\, x_1^2 + \varepsilon_i$$

where $\hat{y}_{surface\ area}$ is the estimating value of surface area (m^2/g), x_1 presents carbonization temperature (℃), x_2 represents the impregnation ratio and ε_i is the error term of model. ε_i is calculated the experimental value (y_i) mines estimated value from regression model ($\varepsilon_i = y_i - \hat{y}_i$).

For adequacy of model and using estimation of surface area, three assumptions should be checked. Errors/residuals distribute Normal, residuals have constant variance and residuals are independent. A normal probability plot and histogram of these residuals in Fig.8.10 (a) – (b) are used for checking Normal distributed. As seen in Fig. 8.10 (a) – (b), there is no severe indication of nonnormality, nor is there any evidence pointing to outlier. So, it is said that the residuals have Normal Distribution. Fig. 8.10 (c) graph shows residuals have constant variance and Fig. 8.10 (d) graph represents that residual are independent.

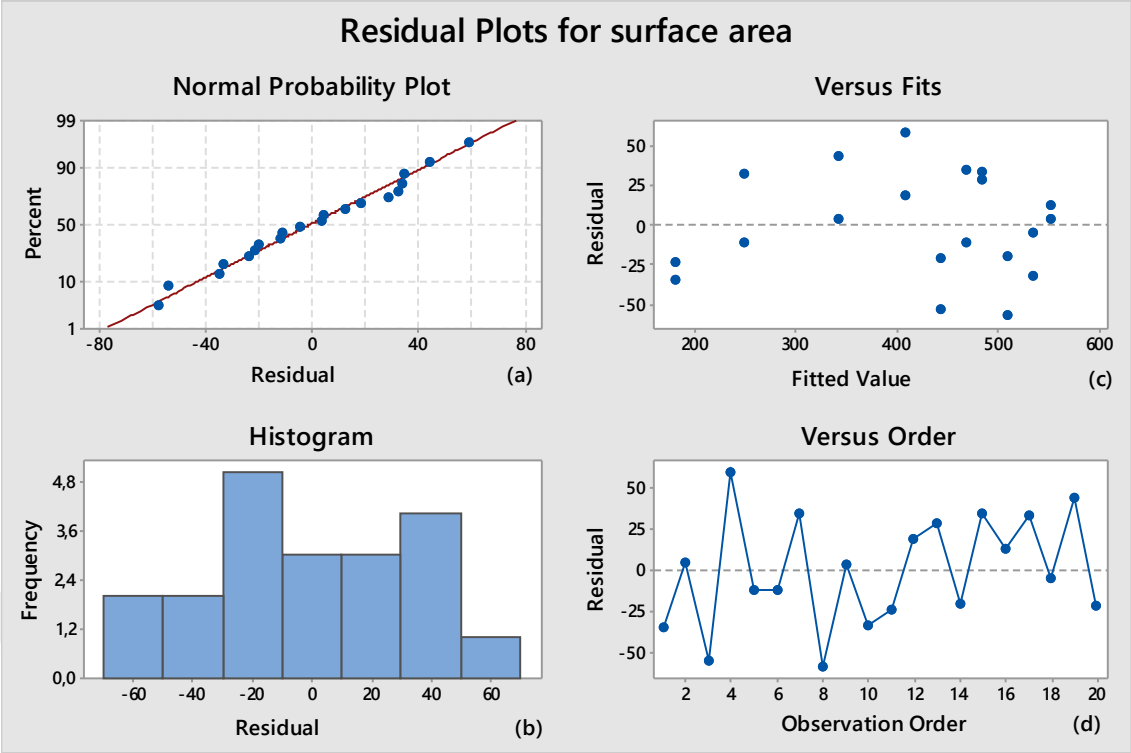

Figure 8.9. *Residual Plots for surface area*

Because the main effects of carbonization temperature and impregnation ratio are affected, main effects plot is given in Fig.8.11. Also, the surface plot and counter plot of factors are given in Fig. 8.12-14, respectively. The optimization plot is drawn in Figure 8.14. According to it, the surface area had a surface area value as a 553.3361 m^2/g at 560.565 ℃ carbonization temperature and impregnation ratio as a 1:2.

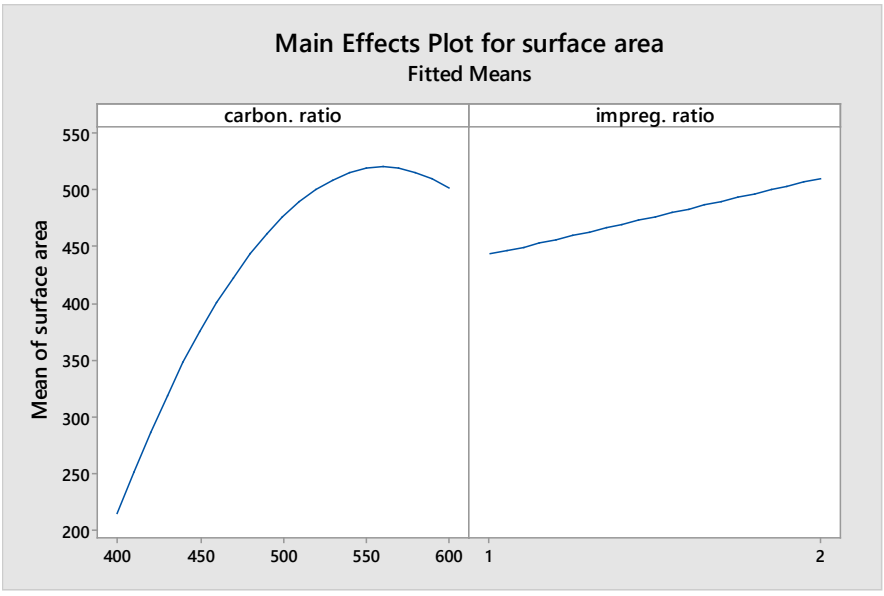

Figure 8.10. *Main effects plot for surface area*

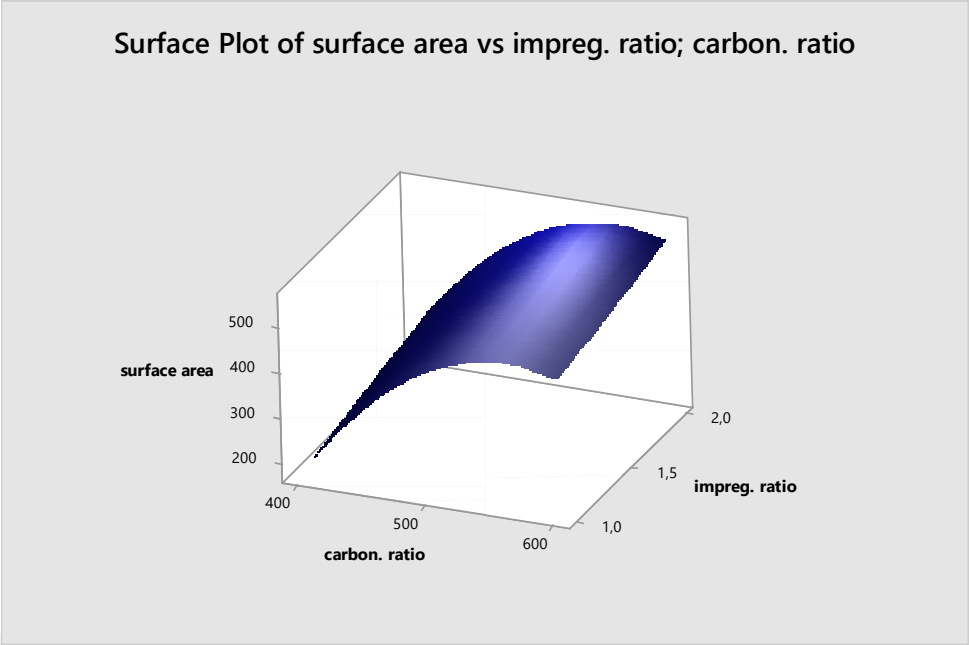

Figure 8.11. *Surface plot of surface area carbonization temperature vs* impregnation ratio

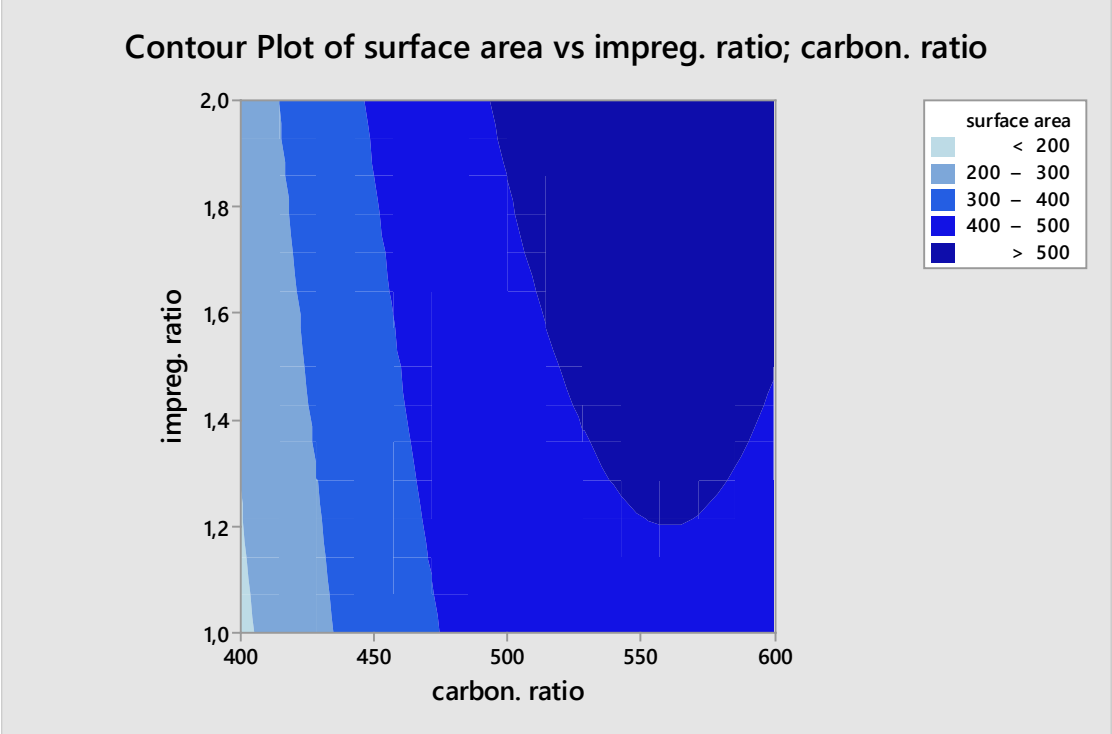

Figure 8.12. Contour Plot of surface area vs carbonization temperature and impregnation ratio

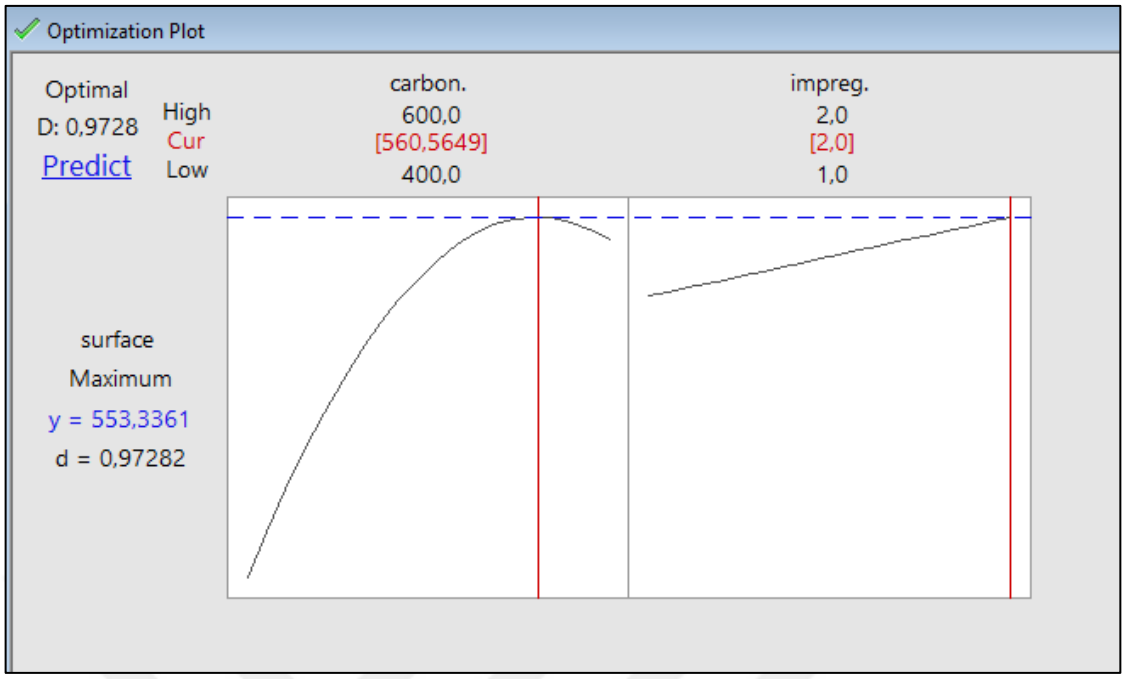

Figure 8.13. *Optimization plot of surface area*

9. CONCLUSIONS

Finally, the key conclusions drawn from the thermogravimetric study of sludge species are discussed in this section. The pyrolysis kinetics of Sludge were investigated using thermogravimetric analysis. In the absence of heat transfer constraint, non-isothermal experiments were carried out at four different heating rates.

Activated sludge as a by-product of biological treatment of industrial or municipal wastewater has a great potential as an organic waste. The present study revealed the available of using catalyst on TGA analysis and pyrolysis method on conversion of sludge obtained from Leather and Textile Industry-Wastewater Treatment Plant to energy. Activation energy was increased with the increasing of conversion degree from 84.66 to 291,18 kJ/mol as conversion degree was increased from 0.1 to 0.8 throughout the non-catalytical pyrolysis. Similar trends can be observed for the catalytical pyrolysis. As a result, it possible to conclude that the activation energy is not stable and is increasing with the increase of the conversion degree.

Both activation energy and pre-exponential factor values were altered by the presence of Al_2O_3 and y-zeolite. During catalytic pyrolysis of sludge, the average activation energy decreased according to all methods applied. When Al_2O_3 was employed as the catalyst, it was reduced from 182.77 to 135.92 kJ/mol, and it was 123.10 kJ/mol when y-zeolite was added, according to KAS model. The similar reduction was observed in the calculations using the Friedman and FWO techniques, indicating that both catalysts were effective at lowering activation energy. Although the pre-exponential factor values reduced marginally, they remained high, ranging between 10^6-10^{18} s-1.

In addition, while the ΔH increased with the increasing conversion degree The catalyst addition decreased the ΔH values, for example, they were in the range of 79.69 to 286.21 kJ/mol during the non-catalytical pyrolysis and decreased to the range of 79.69 to 207.45 kJ/mol in the presence of Al_2O_3, according to KAS model. Y-zeolite addition further lowered the ΔH values, ranging from 68.15 to 192.20 kJ/mol, showing that it was the most effective catalyst in this study.

Gibbs free energy (G) is the increase in a system's total energy required for the creation of the activated complex [100]. According to all three kinetic models, the G

values were in a very narrow range and marginally rose with increasing conversion degree, and were between 156.2 kJ/mol and 150 kJ/mol.

According to the KAS and FWO models, entropy change (S) was negative. The negative values of S imply that the created compounds are more ordered in molecular structure than the initial substances, indicating that substances undergo a chemical or physical aging process before attaining thermodynamic equilibrium.

The product yields (catalytic or non-catalytic models) of sludge sample. Compared to the non-catalytic results, all product yields are differed using catalysts in the experiments. The oil yield increased from 24.7 percent to 25.8 % in the presence of Al_2O_3. In the other hand the oil yield decreased using y-zeolite catalyst. It was also found that the pyrolysis of sludge sample with Al_2O_3 and y-zeolite catalysts results an increasing in gas yield and decreasing in char yield relative to without catalyst.

We focused not only the pyrolysis kinetics and thermodynamic properties of sludge, but also oil quality. Results shows that the influence of both catalysts on the oil product is specific in the view of the compounds created. Activated Al_2O_3 can be described as effective in removing nitrogen-containing components, but on other hand y-zeolite is highly effective in the deoxygenation reactions. The formation of lower molecular weight hydrocarbons is dominant during sludge pyrolysis with y-zeolite. The distribution of carbon in the aliphates obtained is between C9 and C24, and the region where the distribution is concentrated is between C12 and C15. The results demonstrate that the sludge from Leather and Textile Industry-Wastewater Treatment Plant offers a good potential for pyrolysis and the oil produced with the use of y-zeolite can be used as a fuels substitute for fossil fuels.

The effect of carbonization temperature on surface area within the range 400 to 600 °C was investigated for the samples which activated at different impregnation ratio. As a result, both linear and square terms are affected on surface area. Carbonization temperature (°C) is the most effected factors on surface area by 69.07 % contribution with p-value ($0.000 < 0.05$). Also, square term of carbonization temperature (°C) is the second effective factor by 16.47 % with p-value ($0.000 < 0.05$). Impregnation ratio is the third effective factor on surface are by 7.5 % with p-value ($0.001 < 0.05$). The interaction between carbonization temperature and impregnation ratio is insignificant due to the p-

value (0.119 < 0.05). So, this interaction term is removed model and added this sum of square value into the error.

Because the main effects of carbonization temperature and impregnation ratio are affected, the optimum surface area has a surface area value as a 553.3361 m^2/g at 560.565 ℃ carbonization temperature and impregnation ratio as a 1;2.

REFERENCES

[1] S. Khalid, M. Shahid, Natasha, I. Bibi, T. Sarwar, A.H. Shah, N.K. Niazi, A review of environmental contamination and health risk assessment of wastewater use for crop irrigation with a focus on low and high-income countries, Int. J. Environ. Res. Public Health. 15 (2018). https://doi.org/10.3390/ijerph15050895.

[2] Eurostat, Total sewage sludge production from urban wastewater, Eurostat. (2015).

[3] C. Xu, W. Chen, J. Hong, Life-cycle environmental and economic assessment of sewage sludge treatment in China, J. Clean. Prod. 67 (2014) 79–87. https://doi.org/https://doi.org/10.1016/j.jclepro.2013.12.002.

[4] T. Karayildirim, J. Yanik, M. Yuksel, H. Bockhorn, Characterisation of products from pyrolysis of waste sludges, Fuel. 85 (2006) 1498–1508. https://doi.org/10.1016/j.fuel.2005.12.002.

[5] J. Socci, A. Saraeian, S.D. Stefanidis, S.W. Banks, B.H. Shanks, T. Bridgwater, The role of catalyst acidity and shape selectivity on products from the catalytic fast pyrolysis of beech wood, J. Anal. Appl. Pyrolysis. (2019) 104710. https://doi.org/10.1016/j.jaap.2019.104710.

[6] R. Ma, X. Huang, Y. Zhou, L. Fang, S. Sun, P. Zhang, X. Zhang, Bioresource Technology The effects of catalysts on the conversion of organic matter and bio-fuel production in the microwave pyrolysis of sludge at different temperatures, Bioresour. Technol. 238 (2017) 616–623. https://doi.org/10.1016/j.biortech.2017.04.103.

[7] J. Yang, X. Xu, S. Liang, R. Guan, H. Li, Y. Chen, B. Liu, J. Song, W. Yu, K. Xiao, H. Hou, J. Hu, H. Yao, B. Xiao, Enhanced hydrogen production in catalytic pyrolysis of sewage sludge by red mud: Thermogravimetric kinetic analysis and pyrolysis characteristics, Int. J. Hydrogen Energy. 43 (2018) 7795–7807. https://doi.org/10.1016/j.ijhydene.2018.03.018.

[8] G. Xu, X. Yang, L. Spinosa, Development of sludge-based adsorbents: Preparation, characterization, utilization and its feasibility assessment, J. Environ. Manage. 151 (2015) 221–232. https://doi.org/10.1016/j.jenvman.2014.08.001.

[9] R. Font, M.A. Garrido, Friedman and n-reaction order methods applied to pine needles and polyurethane thermal decompositions, Thermochim. Acta. 660 (2018) 124–133. https://doi.org/10.1016/j.tca.2018.01.002.

[10] T. Onsree, N. Tippayawong, A. Zheng, H. Li, Pyrolysis behavior and kinetics of corn residue pellets and eucalyptus wood chips in a macro thermogravimetric analyzer, Case Stud. Therm. Eng. 12 (2018) 546–556. https://doi.org/10.1016/j.csite.2018.07.011.

[11] P.E. Sánchez-Jiménez, L.A. Pérez-Maqueda, A. Perejón, J.M. Criado, Limitations of model-fitting methods for kinetic analysis: Polystyrene thermal degradation, Resour. Conserv. Recycl. 74 (2013) 75–81. https://doi.org/10.1016/j.resconrec.2013.02.014.

[12] H.L. Friedman, Kinetics of thermal degradation of char-forming plastics from

thermogravimetry. Application to a phenolic plastic, J. Polym. Sci. Polym. Symp. 6 (1964) 183–195.

[13] J.H. Flynn, L.A. Wall, General treatment of the thermogravimetry of polymers, J. Res. Natl. Bur. Stand. Sect. A Phys. Chem. 70A (1966) 487. https://doi.org/10.6028/jres.070a.043.

[14] T. Ozawa, A New Method of Analyzing Thermogravimetric Data, Bull. Chem. Soc. Jpn. 38 (1965) 1881–1886. https://doi.org/10.1246/bcsj.38.1881.

[15] H.E. Kissinger, Variation of peak temperature with heating rate in differential thermal analysis, J. Res. Natl. Bur. Stand. (1934). 57 (1956) 217. https://doi.org/10.6028/jres.057.026.

[16] P.S. Low, J.L. Bada, G.N. Somero, Temperature Adaptation of Enzymes: Roles of the Free Energy, the Enthalpy, and the Entropy of Activation, Proc. Natl. Acad. Sci. 70 (1973) 430–432. https://doi.org/10.1073/pnas.70.2.430.

[17] G. Liu, H. Song, J. Wu, Thermogravimetric study and kinetic analysis of dried industrial sludge pyrolysis, Waste Manag. 41 (2015) 128–133. https://doi.org/10.1016/j.wasman.2015.03.042.

[18] D. Kin, W. Gan, A. Chun, M. Loy, B. Lai, F. Chin, S. Yusup, P. Unrean, E. Rianawati, M.N. Acda, Bioresource Technology Kinetics and thermodynamic analysis in one-pot pyrolysis of rice hull using renewable calcium oxide based catalysts, Bioresour. Technol. 265 (2018) 180–190. https://doi.org/10.1016/j.biortech.2018.06.003.

[19] M.J.B. Fong, A.C.M. Loy, B.L.F. Chin, M.K. Lam, S. Yusup, Z.A. Jawad, Catalytic pyrolysis of Chlorella vulgaris: Kinetic and thermodynamic analysis, Bioresour. Technol. 289 (2019) 121689. https://doi.org/10.1016/j.biortech.2019.121689.

[20] M. Goedhuys, N. Janz, P. Mohneny, Knowledge-based productivity in “low-tech” industries: Evidence from firms in developing countries, Ind. Corp. Chang. 23 (2014) 1–23. https://doi.org/10.1093/icc/dtt006.

[21] N. Gao, K. Kamran, C. Quan, P.T. Williams, Thermochemical conversion of sewage sludge: A critical review, Prog. Energy Combust. Sci. 79 (2020) 100843. https://doi.org/10.1016/j.pecs.2020.100843.

[22] C.M. Vivek, P. Ramkumar, P.K. Srividhya, M. Sivasubramanian, Materials Today : Proceedings Recent strategies and trends in implanting of renewable energy sources for sustainability – A review, Mater. Today Proc. (2021). https://doi.org/10.1016/j.matpr.2021.03.208.

[23] U.K. Pata, Linking renewable energy, globalization, agriculture, CO2 emissions and ecological footprint in BRIC countries: A sustainability perspective, Renew. Energy. 173 (2021) 197–208. https://doi.org/10.1016/j.renene.2021.03.125.

[24] A.K. Chandrakar, Energy Resources : Indian Scenario An Assignment on, (2015).

[25] J.S. Tumuluru, S. Sokhansanj, C.T. Wright, R.D. Boardman, N.A. Yancey, A review on biomass classification and composition, co-firing issues and pretreatment methods, Am. Soc. Agric. Biol. Eng. Annu. Int. Meet. 2011, ASABE

2011. 3 (2011) 2053–2083. https://doi.org/10.13031/2013.37191.

[26] S. Uyanik, D. Canan ÇELİKEL, Türk Tekstil Endüstrisi Genel Durumu, 2019.

[27] U. Valİlİğİ, ÇEVRE VE ŞEHİRCİLİK İL MÜDÜRLÜĞÜ UŞAK İLİ 2017 YILI ÇEVRE DURUM RAPORU Uşak Çevre ve Şehircilik İl Müdürlüğü UŞAK 2018, (2018).

[28] J. Werther, T. Ogada, Sewage sludge combustion, Prog. Energy Combust. Sci. 25 (1999) 55–116. https://doi.org/10.1016/S0360-1285(98)00020-3.

[29] M. Anjum, N.H. Al-Makishah, M.A. Barakat, Wastewater sludge stabilization using pre-treatment methods, Process Saf. Environ. Prot. 102 (2016) 615–632. https://doi.org/10.1016/j.psep.2016.05.022.

[30] European Commission, Disposal and recycling routes for sewage sludge. Part 2 – Regulatory report, 2001.

[31] G. Tchobanoglous, F. Burton, H.D. Stensel, Wastewater engineering: An Overview, Wastewater Eng. Treat. Reuse. (1991) 1–24. https://doi.org/10.1016/0309-1708(80)90067-6.

[32] M. Henze, Wastewater treatment: biological and chemical processes, Choice Rev. Online. 33 (1996) 33-4531-33–4531. https://doi.org/10.5860/choice.33-4531.

[33] J.A. Mixon, S. Ave, F.G. Yeager, United States Patent (19), (1981).

[34] W.J. Katz, A. Geinopolos, W.J. Katz, A. Geinopolos, SLUDGE THICKENING BY DISSOLVED-AIR FLOTATION, 39 (2020) 946–957.

[35] L. Appels, J. Baeyens, J. Degrève, R. Dewil, Principles and potential of the anaerobic digestion of waste-activated sludge, Prog. Energy Combust. Sci. 34 (2008) 755–781. https://doi.org/10.1016/j.pecs.2008.06.002.

[36] J. Martín, J.L. Santos, I. Aparicio, E. Alonso, Pharmaceutically active compounds in sludge stabilization treatments: Anaerobic and aerobic digestion, wastewater stabilization ponds and composting, Sci. Total Environ. 503–504 (2015) 97–104. https://doi.org/10.1016/j.scitotenv.2014.05.089.

[37] SCHERLER A, Dewatering of Sewage Sludge By Centrifuge, U S Public Heal. Serv Publ, Inf. Bull. (1969) 2–22.

[38] P. Stasta, J. Boran, L. Bebar, P. Stehlik, J. Oral, Thermal processing of sewage sludge, Appl. Therm. Eng. 26 (2006) 1420–1426. https://doi.org/10.1016/j.applthermaleng.2005.05.030.

[39] G. Chen, P.L. Yue, A.S. Mujumdar, Sludge dewatering and drying, Dry. Technol. 20 (2002) 883–916. https://doi.org/10.1081/DRT-120003768.

[40] E. Yildirir, L. Ballice, Supercritical water gasification of wet sludge from biological treatment of textile and leather industrial wastewater, J. Supercrit. Fluids. 146 (2019) 100–106. https://doi.org/10.1016/j.supflu.2019.01.012.

[41] M. Pellegrini, C. Saccani, A. Bianchini, L. Bonfiglioli, Sewage sludge management in Europe: a critical analysis of data quality, Int. J. Environ. Waste Manag. 18 (2016) 226. https://doi.org/10.1504/ijewm.2016.10001645.

[42] J. Samanya, Increase of energy recovery from sewage sludge, (2013) 236.

[43] G. Barberio, L. Cutaia, V. Librici, TREATMENT AND DISPOSAL OF SEWAGE SLUDGE: COMPARATIVE LIFE CYCLE ASSESSMENT ON ITALIAN CASE STUDY Extended abstract, Environ. Eng. Manag. J. 12 (2013) 7–10.

[44] G. Mininni, A. Sbrilli, E. Guerriero, M. Rotatori, Dioxins and furans formation in pilot incineration tests of sewage sludge spiked with organic chlorine, Chemosphere. 54 (2004) 1337–1350. https://doi.org/10.1016/S0045-6535(03)00252-2.

[45] M. Poffet, Thermal runaway of dried sewage sludge in the storage tanks: from molecular origins to technical measures of smouldering fire prevention, Département Chim. - Univ. Fribg. (2007) 253.

[46] J.P. Hillman, J. Hill, J.E. Morgan, J.M. Wilkinson, Recycling of sewage sludge to grassland: A review of the legislation to control of the localization and accumulation of potential toxic metals in grazing systems, Grass Forage Sci. 58 (2003) 101–111. https://doi.org/10.1046/j.1365-2494.2003.00365.x.

[47] S. McAllister, J.-Y. Chen, A.C. Fernandez-Pello, Fundamentals of Combustion Processes, 2011. https://doi.org/10.1007/978-1-4419-7943-8.

[48] H. Lin, X. Ma, Simulation of co-incineration of sewage sludge with municipal solid waste in a grate furnace incinerator, Waste Manag. 32 (2012) 561–567. https://doi.org/10.1016/j.wasman.2011.10.032.

[49] H. Zhang, Z. Gao, W. Ao, J. Li, G. Liu, J. Fu, C. Ran, Y. Liu, Q. Kang, X. Mao, J. Dai, Microwave pyrolysis of textile dyeing sludge in a continuously operated auger reactor, Fuel Process. Technol. 166 (2017) 174–185. https://doi.org/10.1016/j.fuproc.2017.05.031.

[50] T. Murakami, Y. Suzuki, H. Nagasawa, T. Yamamoto, T. Koseki, H. Hirose, S. Okamoto, Combustion characteristics of sewage sludge in an incineration plant for energy recovery, Fuel Process. Technol. 90 (2009) 778–783. https://doi.org/10.1016/j.fuproc.2009.03.003.

[51] S. Werle, S. Sobek, Gasification of sewage sludge within a circular economy perspective: a Polish case study, Environ. Sci. Pollut. Res. 26 (2019) 35422–35432. https://doi.org/10.1007/s11356-019-05897-2.

[52] S. Werle, Sewage sludge gasification: Theoretical and experimental investigation, Environ. Prot. Eng. 39 (2013) 25–32. https://doi.org/10.5277/EPE130203.

[53] D. Mohan, C.U. Pittman, P.H. Steele, Pyrolysis of wood/biomass for bio-oil: A critical review, Energy and Fuels. 20 (2006) 848–889. https://doi.org/10.1021/ef0502397.

[54] S.R. Naqvi, R. Tariq, Z. Hameed, I. Ali, M. Naqvi, W.H. Chen, S. Ceylan, H. Rashid, J. Ahmad, S.A. Taqvi, M. Shahbaz, Pyrolysis of high ash sewage sludge: Kinetics and thermodynamic analysis using Coats-Redfern method, Renew. Energy. 131 (2019) 854–860. https://doi.org/10.1016/j.renene.2018.07.094.

[55] M.I. Jahirul, M.G. Rasul, A.A. Chowdhury, N. Ashwath, Biofuels production through biomass pyrolysis- A technological review, Energies. 5 (2012) 4952–

5001. https://doi.org/10.3390/en5124952.

[56] N. Tippayawong, J. Kinorn, S. Thavornun, Yields and gaseous composition from slow pyrolysis of refuse-derived fuels, Energy Sources, Part A Recover. Util. Environ. Eff. 30 (2008) 1572–1580. https://doi.org/10.1080/15567030701258550.

[57] A. V. Bridgwater, Review of fast pyrolysis of biomass and product upgrading, Biomass and Bioenergy. 38 (2012) 68–94. https://doi.org/10.1016/j.biombioe.2011.01.048.

[58] D. Meier, B. Van De Beld, A. V. Bridgwater, D.C. Elliott, A. Oasmaa, F. Preto, State-of-the-art of fast pyrolysis in IEA bioenergy member countries, Renew. Sustain. Energy Rev. 20 (2013) 619–641. https://doi.org/10.1016/j.rser.2012.11.061.

[59] H. Fan, H. Zhou, J. Wang, Pyrolysis of municipal sewage sludges in a slowly heating and gas sweeping fixed-bed reactor, Energy Convers. Manag. 88 (2014) 1151–1158. https://doi.org/10.1016/j.enconman.2014.05.043.

[60] T. Lu, H.R. Yuan, S.G. Zhou, H.Y. Huang, K. Noriyuki, Y. Chen, On the pyrolysis of sewage sludge: The influence of pyrolysis temperature on biochar, liquid and gas fractions, Adv. Mater. Res. 518–523 (2012) 3412–3420. https://doi.org/10.4028/www.scientific.net/AMR.518-523.3412.

[61] A. Domínguez, J.A. Menéndez, M. Inguanzo, J.J. Pís, Production of bio-fuels by high temperature pyrolysis of sewage sludge using conventional and microwave heating, Bioresour. Technol. 97 (2006) 1185–1193. https://doi.org/10.1016/j.biortech.2005.05.011.

[62] I.C. Kantarli, J. Yanik, Use of waste sludge from the tannery industry, Energy and Fuels. 23 (2009) 3126–3133. https://doi.org/10.1021/ef8011068.

[63] E. Pokorna, N. Postelmans, P. Jenicek, S. Schreurs, R. Carleer, J. Yperman, Study of bio-oils and solids from flash pyrolysis of sewage sludges, Fuel. 88 (2009) 1344–1350. https://doi.org/10.1016/j.fuel.2009.02.020.

[64] J.P. Cao, L.Y. Li, K. Morishita, X. Bin Xiao, X.Y. Zhao, X.Y. Wei, T. Takarada, Nitrogen transformations during fast pyrolysis of sewage sludge, Fuel. 104 (2013) 1–6. https://doi.org/10.1016/j.fuel.2010.08.015.

[65] X. Huang, J.P. Cao, P. Shi, X.Y. Zhao, X.B. Feng, Y.P. Zhao, X. Fan, X.Y. Wei, T. Takarada, Influences of pyrolysis conditions in the production and chemical composition of the bio-oils from fast pyrolysis of sewage sludge, J. Anal. Appl. Pyrolysis. 110 (2014) 353–362. https://doi.org/10.1016/j.jaap.2014.10.003.

[66] J. Alvarez, M. Amutio, G. Lopez, J. Bilbao, M. Olazar, Fast co-pyrolysis of sewage sludge and lignocellulosic biomass in a conical spouted bed reactor, Fuel. 159 (2015) 810–818. https://doi.org/10.1016/j.fuel.2015.07.039.

[67] Y. Lin, Y. Liao, Z. Yu, S. Fang, X. Ma, A study on co-pyrolysis of bagasse and sewage sludge using TG-FTIR and Py-GC/MS, Energy Convers. Manag. 151 (2017) 190–198. https://doi.org/10.1016/j.enconman.2017.08.062.

[68] S. Deng, H. Tan, X. Wang, F. Yang, R. Cao, Z. Wang, R. Ruan, Investigation on the fast co-pyrolysis of sewage sludge with biomass and the combustion reactivity

of residual char, Bioresour. Technol. 239 (2017) 302–310. https://doi.org/10.1016/j.biortech.2017.04.067.

[69] Z. Huang, L. Qin, Z. Xu, W. Chen, F. Xing, The effects of Fe 2 O 3 catalyst on the conversion of organic matter and bio-fuel production during pyrolysis of sewage sludge, J. Energy Inst. 92 (2019) 835–842. https://doi.org/10.1016/j.joei.2018.06.015.

[70] Y. Sun, B. Jin, W. Wu, W. Zuo, Y. Zhang, Y. Zhang, Y. Huang, Effects of temperature and composite alumina on pyrolysis of sewage sludge, J. Environ. Sci. (China). 30 (2015) 1–8. https://doi.org/10.1016/j.jes.2014.10.010.

[71] Y. Yu, J. Yu, B. Sun, Z. Yan, Influence of catalyst types on the microwave-induced pyrolysis of sewage sludge, J. Anal. Appl. Pyrolysis. 106 (2014) 86–91. https://doi.org/10.1016/j.jaap.2014.01.003.

[72] Q. Xie, P. Peng, S. Liu, M. Min, Y. Cheng, Y. Wan, Y. Li, X. Lin, Y. Liu, P. Chen, R. Ruan, Fast microwave-assisted catalytic pyrolysis of sewage sludge for bio-oil production, Bioresour. Technol. 172 (2014) 162–168. https://doi.org/10.1016/j.biortech.2014.09.006.

[73] H.J. Park, H.S. Heo, Y.K. Park, J.H. Yim, J.K. Jeon, J. Park, C. Ryu, S.S. Kim, Clean bio-oil production from fast pyrolysis of sewage sludge: Effects of reaction conditions and metal oxide catalysts, Bioresour. Technol. 101 (2010) S83–S85. https://doi.org/10.1016/j.biortech.2009.06.103.

[74] J.E. White, W.J. Catallo, B.L. Legendre, Biomass pyrolysis kinetics: A comparative critical review with relevant agricultural residue case studies, J. Anal. Appl. Pyrolysis. 91 (2011) 1–33. https://doi.org/10.1016/j.jaap.2011.01.004.

[75] S. Vyazovkin, K. Chrissafis, M.L. Di Lorenzo, N. Koga, M. Pijolat, B. Roduit, N. Sbirrazzuoli, J.J. Suñol, ICTAC Kinetics Committee recommendations for collecting experimental thermal analysis data for kinetic computations, Thermochim. Acta. 590 (2014) 1–23. https://doi.org/10.1016/j.tca.2014.05.036.

[76] L.N. Samuelsson, Isoconversional analysis for the prediction of mass-loss rates during pyrolysis of biomass, 2016.

[77] W. Hemminger, S.M. Sarge, Chapter 1 Definitions, Nomenclature, Terms and Literature, Elsevier Masson SAS, 1998. https://doi.org/10.1016/S1573-4374(98)80004-6.

[78] T. Willner, G. Brunner, Pyrolysis kinetics of wood and wood components, Chem. Eng. Technol. 28 (2005) 1212–1225. https://doi.org/10.1002/ceat.200500206.

[79] M.Z. (Norwegian U. of S. and T. Alonso, A thermogravimetric and kinetic study on devolatilization of woody biomass, (2016) 1–123.

[80] C. Di Blasi, Modeling intra- and extra-particle processes of wood fast pyrolysis, AIChE J. 48 (2002) 2386–2397. https://doi.org/10.1002/aic.690481028.

[81] C. Di Blasi, C. Branca, Temperatures of wood particles in a hot sand bed fluidized by nitrogen, Energy and Fuels. 17 (2003) 247–254. https://doi.org/10.1021/ef020146e.

[82] S. Vyazovkin, A.K. Burnham, J.M. Criado, L.A. Pérez-Maqueda, C. Popescu, N. Sbirrazzuoli, ICTAC Kinetics Committee recommendations for performing kinetic computations on thermal analysis data, Thermochim. Acta. 520 (2011) 1–19. https://doi.org/10.1016/j.tca.2011.03.034.

[83] S.A. El-Sayed, M.E. Mostafa, Pyrolysis characteristics and kinetic parameters determination of biomass fuel powders by differential thermal gravimetric analysis (TGA/DTG), Energy Convers. Manag. 85 (2014) 165–172. https://doi.org/10.1016/j.enconman.2014.05.068.

[84] Z. Shuping, W. Yulong, Y. Mingde, L. Chun, T. Junmao, Pyrolysis characteristics and kinetics of the marine microalgae Dunaliella tertiolecta using thermogravimetric analyzer, Bioresour. Technol. 101 (2010) 359–365. https://doi.org/10.1016/j.biortech.2009.08.020.

[85] M.J. Starink, The determination of activation energy from linear heating rate experiments: A comparison of the accuracy of isoconversion methods, Thermochim. Acta. 404 (2003) 163–176. https://doi.org/10.1016/S0040-6031(03)00144-8.

[86] B.N. Langtry, Identity And Spatio-Temporal Continuity, Australas. J. Philos. 50 (1972) 184–189. https://doi.org/10.1080/00048407212341221.

[87] K. Slopiecka, P. Bartocci, F. Fantozzi, Thermogravimetric analysis and kinetic study of poplar wood pyrolysis, Appl. Energy. 97 (2012) 491–497. https://doi.org/10.1016/j.apenergy.2011.12.056.

[88] Y. Guan, C. Liu, Q. Peng, F. Zaman, H. Zhang, Z. Jin, A. Wang, W. Wang, Y. Huang, Pyrolysis kinetics behavior of solid leather wastes, Waste Manag. 100 (2019) 122–127. https://doi.org/10.1016/j.wasman.2019.09.005.

[89] X.J. Lee, L.Y. Lee, S. Gan, S. Thangalazhy-Gopakumar, H.K. Ng, Biochar potential evaluation of palm oil wastes through slow pyrolysis: Thermochemical characterization and pyrolytic kinetic studies, Bioresour. Technol. 236 (2017) 155–163. https://doi.org/10.1016/j.biortech.2017.03.105.

[90] J.M. Criado, P.E. Sánchez-Jiménez, L.A. Pérez-Maqueda, Critical study of the isoconversional methods of kinetic analysis, J. Therm. Anal. Calorim. 92 (2008) 199–203. https://doi.org/10.1007/s10973-007-8763-7.

[91] J. Cai, D. Xu, Z. Dong, X. Yu, Y. Yang, S.W. Banks, A. V. Bridgwater, Processing thermogravimetric analysis data for isoconversional kinetic analysis of lignocellulosic biomass pyrolysis: Case study of corn stalk, Renew. Sustain. Energy Rev. 82 (2018) 2705–2715. https://doi.org/10.1016/j.rser.2017.09.113.

[92] H. Shahbeig, M. Nosrati, Pyrolysis of municipal sewage sludge for bioenergy production: Thermo-kinetic studies, evolved gas analysis, and techno-socio-economic assessment, Renew. Sustain. Energy Rev. 119 (2020) 109567. https://doi.org/10.1016/j.rser.2019.109567.

[93] M.J.B. Fong, A.C.M. Loy, B.L.F. Chin, M.K. Lam, S. Yusup, Z.A. Jawad, Catalytic pyrolysis of Chlorella vulgaris: Kinetic and thermodynamic analysis, Bioresour. Technol. 289 (2019) 121689. https://doi.org/10.1016/j.biortech.2019.121689.

[94] Y. Qu, A. Li, D. Wang, L. Zhang, G. Ji, Kinetic study of the effect of in-situ mineral solids on pyrolysis process of oil sludge, Chem. Eng. J. 374 (2019) 338–346. https://doi.org/10.1016/j.cej.2019.05.183.

[95] W. Miao, X. Li, Y. Wang, Y. Lv, Pyrolysis characteristics of oil-field sludge and the comparison of kinetic analysis with two representative methods, J. Pet. Sci. Eng. 182 (2019) 106309. https://doi.org/10.1016/j.petrol.2019.106309.

[96] X. Yang, Z. Jiang, Kinetic studies of overlapping pyrolysis reactions in industrial waste activated sludge, Bioresour. Technol. 100 (2009) 3663–3668. https://doi.org/10.1016/j.biortech.2009.03.002.

[97] M.R. Othman, Y.H. Park, T.A. Ngo, S.S. Kim, J. Kim, K.S. Lee, Thermogravimetric characteristics and pyrolysis kinetics of Giheung Respia sewage sludge, Korean J. Chem. Eng. 27 (2010) 163–167. https://doi.org/10.1007/s11814-009-0338-9.

[98] Y. Zhai, W. Peng, G. Zeng, Z. Fu, Y. Lan, H. Chen, C. Wang, X. Fan, Pyrolysis characteristics and kinetics of sewage sludge for different sizes and heating rates, J. Therm. Anal. Calorim. 107 (2012) 1015–1022. https://doi.org/10.1007/s10973-011-1644-0.

[99] R. Kaur, P. Gera, M.K. Jha, T. Bhaskar, Pyrolysis kinetics and thermodynamic parameters of castor (Ricinus communis) residue using thermogravimetric analysis, Bioresour. Technol. 250 (2018) 422–428. https://doi.org/10.1016/j.biortech.2017.11.077.

[100] X. Zhang, Y. Han, Y. Li, Y. Sun, Effect of Heating Rate on Pyrolysis Behavior and Kinetic Characteristics of Siderite, Minerals. 7 (2017) 211. https://doi.org/10.3390/min7110211.

[101] V.Q. Dinh, V.D. Son Tho, Study on Thermogravimetric and Kinetic of Agricultural Residues in Vietnam, Vietnam J. Sci. Technol. 55 (2017) 436–442. https://doi.org/10.15625/2525-2518/55/4/9027.

[102] W. Ouyang, X. Zhao, M. Tysklind, F. Hao, F. Wang, Optimisation of corn straw biochar treatment with catalytic pyrolysis in intensive agricultural area, Ecol. Eng. 84 (2015) 278–286. https://doi.org/10.1016/j.ecoleng.2015.09.003.

[103] R. Gottipati, Preparation and Characterization of Microporous Activated Carbon from Biomass and its Application in the Removal of Chromium (VI) from Aqueous Phase Department of Chemical Engineering, Dep. Chem. Eng. Natl. Inst. Technol. Rourkela Odisha, India. (2012) 1–242.

[104] L. Wang, M. Zhao, H. Ma, G. Han, D. Yang, D. Chen, Y. Zhang, J. Zhou, Extraction of SiO2 from gasified rice husk carbon simultaneously rice husk activated carbon production: Restudy on product properties, activation mechanism, and evolution law of pore structure, Energy Reports. 6 (2020) 3094–3103. https://doi.org/10.1016/j.egyr.2020.11.031.

[105] H.K. Yağmur, İ. Kaya, Synthesis and characterization of magnetic ZnCl2-activated carbon produced from coconut shell for the adsorption of methylene blue, J. Mol. Struct. 1232 (2021) 130071. https://doi.org/10.1016/j.molstruc.2021.130071.

[106] M.J. Livani, M. Ghorbani, H. Mehdipour, Preparation of an activated carbon from hazelnut shells and its composites with magnetic NiFe2O4 nanoparticles, Xinxing Tan Cailiao/New Carbon Mater. 33 (2018) 578–586. https://doi.org/10.1016/S1872-5805(18)60358-0.

[107] C. Saka, O. Baytar, Y. Yardim, Ö. Şahin, Improvement of electrochemical double-layer capacitance by fast and clean oxygen plasma treatment on activated carbon as the electrode material from walnut shells, Biomass and Bioenergy. 143 (2020). https://doi.org/10.1016/j.biombioe.2020.105848.

[108] Ş. Karadirek, H. Okkay, Statistical modeling of activated carbon production from spent mushroom compost, J. Ind. Eng. Chem. 63 (2018) 340–347. https://doi.org/10.1016/j.jiec.2018.02.034.

[109] O.C. Iheanacho, J.T. Nwabanne, C.C. Obi, C.E. Onu, Packed bed column adsorption of phenol onto corn cob activated carbon: linear and nonlinear kinetics modeling, South African J. Chem. Eng. 36 (2021) 80–93. https://doi.org/10.1016/j.sajce.2021.02.003.

[110] K.M. Smith, G.D. Fowler, S. Pullket, N.J.D. Graham, Sewage sludge-based adsorbents: A review of their production, properties and use in water treatment applications, Water Res. 43 (2009) 2569–2594. https://doi.org/10.1016/j.watres.2009.02.038.

[111] D. Prahas, Y. Kartika, N. Indraswati, S. Ismadji, Activated carbon from jackfruit peel waste by H3PO4 chemical activation: Pore structure and surface chemistry characterization, Chem. Eng. J. 140 (2008) 32–42. https://doi.org/10.1016/j.cej.2007.08.032.

[112] M. Molina-Sabio, F. Rodríguez-Reinoso, Role of chemical activation in the development of carbon porosity, Colloids Surfaces A Physicochem. Eng. Asp. 241 (2004) 15–25. https://doi.org/10.1016/j.colsurfa.2004.04.007.

[113] O.A. Ioannidou, A.A. Zabaniotou, G.G. Stavropoulos, M.A. Islam, T.A. Albanis, Preparation of activated carbons from agricultural residues for pesticide adsorption, Chemosphere. 80 (2010) 1328–1336. https://doi.org/10.1016/j.chemosphere.2010.06.044.

[114] G. ÖZSĠN, Production and Characterization of Activated Carbon From Pistachio-Nut Shell a Thesis Submitted To the Graduate School of Natural and Applied Sciences of the Middle East Technical University By Gamzenur Özsġn in Partial Fulfillment of the Requirements for, (2011) 190.

[115] B. Yang, Y. Liu, Q. Liang, M. Chen, L. Ma, L. Li, Q. Liu, W. Tu, D. Lan, Y. Chen, Evaluation of activated carbon synthesized by one-stage and two-stage co-pyrolysis from sludge and coconut shell, Ecotoxicol. Environ. Saf. 170 (2019) 722–731. https://doi.org/10.1016/j.ecoenv.2018.11.130.

[116] T.L. Silva, A. Ronix, O. Pezoti, L.S. Souza, P.K.T. Leandro, K.C. Bedin, K.K. Beltrame, A.L. Cazetta, V.C. Almeida, Mesoporous activated carbon from industrial laundry sewage sludge: Adsorption studies of reactive dye Remazol Brilliant Blue R, Chem. Eng. J. 303 (2016) 467–476. https://doi.org/10.1016/j.cej.2016.06.009.

[117] Q. Liang, Y. Liu, M. Chen, L. Ma, B. Yang, L. Li, Q. Liu, Optimized preparation of activated carbon from coconut shell and municipal sludge, Mater. Chem. Phys. 241 (2020) 122327. https://doi.org/10.1016/j.matchemphys.2019.122327.

[118] W. Li, K. Yang, J. Peng, L. Zhang, S. Guo, H. Xia, Effects of carbonization temperatures on characteristics of porosity in coconut shell chars and activated carbons derived from carbonized coconut shell chars, Ind. Crops Prod. 28 (2008) 190–198. https://doi.org/10.1016/j.indcrop.2008.02.012.

[119] J. Katesa, S. Junpiromand, C. Tangsathitkulchai, Effect of Carbonization Temperature On Properties of Char And Activated Carbon From Coconut Shell, Suranaree J. Sci. Technol. 20 (2013) 269–278.

[120] T. Varil, D. Bergna, R. Lahti, H. Romar, T. Hu, U. Lassi, Activated carbon production from peat using ZnCl2: Characterization and applications, BioResources. 12 (2017) 8078–8092. https://doi.org/10.15376/biores.12.4.8078-8092.

[121] F. Ateş, H. Büyüktuncer, B. Yaşar, A. Işık, G. Biricik, A.S. Koparal, Comparison of non-catalytic and catalytic fast pyrolysis of pomegranate and grape marcs under vacuum and inert atmospheres, Fuel. 255 (2019) 115788. https://doi.org/10.1016/j.fuel.2019.115788.

[122] A.C.M. Loy, S. Yusup, B.S. How, C.L. Yiin, B.L.F. Chin, M. Muhammad, Y.L. Gwee, Uncertainty estimation approach in catalytic fast pyrolysis of rice husk: Thermal degradation, kinetic and thermodynamic parameters study, Bioresour. Technol. 294 (2019) 122089. https://doi.org/10.1016/j.biortech.2019.122089.

[123] A.G. Barneto, J.A. Carmona, J.E.M. Alfonso, J.D. Blanco, Kinetic models based in biomass components for the combustion and pyrolysis of sewage sludge and its compost, J. Anal. Appl. Pyrolysis. 86 (2009) 108–114. https://doi.org/10.1016/j.jaap.2009.04.011.

[124] J.A. Conesa, A. Marcilla, D. Prats, M. Rodriguez-Pastor, Kinetic Study of the Pyrolysis of Sewage Sludge, Waste Manag. Res. 15 (1997) 293–305. https://doi.org/10.1177/0734242X9701500307.

[125] M. Djaeni, P. Bartels, J. Sanders, G. van Straten, A.J.B. van Boxtel, Multistage Zeolite Drying for Energy-Efficient Drying, Dry. Technol. 25 (2007) 1053–1067. https://doi.org/10.1080/07373930701396535.

[126] J.C.G. da Silva, J.L.F. Alves, W.V. de A. Galdino, S.L.F. Andersen, R.F. de Sena, Pyrolysis kinetic evaluation by single-step for waste wood from reforestation, Waste Manag. 72 (2018) 265–273. https://doi.org/10.1016/j.wasman.2017.11.034.

[127] É.D.G. Baroni, K. Tannous, Y.J. Rueda-Ordóñez, L.K. Tinoco-Navarro, The applicability of isoconversional models in estimating the kinetic parameters of biomass pyrolysis, J. Therm. Anal. Calorim. 123 (2016) 909–917. https://doi.org/10.1007/s10973-015-4707-9.

[128] L. Abdelouahed, S. Leveneur, L. Vernieres-Hassimi, • Laurent Balland, • Bechara Taouk, Comparative investigation for the determination of kinetic parameters for biomass pyrolysis by thermogravimetric analysis, J. Therm. Anal. Calorim. 129 (2017) 1201–1213. https://doi.org/10.1007/s10973-017-6212-9.

[129] S.A. Scott, J.S. Dennis, J.F. Davidson, A.N. Hayhurst, Thermogravimetric measurements of the kinetics of pyrolysis of dried sewage sludge, Fuel. 85 (2006) 1248–1253. https://doi.org/10.1016/j.fuel.2005.11.003.

[130] C. Casajus, J. Abrego, F. Marias, J. Vaxelaire, J.L. Sánchez, A. Gonzalo, Product distribution and kinetic scheme for the fixed bed thermal decomposition of sewage sludge, Chem. Eng. J. 145 (2009) 412–419. https://doi.org/10.1016/j.cej.2008.08.033.

[131] A. Soria-Verdugo, E. Goos, A. Morato-Godino, N. García-Hernando, U. Riedel, Pyrolysis of biofuels of the future: Sewage sludge and microalgae – Thermogravimetric analysis and modelling of the pyrolysis under different temperature conditions, Energy Convers. Manag. 138 (2017) 261–272. https://doi.org/10.1016/j.enconman.2017.01.059.

[132] C. Jindarom, V. Meeyoo, T. Rirksomboon, P. Rangsunvigit, Thermochemical decomposition of sewage sludge in CO2 and N2 atmosphere, Chemosphere. 67 (2007) 1477–1484. https://doi.org/10.1016/j.chemosphere.2006.12.066.

[133] E. Müsellim, M.H. Tahir, M.S. Ahmad, S. Ceylan, Thermokinetic and TG/DSC-FTIR study of pea waste biomass pyrolysis, Appl. Therm. Eng. 137 (2018) 54–61. https://doi.org/10.1016/j.applthermaleng.2018.03.050.

[134] Y. Xiang, Y. Xiang, L. Wang, Kinetics of the thermal decomposition of poplar sawdust, Energy Sources, Part A Recover. Util. Environ. Eff. 39 (2017) 213–218. https://doi.org/10.1080/15567036.2016.1212291.

[135] R.E. Guedes, A.S. Luna, A.R. Torres, Operating parameters for bio-oil production in biomass pyrolysis: A review, J. Anal. Appl. Pyrolysis. 129 (2018) 134–149. https://doi.org/10.1016/J.JAAP.2017.11.019.

[136] J. Akhtar, N. Saidina Amin, A review on operating parameters for optimum liquid oil yield in biomass pyrolysis, Renew. Sustain. Energy Rev. 16 (2012) 5101–5109. https://doi.org/10.1016/J.RSER.2012.05.033.

[137] X. Wang, S. Deng, H. Tan, A. Adeosun, M. Vujanović, F. Yang, N. Duić, Synergetic effect of sewage sludge and biomass co-pyrolysis: A combined study in thermogravimetric analyzer and a fixed bed reactor, Energy Convers. Manag. 118 (2016) 399–405. https://doi.org/10.1016/J.ENCONMAN.2016.04.014.

[138] Y.F. Huang, C.H. Shih, P. Te Chiueh, S.L. Lo, Microwave co-pyrolysis of sewage sludge and rice straw, Energy. 87 (2015) 638–644. https://doi.org/10.1016/j.energy.2015.05.039.

[139] J. Lin, S. Sun, R. Ma, L. Fang, P. Zhang, J. Qu, X. Zhang, H. Geng, X. Huang, Characteristics and Reaction Mechanisms of Sludge-Derived Bio-Oil Produced through Microwave Pyrolysis at Different Temperatures, Energy Convers. Manag. 160 (2018) 403–410. https://doi.org/10.1016/j.enconman.2018.01.060.

[140] D. Wang, R. Xiao, H. Zhang, G. He, Comparison of catalytic pyrolysis of biomass with MCM-41 and CaO catalysts by using TGA-FTIR analysis, J. Anal. Appl. Pyrolysis. 89 (2010) 171–177. https://doi.org/10.1016/j.jaap.2010.07.008.

[141] M. C. Samolada, A. Papafotica, I. A. Vasalos, Catalyst Evaluation for Catalytic

Biomass Pyrolysis, Energy & Fuels. 14 (2000) 1161–1167. https://doi.org/10.1021/ef000026b.

[142] M.F. Gómez-Rico, R. Font, A. Fullana, I. Martín-Gullón, Thermogravimetric study of different sewage sludges and their relationship with the nitrogen content, in: J. Anal. Appl. Pyrolysis, 2005: pp. 421–428. https://doi.org/10.1016/j.jaap.2004.11.029.

[143] N.H. Zainan, S.C. Srivatsa, F. Li, S. Bhattacharya, Quality of bio-oil from catalytic pyrolysis of microalgae Chlorella vulgaris, Fuel. 223 (2018) 12–19. https://doi.org/10.1016/j.fuel.2018.02.166.

[144] A.I. Rushdi, G. Ritter, J.O. Grimalt, B.R.T. Simoneit, Hydrous pyrolysis of cholesterol under various conditions, Org. Geochem. 34 (2003) 799–812. https://doi.org/10.1016/S0146-6380(03)00016-0.

CURRICULUM VITAE

ÖZGEÇMİŞ			
Name, Surname	Mostafa		Abdul Wahab
Birthplace and Date			
Languages	Arabic Native English Advanced French Intermediate		
Education Status	**Start – Completion Year**		**Institution Name**
Lise	2010	2013	George Sarraf
Bachelor's Degree	2014	2018	Usak University
Master's degree	2018	2022	Eskisehir Technical University
Work Experience			
Company Name	Provable Cosmetics		
Start Year	June 2019		
Position	Business Planning and development Manager		
Papers	Investigation of thermal degradation kinetics and catalytic pyrolysis of industrial sludge produced from textile and leather industrial wastewater		
Phone Number			
E-mail			